



Universidad de Concepción
Dirección de Postgrado
Facultad de Farmacia -Programa de Ciencias y Tecnología Analítica.

**Estilbenoides y proantocianidinas en sarmientos de vides:
Caracterización, incidencia de las condiciones de guarda post-poda,
actividad antioxidante y antiproliferativa en células cancerosas.**

Tesis para optar al grado de Doctor en Ciencias y Tecnología Analítica.

Vania Stephanie Sáez Pulgar
CONCEPCIÓN-CHILE
2018

Profesor Guía: Dr. Dietrich von Baer von Lochow
Profesor Co-Guía: Dra. Claudia Mardones Peña
Dpto. de Análisis Instrumental, Facultad de Farmacia.
Universidad de Concepción



Tabla de contenidos.

Índice de figuras.....	vii
Índice de tablas.....	xi
Resumen.....	xiii
Capítulo 1: Introducción.....	1
1.1. Industria vitivinícola en Chile.....	2
1.2. Alternativas de manejo de residuos de la industria vitivinícola.	3
1.3. (Poli)fenoles bioactivos en <i>Vitis vinífera</i>	6
1.3.1. Flavonoides:	6
1.3.2. Proantocianidinas:	7
1.4. No flavonoides:	10
1.4.1. Ácidos fenólicos:.....	10
1.4.2. Estilbenoides:	11
1.5. Sarmientos como fuente de compuestos bioactivos.....	17
1.5.1. Flavonoides en sarmientos:	17
1.5.2 Concentración de compuestos no flavonoides en sarmientos:	19
1.5.3. Factores que influyen en la concentración de estilbenoides en sarmientos de <i>Vitis vinifera</i>	23
1.6. Aislamiento de estilbenoides en órganos de la vid.....	25
1.7. Test de reducción de tetrazolio (MTT) para la medición <i>in vitro</i> de viabilidad celular.....	29
1.8. Análisis de estilbenoides y procianidinas por HPLC.....	31
1.8.1. Cromatografía bidimensional.....	35
2. Hipótesis y Objetivos.....	39
2.1. Hipótesis:	39
2.2. Objetivo General:	39
2.3. Objetivos específicos:	40
3. Estrategia analítica para el análisis de estilbenoides y procianidinas en sarmientos.....	41
3.1. Aislamiento de estilbenoides desde sarmientos.....	41
3.2. Caracterización y elucidación estructural de oligoestilbenoides	42
3.3. Ensayos de actividad antiproliferante de estilbenoides en células cancerosas	42

3.4. Determinación cuantitativa de estilbenoides y proantocianidinas en sarmientos: incidencia de condiciones el proceso de guarda post-poda	42
3.5. Perfil de estilbenoides y procianidinas en sarmientos mediante LC x LC	43
4. Referencias:	44

Capítulo 2: Oligostilbenoids in Pinot Noir Grape Cane Extract: Isolation, Characterization, Antioxidant Capacity and *in vitro* Anti-proliferative Effect on Cancer Cells

Abstract.....	66
1. Introduction	68
2. Material and methods	71
2.1 Solvents and reagents.....	71
2.2 Grape cane extract	72
2.3 Purification of extract by centrifugal partition chromatography	72
2.4 Identity assignment by HPLC-DAD-QToF and quantification by HPLC-DAD-FL..	73
2.5 Isolation of oligostilbenoids by semi-preparative HPLC-UV	74
2.6 Structural determination of isolated oligostilbenoids by NMR spectroscopy	74
2.7 Antioxidant capacity of isolated oligostilbenoids.....	75
2.8 Antiproliferative assay in human cell lines.....	75
3. Results and Discussion.....	76
3.1 Purification of grape cane extract by CPC.....	76
3.2 Purificación of the major and minor oligostilbenoids by semi-preparative HPLC-UV.....	83
3.3 Antioxidant capacity of stilbenoids	90
3.4 Antiproliferative assay in human cell lines.....	94
4. Conclusions	97
Acknowledgments	97
References:	98
Supplementary material:.....	105

Capítulo 3: sección 1, C18 core-shell column with in-series absorbance and fluorescence detection for simultaneous monitoring of changes in stilbenoid and proanthocyanidin concentrations during grape cane storage	123
Abstract.....	124
1. Introduction	126
2. Materials and methods.....	129
2.1 Chemicals used	129
2.2 Plant material used.....	130
2.3 Extraction method used.....	130
2.4 Identification of analytes using HPLC-DAD-FL-ESI-MS/MS	131
2.5 HPLC-DAD-FL conditions for quantitative determination of analytes	132
2.6 Calculations	132
3. Results and discussion.....	133
3.1 Identification of analytes using HPLC-DAD-FL-ESI-MS/MS	133
3.2 Chromatographic separation	137
3.3 Quantification of proanthocyanidins and stilbenoids in grape canes	139
3.4. Effect of relative humidity during post-pruning storage on stilbenoid concentrations.....	142
3. 5. Changes in proanthocyanidin levels in canes during post-pruning storage.....	146
4. Conclusions	148
Acknowledgements	149
References	150

Capítulo 3: Sección 2, Hidrólisis alcalina, enzimática y golpe de calor aplicados en sarmientos de vides: evidencias claves que apoyan el origen biosintético de estilbenos monoméricos en sarmientos con guarda post-poda.	158
Resumen:	158
1. Materiales y métodos:	159
1.1. Muestras de sarmientos para hidrólisis:.....	159
1.2. Muestras para monitorear estilbenoides luego de un golpe de calor:	159
1.3. Extracción:	159

1.4. Autohidrólisis :	159
1.5. Hidrólisis enzimática e hidrólisis básica:	159
1.6. Cuantificación de (poli)fenoles por HPLC-DAD-FL	161
2. Resultados y discusión:	161
3. Conclusiones:	163
4. Referencia:	164

Capítulo 4: Profiling of *Vitis vinifera* L. canes (poly)phenols compounds using comprehensive two-dimensional liquid chromatography..... 165

Abstract	166
1. Introduction.	167
2. Materials and methods.	170
2.1. Samples and chemicals.	170
2.2. Instrumentation.	170
2.3. LC×LC separation conditions.	171
2.4. Calculations.	172
2.4.1. Peak capacity	172
2.4.2. Orthogonality	174
3. Results and discussion.	174
3.1 Separation method optimization	176
3.2. Characterization of the (poly)phenolic profile of grapevine canes by HILIC×RP.	184
4. Conclusions	194
Acknowledgements	195
References	196
Supplementary data :	201

Capítulo 5 :Conclusiones finales. 204

Índice de figuras.

Capítulo 1: Introducción

Figura 1: Clasificación general de los (poli)fenoles (Adaptado de: Jackson 2000, Garrido & Borges 2013).	7
Figura 2: A: unidades flavan-3-oles, B: estructuras de una procianidina tipo A y B (Adaptado de Hümmel & Schreier 2008).....	8
Figura 3: A: estructuras de ácidos fenólicos (Adaptado de Garrido & Borges, 2013). B: Representación esquemática que muestra el rol principal de los ácidos hidroxicinámicos en la biosíntesis de polifenoles (Adaptado de El- seedi 2012).....	11
Figura 4: Clasificación de los estilbenoides (Adaptado de Shen et al., 2009).....	12
Figura 5: síntesis de estilbenoides a través de la vía de shikimato. PAL: fenilamonio liasa, C4H: cinamato 4-hidroxilasa, 4CL: 4-coumarato CoA ligasa, STS: estilbeno sintasa, CHS: Chalcona sintasa.	13
Figura 6: Efecto del tiempo de guarda A: aumento de estilbenoides en sarmientos Pinot Noir con 2 meses de guarda a 6 meses a temperatura ambiente, B: aumento de (<i>E</i>)-resveratrol y (<i>E</i>)-piceatannol en sarmientos Pinot Noir almacenados hasta 350 días post-poda a temperatura ambiente. Efecto de la temperatura sobre el incremento de las concentraciones de estilbenoides en sarmientos y el estrés mecánico luego de la poda, A: aumento de estilbenoides en sarmientos almacenados con diferentes longitudes, B: PCR-RT, aumento transcripcional de STS y PAL de sarmientos de 0.5 cm de longitud (Adaptado y Modificado de Gorena et al., 2014, Houillé et al., 2015, Billet et al., 2017)...	25
Figura 7: Esquema gráfico del modo de separación en sistemas hidroestáticos mediante CPC. (Adaptado de Bojczuk et al., 2017).....	27
Figura 8: Conversión de MTT en formazan en test de reducción de tetrazolio. (Adaptado de Riss et al., 2013).	30
Figura 9: Representación esquemática de la separación a través de cromatografía bidimensional para una muestra de 20 compuestos, (*) son compuestos que coeluyen. A y B Cromatografía en una sola dimensión, C Separación en serie con las columnas usadas en A y B, D Separación bidimensional continua (LC x LC), E y F corresponden a cromatografía en donde se seleccionan las fracciones a llevar a una segunda dimensión (LC-LC). (Adaptado de Stoll et al., 2016).....	36

Figura 10: Estrategia analítica propuesta. 41

Capítulo 2: Oligostilbenoids in Pinot Noir Grape Cane Extract: Isolation, Characterization, Antioxidant Capacity and in vitro Anti-proliferative Effect on Cancer Cells

Figure 1: HPLC-DAD-FL chromatograms on the core-shell C18 column. (A): Scale-up extract at 280 and 306 nm. (B): Fluorescence detection at 330 and 374 nm for excitation and emission, respectively. For the peak numbers, see Table 1. 78

Figure 2: Chemical structures of heterodimers isolated from the pilot plant extract of Pinot Noir grape canes, and the proposed fragmentation pathways. 90

Figure S.1: HPLC-DAD-FL chromatogram on core shell C18 column. Pooled fractions by CPC: Fraction 1 (F1), Fraction2 (F2), Fraction 3 (F3), Fraction 4 (F4) and Fraction 5 (F5). Peak number are indicated in table 1. 105

Figure S.2: Chemical structure of stilbenoids isolated from grape canes. 107

Figure S.3: Antioxidant capacity measured by ORAC-FL assay for increased concentrations of oligostilbenoids isolated from grape cane extract: monomeric stilbenoids (A), oligostilbenoids (B), comparison between vitisin B after isolation and vitisin B with presence of second tetramer (C). 121

Capítulo 3, sección 1: C18 core-shell column with in-series absorbance and fluorescence detection for simultaneous monitoring of changes in stilbenoid and proanthocyanidin concentrations during grape cane storage

Figure 1: Schematic diagram illustrating the formation of stilbenoids and proanthocyanidins derived from the phenylpropanoid pathway. Adapted from references 9, 13, 27 and 28. 127

Figure 2: HPLC-DAD-FL quantitative chromatograms for grape cane extracts. Peak numbers are as listed in Table 1. (A) Absorbance at 306 nm, (B) absorbance at 280 nm, (C) fluorescence detection at 330 and 374 nm, and (D) fluorescence detection at 230 and 320 nm. 138

Figure 3: Stilbenoid levels (mg/kg dry weight) as functions of time during grape cane storage at 60% and 70% relative humidity (RH). Grape varieties: PN: Pinot Noir; CS:

Cabernet Sauvignon; TN: Tintorera. Concentrations of (*E*)-piceid as (*E*)-resveratrol equivalents. Error bars correspond to analytical standard deviations. 143

Figure 4: Proanthocyanidin levels (mg/kg dry weight) as functions of time during grape cane storage at 60% and 70% relative humidity (RH). Grape varieties: PN: Pinot Noir; CS: Cabernet Sauvignon; TN: Tintorera. Concentrations of prodelphinidin dimer as procyanidin B1 equivalents. Error bars correspond to analytical standard deviations..... 147

Figure S.1: HPLC-DAD-MS/MS chromatogram for identification of stilbenoids and proanthocyanidins for cane extract. (A) absorbance at 306 nm, (B) absorbance at 280 nm, (C) fluorescence detection at 330 nm and 374 nm, (D) fluorescence detection at 230 and 320 nm..... 154

Figure S.2: HPLC-DAD-FL chromatograms for grape cane extract column I. Peaks number are in table n°1. (A) absorbance at 306 nm, (B) absorbance at 280 nm, (C) Fluorescence detection at 230 and 320 nm..... 156

Figure S.3: Fluorescence spectra obtained in spectrum scan mode for excitation (1) and emission (2) by FL detector for: (A) (*E*)-resveratrol, (B) vitisin B and (C) ampelopsin A. (D) HPLC-DAD-FL chromatograms for ampelopsin A standard. 157

Capítulo 3, sección 2: Hidrólisis alcalina, enzimática y golpe de calor aplicados en sarmientos de vides: evidencias claves que apoyan el origen biosintético de estilbenos monoméricos en sarmientos con guarda post-poda

Figura 1: esquema ilustrativo de las hidrólisis efectuadas en residuos de sarmientos de vides..... 160

Figura 2: Niveles de estilbenoides sin y con procesos hidrolíticos del residuo de extracción de sarmientos de vides Pinot Noir con distintos tiempos de guarda post-poda. Sólo Extr: extracción con etanol: agua (80:20 v/v) asistida con ultrasonido, Au: Autohidrólisis, H. Enz: hidrólisis enzimática, H. Bás: hidrólisis básica. La barra de error corresponde a la desviación estándar de la suma de los estilbenoides. 162

Figura 3: Estilbenoides monitoreados luego de la poda en sarmientos expuestos a un golpe de calor previo a la guarda post-poda a 70% de humedad relativa y 20°C. 163

Capítulo 4: Profiling of *Vitis vinifera* L. canes (poly)phenols compounds using comprehensive two-dimensional liquid chromatography

Figure 1: Chemical structure of some representative polyphenols present in grapevine (*Vitis vinifera* L.) canes. A) Resveratrol tetramer (Vitisin A); B) Procyanidin trimer digallate; C) Prodelphinidin tetramer (3(E)C-(E)GC)..... 175

Figure 2. First dimension chromatograms (280 nm) corresponding to the separation of the polyphenols found in a grapevine cane extract under optimum conditions for each column. For separation conditions. 179

Figure 3. Two-dimensional plots and orthogonality values (A_0) obtained using each first dimension column studied (A, diol; B, PEG; C, ZIC-HILIC) coupled to the partially porous C_{18} column in the second dimension under optimized conditions... ..183

Figure 4: Two-dimensional HILIC \times RP plots (280 nm) corresponding to the (poly)phenolic profile of Pinot Noir (A) and Cabernet Sauvignon (B) grapevine canes under optimum separation conditions..... 191

Figure S1. MS spectra and MS/MS fragmentation patterns as well as tentatively proposed chemical structure of A) resveratrol heptamer (peak 47), B) procyanidin trimer digallate (peak 67), and C) prodelphinidin tetramer trigallate (peak 72) and its alternative identification D) prodelphinidin pentamer monogallate (peak 72).....202

Índice de Tablas.

Capítulo 1: Introducción

Tabla 1: Resumen de la industria vitivinícola en Chile.....	2
Tabla 2: destino habitual de los residuos de la industria vitivinícola y alternativas estudiadas para su reciclaje.....	4
Tabla 3: Efectos beneficiosos sobre la salud de las proantociandinas.	9
Tabla 4: Efectos beneficiosos sobre la salud de estilbenoides.	15
Tabla 5: Concentración de compuestos flavonoides reportados en sarmientos.	18
Tabla 6: ácidos fenólicos cuantificados en sarmientos.	19
Tabla 7: Concentración de estilbenoides en residuos de la industria vitivinícola (Modificado de Gorena et al., 2015).....	20
Tabla 8 : Concentraciones de oligoestilbenoides en sarmientos de vides viníferas.	22
Tabla 9: Citotoxicidad de estilbenoides (IC ₅₀) en líneas celulares cancerosas humanas a través del ensayo MTT.	31

Capítulo 2: Oligostilbenoids in Pinot Noir Grape Cane Extract: Isolation, Characterization, Antioxidant Capacity and in vitro Anti-proliferative Effect on Cancer Cells

Table 1: HPLC-DAD-QToF of oligostilbenoids in the different fractions of CPC separation.....	80
Table 2: ¹ H, ¹³ C and HMBC data for scirpusin A and its structural isomer in acetone-d ₆ and methanol-d ₄	85
Table 3: TEAC _{CUPRAC} , ABTS and ORAC-FL for oligostilbenoids isolated.	92
Table 4: IC ₅₀ values for isolated stilbenoids, whole cane extract and synthetic etoposide on different cell lines expressed in µg mL ⁻¹ and µM (in parenthesis).	96
Table S.1: Collected fractions by CPC of oligostilbenoids from 14 grams of Pinot Noir grape cane extract.	106
Table S.2: NMR data in acetone d ₆ for vitisin B 500 MHz and ampelopsin A at 500 MHz.	108
Table S.3: H-NMR data in acetone-d ₆ for isorhapontigenin at 500 MHz.	111

Table S.4: NMR data for (<i>E</i>)- δ -viniferin at 500 MHz and (<i>E</i>)- ω -viniferin at 400 MHz in acetone- d_6 .	112
Table S.5 : NMR data for pallidol at 500 MHz in acetone- d_6 .	115
Table S.6: NMR data for (<i>E</i>)- <i>trans-cis</i> -miyabenol C at 500 MHz.	117
Table S.7: Calibration curves for TEAC _{cuprac} , TEAC _{ABTS} and ORAC-FL using TROLOX	120
Table S.8: HPLC-DAD-MS/MS for isolated vitisin B after freeze drying and storage at -20°C in darkness and compared with vitisin B repurified.	122

Capítulo 3, Sección 1: Hidrólisis alcalina, enzimática y golpe de calor aplicados en sarmientos de vides: evidencias claves que apoyan el origen biosintético de estilbenos monoméricos en sarmientos con guarda post-poda

Table 1: Identity assignation of phenolic compounds in grape cane extract using HPLC-DAD-FL-MS/MS	135
Table 2: Chromatographic parameters calculated for development method in core shell column.	139
Table 3: Calibration curves and limits of detection (LOD) and quantification (LOQ) for stilbenoids and proanthocyanidins using DAD and fluorescence detection.	141
Table 4: Interday and intraday repeatability for stilbenoid and procyanidin concentrations in Pinot Noir grape canes (n= 3).	142
Table S.1: Chromatographic parameters calculated for a secondary gradient for grape cane extract development in a second C-18 core-shell column (150 x 4.8 mm, 2.6 μ m of particle size, 1.6 μ m of nucleus and 12% of carbon load).	155

Capítulo 4: Profiling of *Vitis vinífera* L. canes (poly)phenols compounds using comprehensive two-dimensional liquid chromatography

Table 1. Comprehensive two-dimensional method parameters applied to the profiling of (poly)phenolic compounds from grapevine canes.	178
Table 2: Main polyphenols detected in the grapevine canes samples using the optimized HILICxRP-DAD-MS/MS method. (E)C, (epi)catechin; (E)GC, (epi)galocatechin; (E)GCG, (epi)galocatechin gallate.	187

Resumen:

Los sarmientos de vides son residuos lignocelulósico que se producen anualmente en los viñedos durante la poda invernal. Debido a los altos niveles de (*E*)-resveratrol, se han propuesto a los sarmientos como una fuente de estilbenoides. Debido a la carencia de estándares de estilbenoides oligoméricos, éstos se purificaron a través de CPC y HPLC-semi.preparativa desde un extracto de sarmientos de Pinot Noir, obteniéndose 12 estilbenoides: (*E*)- ϵ -viniferina, (*E*)-resveratrol, (*E*)-piceatanol, ampelopsin A, vitisina B, (*E*)- δ -viniferina, (*E*)- ω -viniferina, pallidol, scirpusina A, isorapontigenina, (*E*)-*trans-cis*-miyabenol C y un nuevo estilbenoide, denominado iso-scirpusina A. La identidad de los oligoestilbenoides se confirmó a través de HPLC-Q-Tof y mediante $^1\text{H-NMR}$, $^{13}\text{C-NMR}$, $^1\text{H-HCOSY}$, $^1\text{H-}^{13}\text{C-HSQC}$. Los oligoestilbenoides aislados presentaron una mayor capacidad antioxidante *in vitro* a través de ORAC-FL que (*E*)-resveratrol. (*E*)-piceatannol exhibe efecto *in vitro* antiproliferativo a través del ensayo MTT sobre líneas celulares cancerosas humanas (SK-MES-1, AGS, J82), este efecto no es apreciable sobre la línea celular humana normal (MRC-5). Ampelopsina A muestra un efecto antiproliferativo mayor que (*E*)-resveratrol en la línea celular J82 de cáncer de vejiga.

Sorprendentemente, el incremento de los estilbenoides en sarmientos es gatillado por la poda. La magnitud de dicho incremento en el sarmiento metabólicamente activo depende de las condiciones en la guarda post-poda. Para evaluar la evolución de los estilbenoides así como de las procianidinas, una familia de (poli)fenoles asociados con efectos beneficiosos para la salud, se desarrolló y aplicó en tres cultivares de vides un método HPLC-DAD-FL para la cuantificación rápida, selectiva y sensible, empleando tecnología de columna de núcleo sólido y un método HPLC-DAD-FL-MS/MS para la identificación. A 60 % de humedad relativa, se obtiene el doble de (*E*)-resveratrol para el mismo cultivar en

comparación a los sarmientos que se almacenaron en 70 % de humedad relativa. (-)epicatequina disminuye sus niveles durante el almacenamiento post-poda hasta un 75%. por lo que la humedad relativa es una variable importante a considerar en el almacenamiento post-poda de los sarmientos, además del tiempo de guarda, temperatura y longitud del trozo de sarmiento.

Explorando nuevas opciones con mayor poder de separación, se desarrolló y optimizó un método cromatográfico bidimensional (HILIC x RP)-DAD-MS/MS, obteniéndose con una buena separación, capacidad de peak (842) y ortogonalidad ($A_0 = 78\%$). Se separaron 81 compuestos, entre los que destacan estilbenoides altamente polimerizados así como prodelfinidinas y procianidinas oligoméricas reportadas por primera vez en sarmientos de vides.



Agradecimientos:

FONDECYT 1150721, FONDEQUIP Grant EQM150025, Becas Doctorado Nacional CONICYT, PFB-27 y CORFO Grant 14 IDL2-30156.

Capítulo 1: Introducción.



1.1. Industria vitivinícola en Chile.

En el año 2015, el área correspondiente a plantaciones de vides en el mundo alcanzó los 7.5 millones de hectáreas, produciéndose 7.5 millones de toneladas de uva. El 20 % de esta producción corresponde al continente americano. En Chile hay plantadas 211 mil ha con vides, las que producen 3.1×10^5 toneladas de uvas y 10.1 millones de hectólitros de vino (OIV 2016).

Las plantaciones de vides en Chile abarcan desde la región de Tarapacá hasta Los Lagos (Tabla 1). El 71 % de la superficie plantada corresponden a vides para vinificación, un 24 % para uva de mesa y sólo el 4 % para producción de pisco. La mayor superficie de vides para vinificación se encuentra en las regiones del Maule (38 %) y de O'Higgins (33 %). La producción de vino en Chile se concentra en las regiones Metropolitana (1.3 mhl), O'Higgins (3.2 mhl) y del Maule (4.6 mhl). En el año 2016, las exportaciones de vinos de Chile significaron 1845 millones de USD de ingresos para el país, por lo que es una actividad agro-económica relevante (Ministerio de Agricultura 2017).

Tabla 1: Resumen de la industria vitivinícola en Chile.

Región	Superficie de vides para vinificación 2015 (ha)			Producción de vino 2016 (mhl)
	Blancas	Tintas	Total	
Atacama	44	13	57	0.002
Coquimbo	1636	1654	3290	0.324
Valparaíso	6411	3650	10061	0.190
Metropolitana	1700	11358	13058	1.329
Lib. Bernardo O'Higgins	6752	39663	46414	3.225
Maule	14775	39063	53838	4.670
Biobío	5009	10098	15107	0.404
Los Lagos	16	9	25	0.000
Total	36375	105544	141850	10.144

mhl: millones de hectólitros, ha: hectáreas. Adaptado de Boletín del Vino, Ministerio de Agricultura, 2017.

En Chile, de las 141.850 há plantadas con vides para vinificación un 30 % corresponde a Cabernet Sauvignon, seguido de Sauvignon blanc (11 %), Merlot (9 %), Chardonnay (8 %), País (9 %), Carmènère (8 %) y Pinot Noir (3 %). En cuanto a la producción de vino con denominación de origen, el mayor volumen corresponde a Cabernet Sauvignon (33.3%), seguido por Sauvignon Blanc (13.5%) y Merlot (12.6%) (Ministerio de Agricultura 2017).

1.2. Alternativas de manejo de residuos de la industria vitivinícola.

El proceso para la elaboración de vino incluye variadas etapas, en las cuales se generan sub-productos o residuos. El escobajo, la raspa del racimo sin uva, corresponde al 14 % del peso de los residuos sólidos durante el proceso de vinificación, mientras que el orujo, una mezcla de pieles, semillas y escobajos residuales corresponden al 60%. Las lias del vino contienen etanol, ácido tartárico, además de células de levaduras, que corresponden entre el 2 – 6 % del vino producido. Los sarmientos, un residuo lignocelulósico, se generan en las podas anuales de los viñedos en el invierno. De acuerdo al tipo de poda y el vigor de la vid, se pueden generar 1.4 - 4.2 ton por hectárea. (Spigno et al., 2017).

Los residuos de la industria vitivinícola son considerados como desechos de alimentos así como sub-productos, dependiendo de la interpretación de las definiciones actuales (Spigno et al., 2017). La directiva de la Unión Europea 2008/98/EC indica que la prevención en la generación de residuos debe ser la primera prioridad del manejo de residuos y que la reutilización y reciclaje debe preferirse antes de recobrar energía desde el residuo (Sánchez-Gómez et al., 2014). Además, la elaboración de vino genera aguas residuales contaminantes debido a su alto contenido en materia orgánica, salinidad, metales pesados y en N, P, K.

estas aguas requieren tratamiento adicional antes de ser liberadas al medio ambiente (Oliveira & Duarte 2016., Spigno et al., 2017).

Diversas estrategias han sido estudiadas para su posible implementación para un manejo de los residuos, incorporando conceptos de sustentabilidad y el aprovechamiento integral. En la tabla 2 se muestra el principal destino de los residuos o también denominados subproductos de la industria vitivinícola y las posibles alternativas de manejo estudiadas.

Tabla 2: destino habitual de los residuos de la industria vitivinícola y alternativas estudiadas para su reciclaje.

Residuo	Manejo tradicional	Alternativas de uso	Referencias
Orujo	-destilación -agentes colorantes -incineración -alimento para animales	- extracto antioxidante -aplicaciones para comida/ fibra antioxidante -biomasa para la producción de energía	-Antoniolli et al., 2015. -Lavelli et al., 2016. -Romo-Sánchez et al., 2015. -Schönnenbeck et al 2016.
Semillas de orujo	-recuperación de aceite - incineración	-aplicaciones en alimentos -extracción de antioxidantes	- Kim et al., 2014, Correddu et al., 2015. -Maier et al., 2009.
Escobajo	-compostaje -alimentos para animales -combustión -enterrados en el viñedo	-substrato para fermentación -biomasa para la producción de energía. -obtención de compuestos bioactivos y antioxidantes. -carbón activado.	-Spigno et al., 2013. -Amendola et al, 2012.
Lias de vino	-Destilación -extracción de ácido tartárico -agentes colorantes -suplemento	-extracción de antioxidantes -aplicaciones en alimentos -extracción de nutrientes/subtrato de fermentación	-Delgado de la torre et al., 2015, Dimou et al., 2015, Giacobbo et al 2015, Naziri et al 2016, Tao et al., 2014. - Sharma et al., 2015

	natural		-Dimou et al., 2015, Pérez.Bibbins et al., 2015.
Sarmientos	-depositados en el viñedo -incinerados	-antioxidantes / extractos bioestimulantes/actividad antifungica -saborizantes -remoción de compuestos tóxicos -biomasa para la producción de energía/ fracción lignocélulosa	- Romain et al 2012, Gorena et al., 2014, Rahja et al 2015, Sánchez-gómez et al., 2014, Sánchez-Gómez et al 2016a, Houillé et al., 2014. -Delgado de la Torre et al 2014, Sánchez-Gómez et al 2016b. - Karaoglu et al., 2010, Vecino et al., 2015. -Argun & Onaran 2015, Buratti et al., 2015, Cotana et al., 2015, San José et al 2013, Spinelli et al 2012.

Adaptado de Spigno et al., (2017).

La generación de la mayoría de los desechos vitivinícolas no se puede evitar, pero si deben aprovecharse integralmente, pues son generados en altas cantidades y además pueden impactar negativamente al medio ambiente. Por ello es imperativo buscar alternativas sustentables para su manejo. Una de las estrategias que ha suscitado atención es la posibilidad de obtener o recuperar compuestos bioactivos desde los residuos, lo que conlleva una valorización de los residuos y disminuye el impacto negativo que producen (Texeira et al., 2014, Spigno et al., 2017). Los compuestos bioactivos son principalmente (poli)fenoles apreciados en la industria cosmética, farmacéutica y en el sector nutracéutico. La cantidad posible de recuperar así como la proporción relativa de estos compuestos bioactivos en los residuos está condicionada por varios factores, como la variedad de la vid, condiciones climáticas, procedimientos de fertilización, propiedades del suelo, entre otros.

Por otro lado, el proceso específico de producción de vino además del tiempo entre la generación del residuo y el proceso de extracción de compuestos bioactivos, así como las características del reciclaje y el procedimiento de recuperación de los (poli)fenoles, tienen un directo impacto en su concentración final, y por ende en el potencial del residuo como fuente de fitoquímicos bioactivos (Texeira et al 2014).

1.3. (Poli)fenoles bioactivos en *Vitis vinífera*.

Los (poli)fenoles son metabolitos secundarios en las plantas, son antioxidantes putativos, además confieren propiedades organolépticas. Pueden clasificarse de acuerdo a su estructura en **flavonoides** y **no flavonoides**.

1.3.1. Flavonoides:

Poseen una estructura base de 15 carbonos, que comprende dos anillos aromáticos unidos a una cadena de tres carbonos ($C_6-C_3-C_6$) que puede ser o no parte de un anillo. Se clasifican de acuerdo al grado de oxidación que puede tener el anillo pirano. Los flavonoides comprenden a las **flavonas**, **flavonoles**, **flavanonas**, **flavononoles**, **flavanes**, **flavanoles**, **antocianos** y **antocianidinas**. Se incluyen además las chalconas y las dihidrochalconas. Debido a la alta complejidad de las estructuras existen otras clasificaciones, dependiendo si están conjugadas o no (Garrido & Borges 2013).

Clasificación de (Poli)fenoles

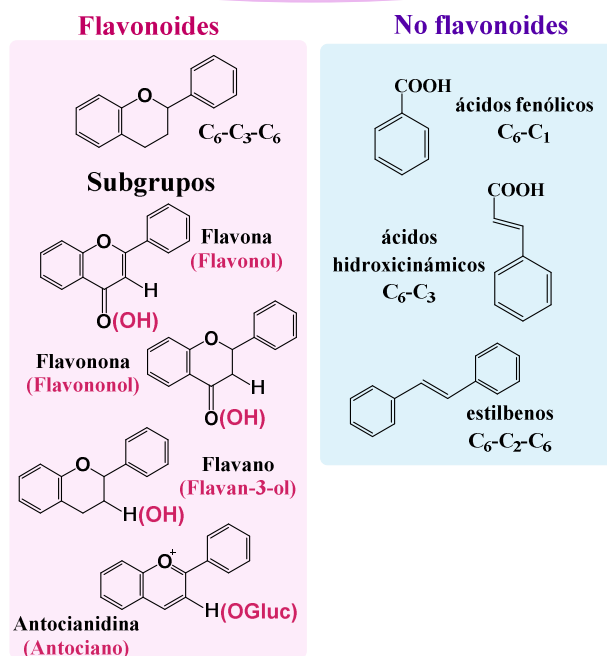


Figura 1: Clasificación general de los (poli)fenoles (Adaptado de: Jackson 2000, Garrido & Borges 2013).

1.3.2. Proantocianidinas:

Las proantocianidinas (**PAC**) son flavanoles que pueden existir en forma monómerica u oligomérica. Fueron descubiertos por Jacques Masquelier en la década de 1940, quien los confundió con vitaminas (De La Iglesia et al., 2010). La clasificación depende de las unidades monómericas, del grado de polimerización y del tipo de enlace interflavan. Las unidades monómericas (flavan-3-ol) y el patrón de hidroxilación para cada proantocianidina se muestran en la figura 2. Las proantocianidinas más abundantes son las procianidinas constituidas por unidades de (epi)catequina y las menos abundantes son aquellas constituidas por unidades de (epi)afzelequina o (epi)galocatequina, llamadas properlargonidinas y prodelfinidinas respectivamente. Las unidades monómericas de las procianidinas pueden poseer la configuración R y S en la unión C₂-C₃, por lo que hay 4 monómeros posibles, que pueden adquirir la configuración *cis* o *trans*. Las unidades flavan-3-ol pueden poseer una unidad acilo o glicosilo. La sustitución más común es ácido

gálico, para formar 3-O-galatos. Las uniones en los enlaces interflavan clasifican a las PAC como B o A. Si la unión es de $C_4 \rightarrow C_8$ o $C_4 \rightarrow C_6$ son tipo B, mientras que si se forma un enlace éster adicional entre C_2 y C_7 es tipo A (Hümmer & Schreier 2008, De la Iglesia et al 2010).

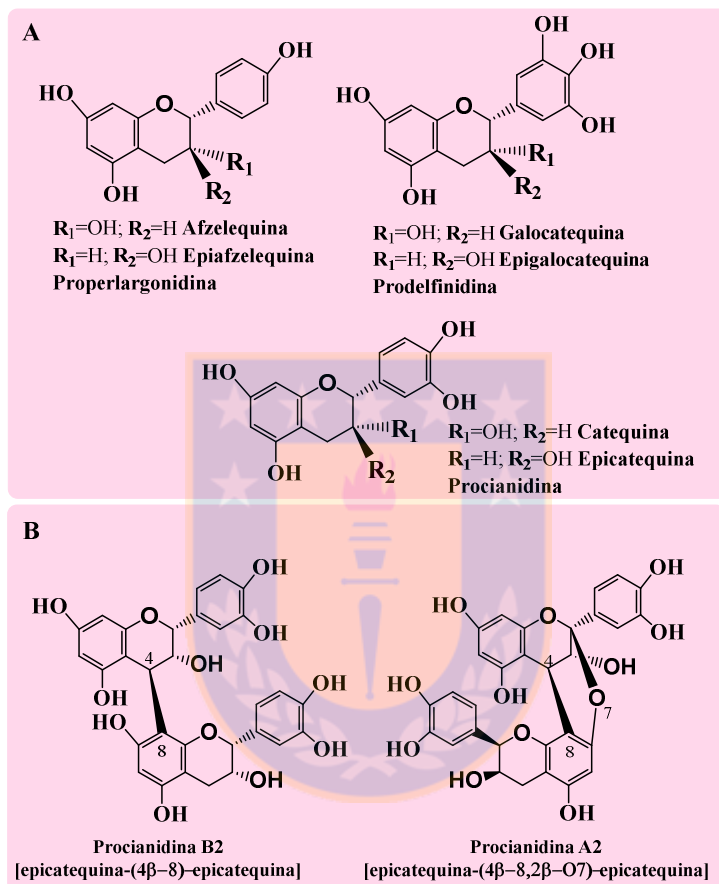


Figura 2: A: unidades flavan-3-oles, B: estructuras de una procianidina tipo A y B (Adaptado de Hümmer & Schreier 2008).

Las proantocianidinas poseen una enorme diversidad estructural debido a la naturaleza de sus monómeros y a los altos grados de polimerización que se pueden encontrar. En frutas se ha observado procianidinas de grado de polimerización de hasta 190. En matrices alimentarias son más comunes las proantocianidinas de tipo B que las de tipo A (Neilson et al 2016).

Las proantocianidinas afectan el sabor, apariencia y el valor nutricional de los alimentos (Ou & Gu 2014). Se han reportado variados efectos positivos sobre la salud. Presentan citotoxicidad frente a diversos tipos de tumor (cáncer de próstata, seno y colon), son agentes quimiopreventivos en el caso de cáncer oral y de próstata, disminuyen el efecto de las infecciones bacterianas debido a que poseen actividad anti-adhesiva, además de disminuir los mediadores de inflamación (De La Iglesia 2010). Algunas de las propiedades atribuidas a las proantocianidinas se resumen en la tabla 2.

Tabla 3: Efectos beneficiosos sobre la salud de las proantocianidinas.

Enfermedad	Efecto	Referencia
Cardiovascular	-Antitrombótico - Disminuye la respuesta anti inflamatoria	-Quiñonez et al., 2013 -De La Iglesia 2010, - Martinez-Micaelo 2011.
Diabetes	-Mejora la homeostasis de la glucosa, modifica la insulinemia y protege a las células β pancreáticas del estrés oxidativo -Disminuye la interacción de los productos finales de glicosilación con su receptor (RAGE). -Disminuye los efectos de resistencia a la insulina debido a que aumenta la expresión de receptores de insulina y transportadores de glucosa.	- Castell-Auví et al., 2012. -Yang & Chan 2017 -De La Iglesia et al., 2010.
Cáncer	-Promueve la apoptosis, disminuye la proliferación y angiogénesis. - Promueve la citotoxicidad de agentes usados para tratar el cancer	- De la Iglesia et al., 2010. - Tyagi et al., 2013. - Mao et al., 2016. -Zhao et al 2013.
Infección bacteriana	-Disminuye los efectos de los mediadores de inflamación y la actividad antiadhesiva	- De La Iglesia et al., 2010

Los efectos de las proantocianidinas son variados así como los mecanismos y vías de señalización en las que intervienen. La absorción de las procianidinas está influenciada por su grado de polimerización. Se absorben en su forma intacta hasta tetrámeros en el intestino delgado (10% como (-)-epicatequina equivalente), mientras que las de grado polimerización mayor son degradadas por la microflora del intestino a fenilvalerolactonas y ácidos fenólicos, siendo los responsables de los efectos bioactivo. Por lo tanto, se puede deducir que los efectos saludables *in vivo* se deben a las procianidinas biodisponibles así como a los metabolitos generados por la microflora del intestino (Ou & Gu 2014).

1.4. No flavonoides:

En el grupo de los no flavonoides se encuentran los ácidos fenólicos que comprende a los ácidos benzoicos (C_6-C_1) y los ácidos hidroxicinámicos (C_6-C_3), y los estilbenoides ($C_6-C_2-C_6$).

1.4.1. Ácidos fenólicos:

Los ácidos fenólicos se dividen en: ácidos hidroxibenzoicos y ácidos hidroxicinámicos (Figura 3). Entre los ácidos hidroxibenzoicos destacan el protocatechuico, vanílico, siríngico y gálico. Este último es un precursor de los taninos hidrolizables (Garrido & Borges, 2013). Los ácidos hidroxicinámicos más comunes son orto, meta y para coumárico, cinámico, cafeico, ferúlico y sinápico. Los (poli)fenoles son sintetizados a partir de vía fenilpropanoide. Esta ruta se subdivide según la enzima que actúe sobre el sustrato para la síntesis de (poli)fenoles de distinta naturaleza. Como se observa en la figura 3, los ácidos hidroxicinámicos poseen un rol relevante y central como precursores de varias familias de (poli)fenoles, incluyendo los estilbenoides (El-Seedi 2012).

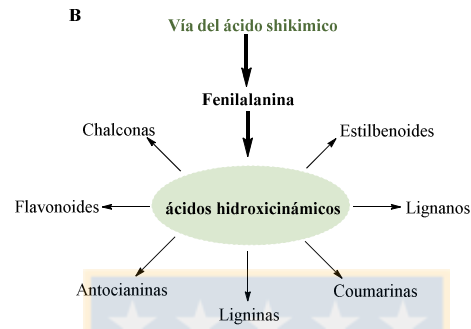
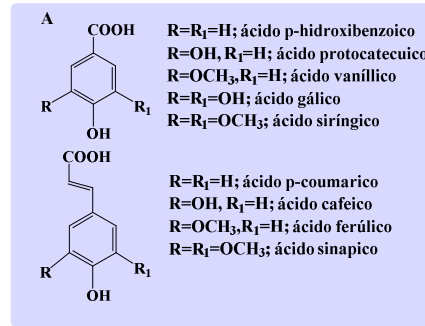


Figura 3: A: estructuras de ácidos fenólicos (Adaptado de Garrido & Borges, 2013). B: Representación esquemática que muestra el rol principal de los ácidos hidroxicinámicos en la biosíntesis de polifenoles (Adpatado de El- seedi 2012).

1.4.2. Estilbenoides:

Los estilbenoides son metabolitos secundarios presentes en un acotado grupo de plantas, entre las que se encuentra en la familia botánica Vitaceae. En esta familia, que incluye 16 géneros, sólo ocho contienen estilbenoides: *Ampelopsis*, *Cayratia*, *Cissus*, *Cyphostemma*, *Muscadinia*, *Parthenocissus* y *Vitis* (Rivière et al., 2012). Los estilbenoides pueden existir en forma monomérica y oligomérica. El estilbenoide más popular es el resveratrol (3,5, 4'-tri-hidroxi-estilbeno), caracterizado por un núcleo 1,2-difeniletileno (figura 4) (Jeandet et al., 2010, Rivière et al., 2012, Keylor et al., 2015). Existen dos formas de clasificar estructuralmente a los estilbenoides. La propuesta por Sotheeswaran en 1993, en que

clasificaba a los oligostilbenoides en dos grupos, A y B. El grupo A posee un heterociclo oxigenado con una estructura de 2-*trans*-arilo-2,3 dihidrofurano, mientras que el grupo B carece del heterociclo oxigenado. Esta clasificación limita a los estilbenos oligoméricos. Una clasificación más reciente, útil para los oligómeros, los clasifica en cinco grupos: aquellos basados en resveratrol, isorhapontigenina, piceatanol, oxiresveratrol y de resveratrol con oxiresveratrol (Shen et al., 2009) (figura 4). Los estilbenoides presentes en Vitaceae son polymerizaciones complejas de resveratrol, exceptuando scirpusina A, que es un dímero conformado por una unidad de piceatanol y resveratrol (Rivière et al., 2012).

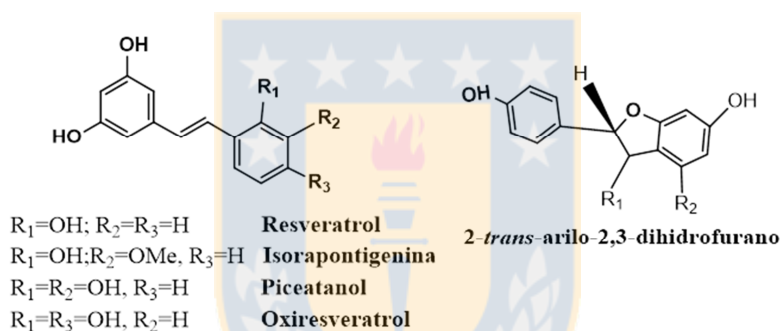


Figura 4: Clasificación de los estilbenoides (Adaptado de Shen et al., 2009).

Si bien los estilbenoides son sintetizados a través de una vía que comparte con los ácidos hidroxicinámicos y flavonoides (Figura 5), es posible inducir su síntesis a través de estímulos como irradiación de luz UV, trauma físico o un ataque de patógenos. Estilbeno sintetasas (STS) es el complejo enzimático responsable de la producción de (*E*)-resveratrol, el que sufre modificaciones estructurales generando monómeros modificados o generando oligómeros. Estas derivatizaciones o modificaciones confieren a los estilbenoides nuevas propiedades anti-fúngicas más potente que el (*E*)-resveratrol. La primera vez que se describió a los estilbenoides en plantas, fue en la década del 70 por Langcake & Price, quienes describieron lesiones fluorescentes en hojas de *Vitis vinífera*, luego de una

infección con patógenos de *Botrytis cinerea* (Moho gris) y *Plasmopora viticola* (Oídio) (Keylor et al., 2015).

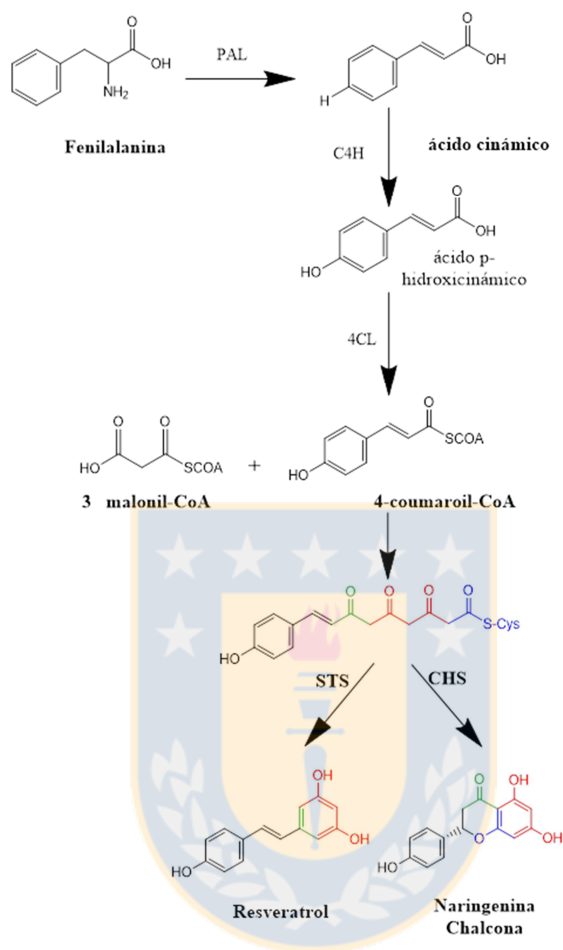


Figura 5: síntesis de estilbenoides a través de la vía de shikimato. PAL: fenilamonioliasa, C4H: cinamato 4-hidroxilasa, 4CL: 4-coumaroil-CoA ligasa, STS: estilbeno sintasa, CHS: Chalcona sintasa.

Si bien los estilbenoides pueden ser constitutivos, también son inducibles luego de un estímulo, por lo cual se consideran fitoalexinas, término propuesto en 1940 por Müller & Börger. Una fitoalexina es una sustancia defensiva de bajo peso molecular producida por

plantas en respuesta a una infección (Jeandet et al., 2010). Resveratrol a veces no se considera *per sé* una fitoalexina, sino como un precursor de ellas (Keylor et al., 2015).

Actualmente existen más de 300 oligómeros de estilbenoides identificados. Esto es debido al avance de las técnicas de espectroscopia RMN, incluyendo las bidimensionales (COSY, HSQC, HMBC) e IR y HPLC con detección UV-vis o DAD y espectrometría de masas. Estas técnicas combinadas permiten descifrar la configuración de estructuras generalmente difíciles de resolver. Sin embargo, en oligoestilbenoides complejos, las constantes de acoplamiento vecinales son pobres predictores de configuración relativa. Es por ello que a veces se requiere NOE(SY) y ROESY. Actualmente la configuración absoluta de oligoestilbenoides sigue siendo un desafío (Keylor et al., 2015).

En Vitaceae, los oligómeros con un anillo 2,3-dihidrobenzohidrofurano son comunes y generalmente se denominan vitisina. Corresponden a dímeros de (*E*)-resveratrol. (*E*)- ϵ -víniferina es el mayor constituyente en *Vitis* y posible intermediario para generar oligómeros (Rivière et al., 2012). En la familia Vitaceae, la diversidad de oligómeros va desde dímeros hasta hexámeros (Rivière et al., 2012).

(*E*)-resveratrol captó particularmente la atención debido a la “paradoja francesa”, un término acuñado en 1992 por Renaud & Lorgeril, que relacionaba los datos epidemiológicos de la población francesa que poseía una baja incidencia de enfermedades coronarias, a pesar una dieta alta en grasas saturadas. Para explicar la discrepancia, se propuso que el consumo moderado de vino (57% del consumo total de alcohol en Francia corresponde a vino), podría disminuir la incidencia de estas enfermedades en la población (Catalgol et al., 2012). En 1992 Siemann & Creasy reportaron concentraciones significativas de (*E*)-resveratrol en vino tinto. Esto suscitó atención debido a que es el mismo principio encontrado en medicina tradicional china y japonesa para la prevención y

tratamiento de enfermedades cardiovasculares (*Polygonum cuspidatum* y *Veratrum grandiflorum*) (Catalgol et al 2012., Gambini et al., 2015, Keylor et al., 2015). La relación entre un compuesto bioactivo y enfermedad crónica no transmisible es relevante, debido a que implica que el estilo de vida, principalmente la dieta, incida favorablemente sobre la salud.

Los estilbenoides han sido asociados con efectos *in vitro* e *in vivo* para la prevención y disminución de efectos en diversas enfermedades, como cáncer, diabetes, neurodegenerativas, VIH (Delmas et al., 2011, Catalgol et al., 2012, Pflieger et al., 2013, Giovanelli et al 2014., Xue et al., 2014).

Además se ha reportado un efecto mimético a la restricción calórica (Timmers et al., 2011). En la tabla 3 se resumen algunos de los efectos de (*E*)-resveratrol y algunos oligoestilbenoides. La evidencia sugiere que los estilbenoides ejercen principalmente sus efectos interfiriendo con las vías o cascadas de señalización o a través de vías epigenéticas, en vez de alguna inhibición de alguna enzima diseñada para un propósito específico (Keylor et al., 2015).

Tabla 4: Efectos beneficiosos sobre la salud de estilbenoides.

Enfermedad	Efecto	Referencia
Cáncer	-Resveratrol y algunos oligómeros afectan a los factores de transcripción y vías de señalización celular. -Regulación del ciclo celular e inducción de apoptosis.	-Catalgol et al., 2012, Xue et al., 2014, Espinoza et al., 2017.
Enfermedades de transmisión sexual	Virus de inmunodeficiencia Humana (VIH) -Agentes activos <i>in vitro</i> para contrarrestar los efectos de la integrasa retroviral (HIV-1). Virus del papiloma Humano (VPH) -Inhibición de oncoproteína HPV-16 e inducción de apoptosis.	-Pflieger et al., 2013, Chan et al., 2017. -Abhijit et al., 2016.

Cardiovascular	-Promueve la agregación plaquetaria, proliferación de células endoteliales, diferenciación de fibroblastos cardiacos, vasodilatación por producción de óxido nítrico e inhibición de la angiotensina II produciendo efectos anti-hipertensivo.	-Catalgol et al., 2012, Bonnefont-Rouselot et al., 2016.
Neurodegenerativa	Enfermedad de Alzheimer -Disminuye la producción de péptido β amiloide, inhibe la β -secretasa y la generación de intermediarios reactivos de oxígeno, además de la agregación del péptido α/β Enfermedad de Huntington - Evita la pérdida de la membrana mitocondrial, aumentan SIRT-3 mitocondrial.	- Tristan et al., 2011, Catalgol et al., 2012. -Fu et al., 2012.
Diabetes y Obesidad	Diabetes tipo 1 -Disminuye los niveles de glicemia y aumenta los niveles de insulina y posee un efecto protector sobre las células β pancreática. Diabetes tipo 2 -Efecto pleiotrópico en distintos tejidos disminuyendo la resistencia la insulina y aumenta los tiempos para las alzas de glucosa luego de la ingesta. Obesidad - Induce cambios metabólicos en humanos obesos imitando los efectos de la restricción calórica.	-Szkudelski & Szkudelska 2016, Berman et al., 2017. -Timmers et al., 2011.

Resveratrol se encuentra en su forma *cis* o *trans* de manera constitutiva, sin embargo la isoforma *trans* es la mayoritaria. Es posible la isomerización de la isoforma *trans* a *cis* cuando es expuesto a luz UV (254 nm, 366 nm) o luz solar. Resveratrol en ambas isoformas posee una baja solubilidad en agua (<0.05mg/mL). Una forma de aumentar su solubilidad es con etanol (50 mg/L) o DMSO (16 mg/mL) (Delmas et al., 2010). Debido a su naturaleza lipofílica la absorción de (*E*)-resveratrol depende de la forma de administración así como de la matriz en la que esta contenida. A pesar de la pobre biodisponibilidad *in vitro*, (*E*)-resveratrol posee una alta eficacia *in vivo*.

Estudios *in vitro* han demostrado que el 90% de (*E*)-resveratrol libre se une a lipoproteínas (LDL), además de que puede unirse a albuminas. Luego de ingerir resveratrol, éste se puede encontrar en tres formas en el plasma: glucuronidado, sulfatado o libre. A nivel intestinal, es absorbido por difusión pasiva o formando complejos con los transportadores de membranas, las integrinas. Resveratrol también interactúa con ácidos grasos, generando un ambiente favorable para la unión de resveratrol libre. Generalmente son usados como vectores por las interacciones específicas con los transportadores de transmembrana en el hígado, donde ocurre la metabolización del resveratrol. La excreción urinaria de metabolitos de (*E*)-resveratrol radiomarcado demostró que el 75 % de (*E*)-resveratrol administrado de forma oral u intravenosa fue absorbido, lo cual es inusualmente alto para un compuesto con pobre solubilidad en agua (Gambini et al., 2015).

1.5. Sarmientos como fuente de compuestos bioactivos.

La poda de las vides es un evento estacional. Su relevancia se debe a que afecta la forma y el tamaño de la vid, contribuyendo en el balance entre la parte vegetativa y la frutal, y por consecuencia la cantidad y la calidad de la producción de uva (Çetin et al., 2011, Sánchez-Gómez et al., 2017). Independiente de la variedad de vid, los sarmientos se componen principalmente de hemicelulosa (68%), lignina (20%) y proteínas (5%). Los componentes minoritarios en sarmientos corresponden a lípidos y a moléculas de bajo peso molecular como estilbenoides, flavonoides y ácidos fenólicos (Sánchez-Gómez et al., 2017).

1.5.1. Flavonoides en sarmientos:

Las concentraciones reportadas de flavonoides en sarmientos se resumen en la tabla 4. En ellos se ha reportado flavonoles, particularmente quercetina, morina y rutina. Mediante

HPLC-MS/MS se ha identificado quercetina-O-glucósido (Püssa 2006). Solamente se ha cuantificado una flavona, luoteolina. Unidades flavan-3-ol como (+)-catequina y (-)-epicatequina se han descrito en sarmientos (Püssa et al., 2006, Çetin et al., 2011, Lambert et al 2013).

Tabla 5: Concentración de compuestos flavonoides reportados en sarmientos.

Flavonoides	Compuesto	Concentración (mg/kg)	Referencia.
Flavonol	Morina	21.8-98.2	Zhang et al., 2013
	Quercetina	50.32-88.0	Zhang et al., 2013
	Rutina	49.7-90.4	Zhang et al., 2013
Procianidinas	Catequina	400-7400	Delgado-Torre et al., 2012
		600-1000	Püssa et al., 2006.
		0.8-2.89	Çetin et al., 2011.
		306.8-776.1	Zhang et al., 2013
	76.4-402.2	Sánchez-Gómez et al., 2014	
Epicatequina	600-1300	Püssa et al., 2006.	
	0.6-1.1	Çetin et al., 2011.	
	402.5-656.9	Zhang et al., 2013	
	62.9-217.7	Sánchez-Gómez et al., 2014	
Flavona	Luoteolina	8.4×10^{-3} - 0.7×10^{-2}	Çetin et al., 2011.

La diferencia de los rangos de las concentraciones de los compuestos flavonoides presentes en sarmientos pueden deberse a que no todos están reportados en base seca, el tipo de cultivar y el método de extracción.

Usualmente se consideran las semillas de uva y las que provienen del orujo como fuente de procianidinas (Maier et al 2009, Khanal et al 2009, Rockenbach et al., 2011). En semillas provenientes del orujo, las concentraciones de (+)-catequina están en el rango de 177-475 mg/kg (Rockenbach et al 2011), en pieles de uva del orujo desde 0.73-132 mg/kg (Katalinic et al., 2010, Rockenbach et al 2011). Las concentraciones de (+)-catequina en sarmientos parecen ser superiores a las de semillas y pieles de uva provenientes desde el orujo.

En sarmientos, las procianidinas identificadas mediante HPLC-MS/MS corresponden a B1 y B2 (Püssa 2006). Posteriormente se corroboró la presencia de (-)-epicatequina y (+)-catequina en sarmientos a través de LC-NMR y LC-MS (Lambert 2013). No se ha evaluado el potencial de los sarmientos como fuente de procianidinas de distinto grado de polimerización.

1.5.2 Concentración de compuestos no flavonoides en sarmientos:

En sarmientos se han cuantificado ácidos fenólicos, tanto hidroxicinámicos como hidroxibenzoicos. Sus concentraciones son disimiles entre sí (tabla 6). Los sarmientos son por excelencia una fuente potencial de estilbenoides, principalmente de (*E*)-resveratrol y (*E*)- ϵ -viniferina. Las concentraciones son mayores que aquellas encontradas en otros residuos vitivinícolas o en el vino (Tabla 6). Las concentraciones de los estilbenoides dependen mucho del cultivar. Pinot Noir y Gewüztraminer son las variedades en donde se han reportado niveles de oligestilbenoides más altos (Vergara et al 2012, Lambert et al 2013, Guerrero et al 2016).

Tabla 6: ácidos fenólicos cuantificados en sarmientos.

Ácidos fenólicos	Compuesto	Concentración (mg/kg)	Referencia
Ácidos hidroxibenzoicos	Ácido gálico	11.5-58.8 7.2-20.5	Zhang et al., 2013 Sánchez-Gómez et al., 2014
	Ácido elágico	3.8-14.1	Sánchez-Gómez et al., 2014
	Ácido vanílico	17.8-48.3 2.7-8.3	Zhang et al., 2013 Sánchez-Gómez et al., 2014
	Ácido protocatecuico	91.6-167.9 3.2-6.94	Zhang et al., 2013 Sánchez-Gómez et al., 2014
	Ácido siríngico	71.7-110.9 4.6-6.5	Zhang et al., 2013 Sánchez-Gómez et al., 2014

	Ácido salicílico	153.5-227.9	Zhang et al., 2013
Ácidos hidroxicinámicos	Ácido p-coumárico	9×10^{-3} - 3.5×10^{-2} 70.3-131.6 5.6-8.4	Çetin et al., 2011. Zhang et al., 2013 Sánchez-Gómez et al., 2014
	Ácido cafeico	5.8×10^{-3} - 1.52×10^{-2} 3.1-63.2 1.9-3.4	Çetin et al., 2011. Zhang et al., 2013 Sánchez-Gómez et al., 2014
	Ácido ferúlico	0.92-2.3	Sánchez-Gómez et al., 2014
	Ácido (<i>E</i>) caftárico	55.2-77.6	Sánchez-Gómez et al., 2014
	Ácido (<i>E</i>)-p-coutárico	14.7-19.3	Sánchez-Gómez et al., 2014

Tabla 7: Concentración de estilbenoides en residuos de la industria vitivinícola (Modificado de Gorena et al., 2015).

Fuente	Concentración total de estilbenoides	Concentración de (<i>E</i>)-resveratrol	Referencia
Vino		0.361-14.3 mg/L	Mark et al., 2005, Boutegrabet et al., 2011, Bavaresco 2012 Fernandez-Marín et al., 2014.
Hojas	478 -1622 µg/g 3.2-5.3 mg/g	11 µg/g 0.71-3.16 mg/g	Vrhovsek et al., 2012 Carre et al., 2017
Orujo	11.2-19.7 µg/g	1.0±0.1 µg/g 6.9-27.5 µg/g	Reis et al., 2017 Fontana et al., 2016
Lias		3.0 ±0.1 µg/g	Reis et al 2017
Escobajos	14.3-225.8 mg/kg 60-480 mg/kg	14.3-225 mg/kg 16-289 mg/kg	Piñeiro et al., 2013 Ewald et al., 2017
Semillas	--	1.11-3.75 mg/100g	Rockenbach et al., 2011
Pieles	3.68 mg/kg	0.09-1.02 mg/kg	Katalinic et al 2010
Sarmientos	936-10000 mg/kg	41-7545 mg/kg	Vergara et al., 2012, Zhang et al., 2013, Lambert et al., 2013, Gorena et al., 2014, Houillé et al 2015, Ewald et al., 2017.

El perfil de estilbenoides en sarmientos de *Vitis vinifera* incluye monómeros como (*E*)-resveratrol , (*E*)-piceatanol, habiéndose reportado (*E*)-piceido (Sánchez-Gómez et al 2014, Gorena et al 2014, Houillé 2015, Guerrero et al 2016), dímeros como (*E*)- ϵ -viniferina (Gorena et al 2014, Gabaston et al 2017, Ewald et al., 2017), ampelopsina A (Schnee et al., 2013, Gorena et al 2014, Guerrero et al 2016) y recientemente se reportó (*E*)- ω -viniferina y (*E*)- δ -viniferina, además del trímero miyabenol C (Gabaston et al ., 2017), tetrámeros como vitisina B, hopeafenol e isohopeafenol (Vergara et al., 2012, Lambert et al., 2013). La variedad de los oligoestilbenoides depende del cultivar y del género de *Vitis* (Pawlus 2013, Guerrero et al 2016). Las *Vitis* no viníferas poseen en su perfil también (*E*)-resveratrolósido, (*E*)-ampelopsina E, (*E*)-amurensina B (Pawlus et al 2013).

Se ha analizado con relativo éxito a través de análisis de componentes principales (PCA) la correlación de la concentración de un oligoestilbenoide a una variedad de sarmiento. La separación se logra con dos componentes, pero con un 53% de varianza explicada (Guerrero et al 2013). Ello se puede deber a que las concentraciones de los estilbenoides en sarmientos son afectados no sólo por el cultivar, sino también por las condiciones de guarda inmediatamente después de la poda (Gorena et al.2014, Houillé et al. 2015, Billet et al 2017, Ewald et al 2017) y esto se ve reflejado en los amplios rangos de concentración de los oligostilbenoides reportados en la tabla 8.

Tabla 8 : Concentraciones de oligoestilbenoides en sarmientos de vides viníferas.

Estilbenoide	Concentración (mg/kg Peso Seco)	Referencia
(<i>E</i>)-resveratrol	1100-3200 383-6533 613.2-1350.9 190-1526 1360-4941 0.7-28.5 41-5100 441-7532	Püssa et al., 2006. Vergara et al., 2012 Zhang et al., 2013 Lambert et al., 2013 Gorena et al., 2014 Sánchez-Gómez et al., 2014 Houillé et al 2015 Ewald 2017
Piceido	0.5-3.8	Sánchez-Gómez et al., 2014
Hopeafenol	339-1468 32-95 859	Lambert et al., 2013 Gorena et al., 2014 Guerrero et al., 2016
(<i>E</i>)- ϵ -viniferina	700-1700 75-868 967-3737 94-656 2810 1743-3504	Püssa et al., 2006. Vergara et al., 2012 Lambert et al., 2013 Gorena et al., 2014 Guerrero et al 2016 Ewald et al 2017
(<i>E</i>)-piceatanol	72-457 190-1710 170-352	Vergara et al., 2012 Lambert et al., 2013 Gorena et al., 2014
(<i>E</i>)-vitisina B	88-1116 27-232 791	Lambert et al., 2014 Gorena et al., 2014 Guerrero et al 2016
Miyabenol C	22-174	Lambert et al., 2013

Algunos autores también han reportado ensayos para determinar la capacidad de absorción de radicales de oxígeno (ORAC-FL) a los extractos de sarmientos, encontrándose valores de 1718-5294 $\mu\text{mol TEAC/g}$. No se reportó relación entre los niveles de oligoestilbenoides y la capacidad antioxidante (Guerrero et al 2013). Además, los valores de capacidad antioxidante no eran comparables con estudios previos, que reportaban un rango entre 300-1300 $\mu\text{mol TEAC/g}$ (Karacabey & Mazza 2010). El perfil (poli)fenólico de los sarmientos es variado y complejo, por lo que la capacidad antioxidante puede ser reflejo de un efecto sinérgico entre más de una familia de (poli)fenoles. Si bien queda establecido que

los sarmientos son una fuente de antioxidantes naturales para diversos propósitos, se requiere un estudio de la capacidad antioxidante de los sarmientos con las muestras en condiciones rigurosamente controladas, para establecer si la capacidad antioxidante coincide con el aumento de los estilbenoides, por los flavonoides o es un efecto sinérgico entre ambas familias de compuestos u otro tipo de fenómeno.

1.5.3. Factores que influyen en la concentración de estilbenoides en sarmientos de *Vitis vinifera*

Actualmente se conocen tres factores que influyen en la concentración de los estilbenoides en sarmientos: tiempo de guarda luego de la poda (Vergara et al., 2012, Gorena et al., 2014, Ewald et al 2017), temperatura de la guarda (Houillé et al., 2015) y recientemente la longitud del corte del sarmiento en la guarda luego de la poda, efecto denominado como estrés mecánico (Billet et al 2017).

El sarmiento luego de la poda sigue metabólicamente activo. El tiempo que se almacena luego de la poda incide en las concentraciones de estilbenoides, principalmente de (*E*)-resveratrol y en menor medida de (*E*)-piceatanol. En sarmientos de la variedad Pinot Noir, se reportó un incremento de los estilbenoides de un 35% a los dos meses de guarda post-poda a temperatura ambiente, para luego disminuir a los tres meses (Vergara et al 2012). El aumento es efectivo cuando se guardan intactos a temperatura ambiente. (*E*)-resveratrol aumenta sus niveles hasta cinco veces en 120 días de guarda luego de la poda. Si la guarda del sarmiento prosigue hasta los 6 meses, el aumento de los estilbenoides puede llegar hasta siete veces (Gorena et al., 2014). En una guarda post-poda prolongada durante 30 meses, se reportó que la concentración de (*E*)-resveratrol llega a un plateau. Los sarmientos alcanzaron sus máximos niveles de (*E*)-resveratrol luego de 6 meses de almacenamiento,

aumentando 400-1400%. Luego de los seis meses tiende a decaer para permanecer en un nivel más constante (Ewald et al., 2017).

La temperatura óptima de guarda para el incremento de estilbenoides es a 20°C, donde se registro un aumento de (*E*)-resveratrol de 19 hasta 106 veces. La temperatura influye también en el tiempo en que se gatilla el incremento. Si los sarmientos se guardan a 28 °C, éstos demoran sólo dos semanas en alcanzar su máximo incremento de estilbenoides, para luego no aumentar más su concentración y llegar a un plateau. Además se señala que si los sarmientos luego de la poda se someten a 60°C por al menos una hora, no aumentan sus concentración de estilbenoides durante la guarda (Houillé et al., 2015). La explicación de este fenómeno estaría en la abundancia transcripcional para la expresión de los genes que participan en la vía shikímica. Luego de los seis meses de guarda post-poda la abundancia transcripcional para STS reporta un aumento, por lo que es inducida a diferencia de los otros genes implicados en la vía (PAL, 4CL, C4H). Esto implica que la síntesis de (*E*)-resveratrol en sarmientos es *de novo* (Houillé et al., 2015).

Recientemente se demostró que el estrés mecánico de cortar los sarmientos en trozos de 0.5 cm luego de la poda estresa al sarmiento, gatillando con ello un aumento de expresión de la STS y por consecuencia de (*E*)-resveratrol y (*E*)-piceatanol en menos tiempo, en sólo seis días y no semanas, alcanzando concentraciones similares cuando el sarmiento es guardado en segmentos más largos por más tiempo. Luego del aumento, la concentración se mantiene constante llegando al plateau. Si se corta a 0.2 cm, el aumento se gatilla antes, pero luego decrece y para permanecer constante. El uso del estrés mecánico se propuso recientemente como una estrategia para aumentar rápidamente la concentración de estilbenos (Billet et al 2017). Sin embargo, si se muelen los sarmientos luego de colectarlos, tampoco se observa un incremento relevante de estilbenoides (Gorena et al., 2014). En todos los estudios hay

concordancia de que el aumento es de (*E*)-resveratrol y (*E*)-piceatanol, mientras que los oligoestilbenoides no son inducibles.

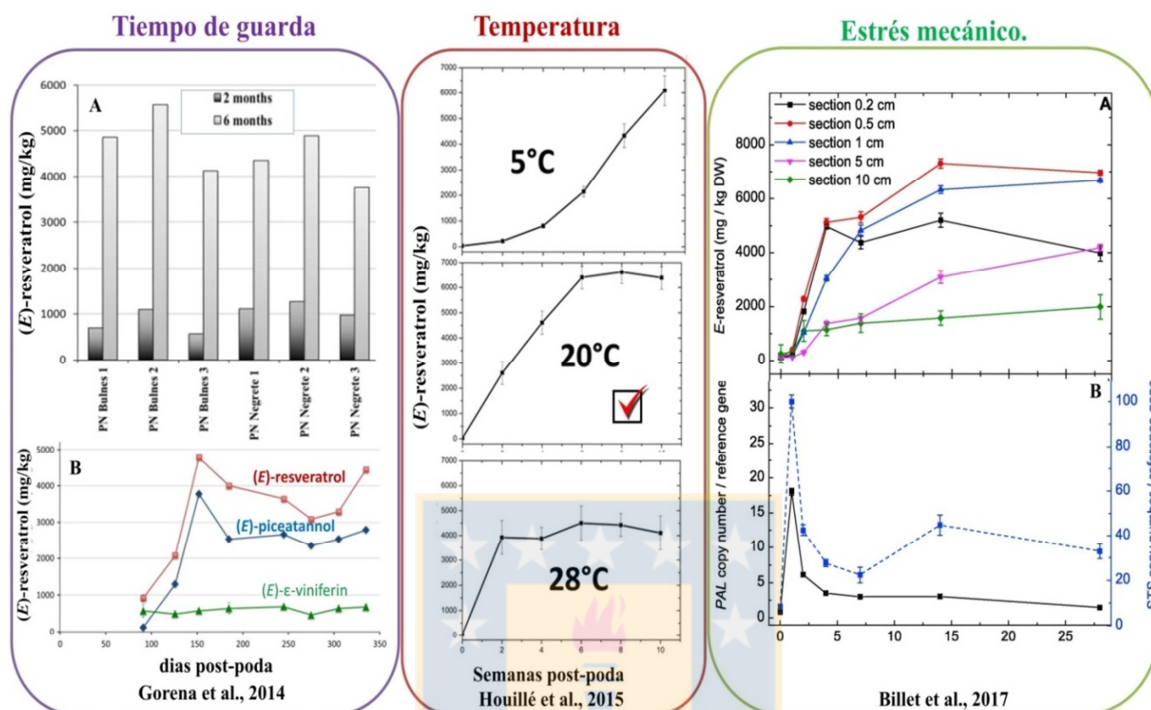


Figura 6: Efecto del **tiempo de guarda** A: aumento de estilbenoides en sarmientos Pinot Noir con 2 meses de guarda a 6 meses a temperatura ambiente, B: aumento de (*E*)-resveratrol y (*E*)-piceatannol en sarmientos Pinot Noir almacenados hasta 350 días post-poda a temperatura ambiente. **Efecto de la temperatura** sobre el incremento de las concentraciones de estilbenoides en sarmientos y el **estrés mecánico** luego de la poda, A: aumento de estilbenoides en sarmientos almacenados con diferentes longitudes, B: PCR-RT, aumento transcripcional de STS y PAL de sarmientos de 0.5 cm de longitud (Adaptado y Modificado de Gorená et al., 2014, Houillé et al., 2015, Billet et al., 2017).

1.6. Aislamiento de estilbenoides en órganos de la vid

La cromatografía en contracorriente (CCC) ha demostrado ser una técnica útil para la purificación de estilbenoides en gran escala, especialmente la cromatografía de partición

centrífuga (CPC), ya que a diferencia de la cromatografía flash o semi-preparativa, los (poli)fenoles no se adsorben irreversiblemente (Bisson et al., 2011), por lo que se puede recuperar la muestra totalmente, además de poseer una alta capacidad de carga (Michel et al., 2014). En CPC se emplean sistemas bifásicos en los que los (poli)fenoles se separan de acuerdo a sus coeficientes de partición o a veces denominado razón de proporción (K_d) (Zga et al 2009, Bisson et al., 2011). Es posible predecir el orden de elución de los (poli)fenoles calculando su respectiva K_d (Bisson et al., 2011). CPC posee un sistema de equilibrio hidrostático, en el cual se retiene una fase a través de una fuerza centrífuga aplicada de manera constante y la otra fase se bombea a través de la fase estacionaria (figura 7). Este sistema se caracteriza por tener pequeñas cámaras de elución o canales interconectadas en discos montados uno sobre otro y rotando en un solo eje (Michel et al., 2013, Bojczuk et al., 2017). Dependiendo de la densidad de las fases, se puede operar en dos modos. Cuando la fase más ligera (menos densa) es fase móvil, se denomina modo ascendente, mientras que cuando la de mayor densidad fluye a través de la menos densa se denomina descendente (Bojczuk et al., 2017). Un punto relevante a considerar es la solubilidad de los compuestos a separar y su razón de K_d entre las fases inmiscibles. Si bien existen diversas combinaciones de sistemas de solventes, una de las más usadas para fraccionar extractos ricos en polifenoles se compone de acetato de etilo, heptano, agua y metanol, formando 23 posibles combinaciones (A hasta la Z), llamado comúnmente sistema Arizona (das Neves Costa & Leitao 2010, Bojczuk et al., 2017). Debido a la modalidad de usos, la posibilidad de generar un sistema bifásico en un amplio rango de polaridades, CPC es una técnica idónea para la separación y purificación de (poli)fenoles desde extractos de plantas.

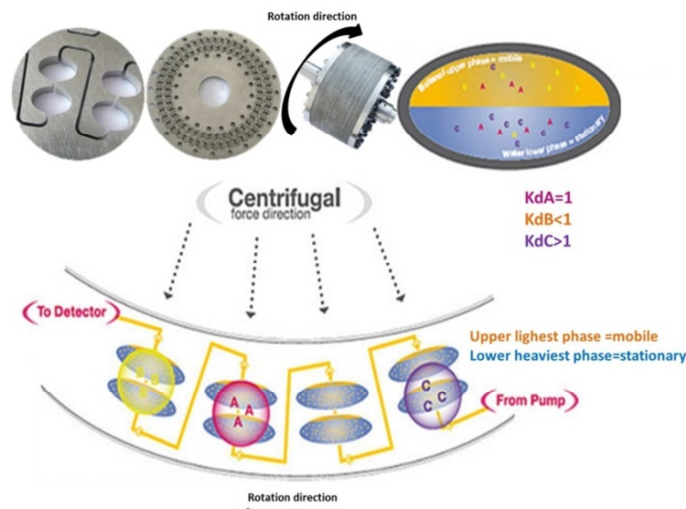


Figura 7: Esquema gráfico del modo de separación en sistemas hidroestáticos mediante CPC. (Adaptado de Bojczuk et al., 2017).

El principal objetivo de la purificación es obtener los compuestos con un alto grado de pureza en la menor cantidad de pasos posibles con un rendimiento adecuado. El requerimiento es que el extracto debe poseer una alta concentración. Es por ello que raíces, escobajos y recientemente sarmientos de vides son usados como fuente de estilbenoides. Desde extracto de escobajos de Chardonnay se purificó (*E*)- ϵ -viniferina, (*E*)-piceatannol, vitisina C, (*E*)-resveratrol y (-)-ampelopsina A (Zga et al., 2009) con el sistema K de la escala Arizona en modo ascendente y se puede extraer desde un solo paso (+)-ampelopsina A en modo dual. La obtención de compuestos bioactivos en modo dual, es cuando la fase estacionaria pasa a ser la fase móvil y viceversa, por lo que compuestos antes retenidos ahora son eluidos. Esta es una estrategia elegante para separar mezclas complejas. Incluso es posible el uso modo multi-dual, con un aumento de los platos teóricos en el aislamiento, pero conllevando un aumento de tiempo en la separación (Bojczuk et al., 2017). El uso del sistema M ascendente de la escala Arizona sirve para separar (*E*)-resveratrol de (*E*)- ϵ -

viniferina, mientras que el sistema M en modo descendente para la obtención de vitisina C (Zga et al., 2009).

Desde un extracto de raíces de *V. riparia* × *V. berlandieri* que contiene estilbenoides constitutivamente sintetizados con un alto contenido de vitisina C, se ensayó el aislamiento de estilbenoides con un paso previo de concentración en Amberlita XAD-7 y luego mediante CPC acoplada con un detector de masas con trampa de iones, empleando un sistema de elución híbrido (Bisson et al 2011). En ese estudio se implementó el “paso inverso”. Generalmente en las eluciones en CPC con gradiente se emplea un solvente que posea menos fuerza de elución a uno mayor. El proceso contrario de uno mayor a uno menor es lo que se denomina “paso inverso” o “gradiente inverso”. El trabajo esclarece que el uso del sistema Arizona K y L fue adecuado para la separación de estilbenoides en particular para (*E*)- ϵ -viniferina, (*E*)-piceatanol y algunos trómeros.

Los trabajos de Pawlus et al., 2013 y Houillé et al., 2014., emplean gradientes de elución, con los sistemas L en modo ascendente y luego K, ya sea en modo ascendente o descendente para extractos de sarmientos de vides no viníferos o para extractos de Malbec, respectivamente. Luego de separar por CPC, obtienen 3 fracciones de interés, Houillé et al., 2014 aplican el sistema H a la tercera fracción obtenida con M ascendente, separando ampelopsina A de hopeaphenol. A partir de los extractos de *Vitis viníferas* y *Muscadinia*, luego de obtener 10 fracciones enriquecidas de estilbenoides, separan a través de Sephadex la primera fracción para luego utilizar HPLC semi-preparativa, con ello obtienen: (*E*) y (*Z*) amurensis B, (*E*)- ϵ -viniferina, (*E*)- ω -viniferina, (*E*) y (*Z*) ampelopsina E, (*E*) y (*Z*) miyabenol C, (*E*) y (*Z*) Vitisin C de las distintas fracciones (Pawlus et al., 2013).

Otra estrategia es fraccionar el extracto consecutivamente en CPC, es decir inyectar sucesivamente para obtener un alto número de fracciones con alta concentración de

estilbenoides, para luego volver a fraccionarlas por CPC. Esta estrategia fue adoptada por Papastamoulis et al., 2014, para extractos de sarmientos de Merlot obtenidos con metil-ter-butil éter y fue replicada por Pavela et al 2017., para sarmientos de Cabernet Sauvignon preconcentrados en Amberlita. Papastamoulis et al 2014., inyectaron 1.8 g de extracto cuatro veces sucesivas y obtuvieron 19 fracciones, de las cuales 16 fueron en modo M ascendente y descendente. Los sistemas L, F y J fueron empleados para purificar los aislar los estilbenoides desde las fracciones.

A pesar del buen funcionamiento de las estrategias para aislar estilbenoides en gran parte de las purificaciones fue imprescindible el uso de HPLC preparativa para obtener los estilbenoides con un alto grado de pureza luego de fraccionar por CPC.

1.7. Test de reducción de tetrazolio (MTT) para la medición *in vitro* de viabilidad celular

Los test de proliferación celular *in vitro* son una herramienta para determinar si una molécula sintetizada o aislada posee efectos directos sobre la proliferación celular o si poseen efectos citotóxicos que conlleven a la muerte celular. Entre estos métodos se incluyen aquellos que utilizan sales de tetrazolio, resazurina, marcadores de proteasas y detección de ATP.

El test MTT ((3-[4,5 -dimethylthiazol-2-yl]-2,5 diphenyl tetrazolio bromuro), es un test basado en sales de tetrazolio, el MTT posee una carga positiva y penetra fácilmente a las células viables. Este test ha sido ampliamente aceptado y difundido. Además es considerado uno de los test más sensibles para medir citotoxicidad (Riss et al., 2013; Vinken & Blaauboer., 2017). El nombre se debe a que antiguamente se denominaba metiltiozolib-tetrazolio (Storcket et al., 2012). Las células viables al estar expuestas a la sal de

tetrazolio, lo acumulan y lo biotransforman a formazán, el cual es de color púrpura, por lo que la absorbancia a 570 nm es útil para saber cuántas células viables hay luego de la exposición a un agente citotóxico o que promueve la muerte celular (Riss et al., 2013).

El mecanismo de acción para la generación del formazán desde MTT debe incluir dadores de electrones. Las coenzimas o enzimas como nicotinamida adenina dinucleótido de hidrógeno (NADH) (Figura 8) o succinato deshidrogenasa (SDH) respectivamente, podrían llegar a ejercer este rol (Riss et al., 2013; Vinken & Blaauboer., 2017), por lo que una célula metabólicamente activa es solamente capaz de reducir el MTT. Es común que en literatura se señale que el lugar de reducción del MTT sea la mitocondria y que las deshidrogenasas mitocondriales sean parte del mecanismo. Sin embargo, existe evidencia de que el lugar donde ocurre la reducción es en el citoplasma y que principalmente por causa de NADH y de las deshidrogenasas asociadas al retículo endoplasmático se forme el formazán (Stockert et al., 2012).

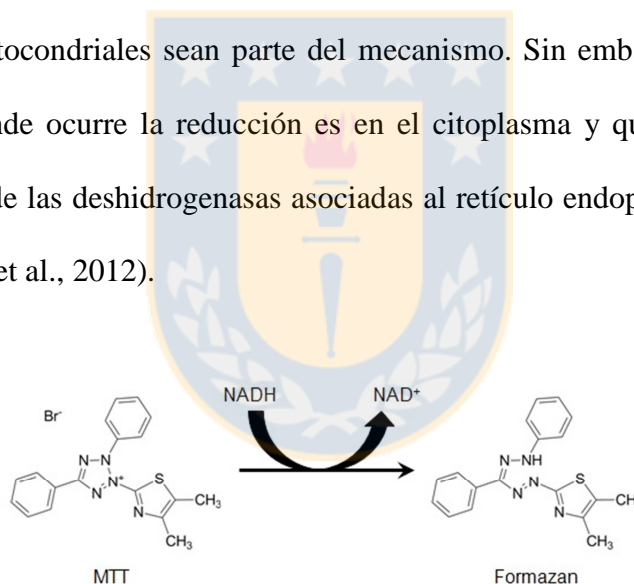


Figura 8: Conversión de MTT en formazan en test de reducción de tetrazolio. (Adaptado de Riss et al., 2013).

En la tabla 8 se describen los efectos citotóxicos reportados para algunos estilbenoides en modelos celulares cancerígenos de humanos expresados como concentración mínima inhibitoria (IC₅₀) (Tabla 8), es decir, la concentración requerida de un compuesto para disminuir en un 50% la población celular.

Tabla 9: Citotoxicidad de estilbenoides (IC₅₀) en líneas celulares cancerosas humanas a través del ensayo MTT.

Estilbenoide	Línea celular (modelo celular)	IC ₅₀ (μM)	Referencia
<i>(E)</i> -resveratrol	K562 (leucemia)	30	Ha et al., 2009
	HCT116 (carcinoma colon rectal)	28	Ha et al., 2009
	A549 (carcinoma de pulmón)	33	Chen et al., 2010
	MCF-7 (adenocarcinoma mamario)	9.2	Wu et al 2010
	MDA-MB-23 (adenocarcinoma mamario)	12	Wu et al 2010
	HT-144 (melanoma)	93	Nivelle et al., 2017
<i>(E)</i> -piceatanol	WM-266-4 (melanoma)	29	Du et al., 2017
	A2058 (melanoma)	15	Du et al., 2017
<i>(E)</i> -ε-viniferina	HT-144 (melanoma)	82	Nivelle et al., 2017
	SKMEL-28 (melanoma)	86	Nivelle et al., 2017
<i>(E)</i> -piceido	K562 (leucemia)	24	Ha et al., 2009
Amurensis G	K562 (leucemia)	23	Ha et al., 2009
	HCT116 (carcinoma colon rectal)	17	Ha et al., 2009
Ampelopsina A	K562 (leucemia)	38	Ha et al., 2009
Scirpusina A	MCF-7 (adenocarcinoma mamario)	64	Wu et al., 2010
	MDA-MB-23 (adenocarcinoma mamario)	82	Wu et al., 2010

1.8. Análisis de estilbenoides y procianidinas por HPLC.

Los estilbenoides se han determinado en diversas matrices a través de HPLC con columnas en fase inversa C18 rellenas con partículas porosas porosas (Pawlus et al 2013., Gorena et al., 2014., Guerrero et al., 2016, Esatbeyoglu et al.,2016) y además empleando columnas con partículas de tamaños sub 2.1 μm en modo UHPLC (Boutegrabet et al., 2011, Xie & Bolling., 2014, Gabaston et al 2017) acoplado a diversos detectores DAD (Esatbeyoglu et al 2016, Guerrero et al., 2016), espectrómetro de masas: triple cuadrupolo (Vergara et al., 2012, Gorena et al 2014.), Q-ToF (Moss et al., 2013, Gabaston et al 2017), tanto en modo positivo como negativo. El método más empleado para cuantificar es a través de DAD.

Las columnas cortas (5-10 cm) y de diámetro angosto (2.1 mm) rellenas con partículas sub 2.1 μm responden a la demanda de obtener separaciones rápidas en tiempos más cortos, obteniendo peaks estrechos y aumentando la eficiencia con el inconveniente de un aumento de presión (Formula 1) en el rango de 18000-19500 psi (Fekete et al 2012), por lo cual se requieren bombas especiales para dichas presiones, denominadas de UPLC o UHPLC.

$$\Delta P = \frac{250LQ\eta}{dp^2 dc^2} \quad (1)$$

ΔP : Presión, Q: caudal, L: longitud de columna, η : viscosidad de la fase móvil, dp: diámetro de la partícula, dc: diámetro de la columna.

Al ser las partículas tan pequeñas, ocurre un fenómeno de calor friccional, generándose un gradiente de temperatura en la columna. Esto es más crítico cuando la columna es más corta, perdiendo eficiencia (Fekete et al 2012).

Las partículas porosas poseen una mayor resistencia a la transferencia de masa (termino C) (Formula 2) que aquellas no porosas, pero ofrecen una superficie mayor por lo tanto una mayor capacidad de carga de muestra. Una alternativa a las columnas UHPLC son las columnas de núcleo sólido, que combinan las ventajas de las partículas porosas y no porosas. Las partículas poseen un núcleo sólido de sílica (1.7 μm de diámetro), recubierto con una superficie porosa para generar una esfera (Fekete et al., 2012, González-Ruiz et al., 2014). El desarrollo de la tecnología responde a la necesidad de alta eficiencia en cortos periodos de tiempos, pero con presiones abordables con una bomba de HPLC convencional.

$$h = \frac{B}{v} + A + Cv \quad (2)$$

h: altura reducida de platos, v: velocidad reducida, A, B y C son coeficientes numéricos asociados a dispersión por efecto de camino múltiple o efecto de remolino, difusión longitudinal o axial y transferencia de masa, respectivamente (Hayes et al., 2014).

Originalmente, la idea de las partículas de núcleo sólido era aumentar la eficiencia, disminuyendo los caminos que el compuesto debe recorrer y por lo tanto mejorar la transferencia de masas. Se esperaba que la partícula de núcleo sólido contribuyera a la eficiencia debido a la disminución de la difusión axial (término B) y la dispersión de camino múltiple (término A) en la formula 2. Estos términos están asociados al diámetro externo de la partícula, mientras que la transferencia de masas a la delgada capa fina porosa que recubre el núcleo de la partícula (Fekete et al., 2012). Si bien existen varios modelos matemáticos que tratan de explicar el comportamiento de las columnas de núcleo sólido, sólo se explican los aspectos relevantes en donde hay consenso. Efectivamente, el termino A se afecta por la calidad del empaque y el tamaño de la partícula. La explicación lógica es que el empaque es mejor en comparación a las columnas porosas y de partícula sólida (Fekete et al., 2012., Hayes et al., 2014, González-Ruiz et al., 2015).

La reducción del volumen muerto de las columnas mejora la eficiencia, a diferencia de las columnas porosas que sólo ocupan un con relleno un tercio del volumen interno de la columna. Al emplear partículas de núcleo sólido, el volumen ocupado aumenta entre un 20-30 %, lo que se traduce en una menor difusión longitudinal, disminuyendo el término B. Si bien el termino C contribuye a la disminución del ancho de banda, no es el coeficiente más importante, cómo originalmente se promovía. La contribución del término B es inversamente proporcional a la velocidad lineal de la fase y a su vez la difusión longitudinal reducida se puede expresar como la razón entre el término B y C, por lo que a altas velocidades la contribución del termino C es menos significativa (Fekete et al., 2012, Hayes et al., 2014). La tecnología de núcleo sólido se asocia a una conductividad térmica alta, evitando la generación del gradiente de temperatura y el ensachamiento del peak (González-Ruiz et al., 2015), por lo que actualmente esta tecnología sustenta la generación

de metodologías cromatográficas rápidas con alta eficiencia para la cuantificación de (poli)fenoles, comparable a UHPLC, pero con caídas de presión significativamente menores.

Las proantocianidinas son complejas de analizar a través de HPLC, en particular en fase inversa, que es la técnica preferida para separar (poli)fenoles de extractos vegetales. Sin embargo, la resolución sólo alcanza hasta tetrámeros, debido a dos fenómenos: el primero es que las concentraciones de las procianidinas de mayor DP en general son menores, además que aumentan las posibilidades de isomerización, por lo que la capacidad del peak es reducida. Además, al aumentar el DP disminuye la absorbancia así como la señal fluorescente. En fase normal se logra la separación de hasta DP 14, eluyendo de acuerdo a su DP, pero con peaks poco definidos (Hümmer & Schreier 2008). Actualmente, la cromatografía de interacción hidrofílica (HILIC) ofrece una alternativa para mejorar la eficiencia y aumentar el grado de separación de las procianidinas en muestras como orujo (Winterhalter et al., 2015), escobajos (Barros et al., 2014) y en extractos de manzana (Hollands et al., 2017). Esto es porque retiene (poli)fenoles altamente polares, además de ser un método reproducible entre laboratorios (Hollands et al., 2017).

A diferencia de la cromatografía en fase normal, en HILIC se utiliza 2-3% de agua en sus fases móviles, mientras que en la cromatografía normal se evita, por lo que HILIC no se considera como cromatografía de fase normal. Existe evidencia de que en HILIC se forma una capa de agua en las partículas de sílica o enlazadas con fase estacionaria y que el mecanismo principal sería el de reparto entre la fase móvil y la capa de agua que rodea la fase estacionaria (Guo & Gaiki et al., 2011, McCalley et al., 2017).

Otra alternativa que ha cobrado importancia para la cuantificación de procianidinas en matrices alimentarias es el uso de UHPLC-MS/MS, que ofrece métodos reproducibles, con

bajos límites de cuantificación y alta sensibilidad (Ortega et al., 2010, Jungfer et al., 2012). Sin embargo, los tiempos de análisis bordean entre 12-25 minutos y emplear un espectrómetro de masas que encarece el costo de análisis rutinarios.

1.8.1. Cromatografía bidimensional

La cromatografía bidimensional es una técnica de separación para componentes de una mezcla extremadamente compleja, usando dos dimensiones distintas (D), conectadas una con la otra, pero independientes entre sí, con lo que proveen diferentes selectividades. Esta propiedad se denomina ortogonalidad (Matos et al., 2012, Cacciola et al., 2017). La definición de ortogonalidad implica que dos sistemas cromatográficos no tengan entre sí correlación estadística entre los tiempos de retención en cada dimensión, por lo que el mecanismo de separación no debe ser necesariamente distinto en la primera y en la segunda dimensión para poseer ortogonalidad (D'Attoma et al., 2012).

Existen dos modos de llevar a cabo la cromatografía líquida bidimensional: recortar el corazón de las fracciones, conocida como “heart-cutting” (LC-LC), en donde se llevan desde 1D a 2D las fracciones de interés, mientras que el modo “comprehensive” (LC x LC), que se puede traducir como exhaustivo, corresponde a toda la muestra que va desde 1D hacia 2D .

Los puntos críticos a considerar al desarrollar una metodología LC x LC “on line” los solventes que componen las fases móviles en 1D , que deben ser compatibles en 2D y el corto tiempo de análisis en 2D (Stoll et al., 2016, Cacciola et al., 2017). Al implementar una cromatografía bidimensional se debe optimizar cada dimensión por separado. Un detalle no menor es que en 1D el análisis debe ser lento, mientras que en 2D debe ser extremadamente rápido, por lo que generalmente se acopla en 2D un detector de masas para una rápida

adquisición de datos. A veces se considera los datos obtenidos a través de espectrometría de masas como una tercera dimensión (Cacciola et al., 2017).

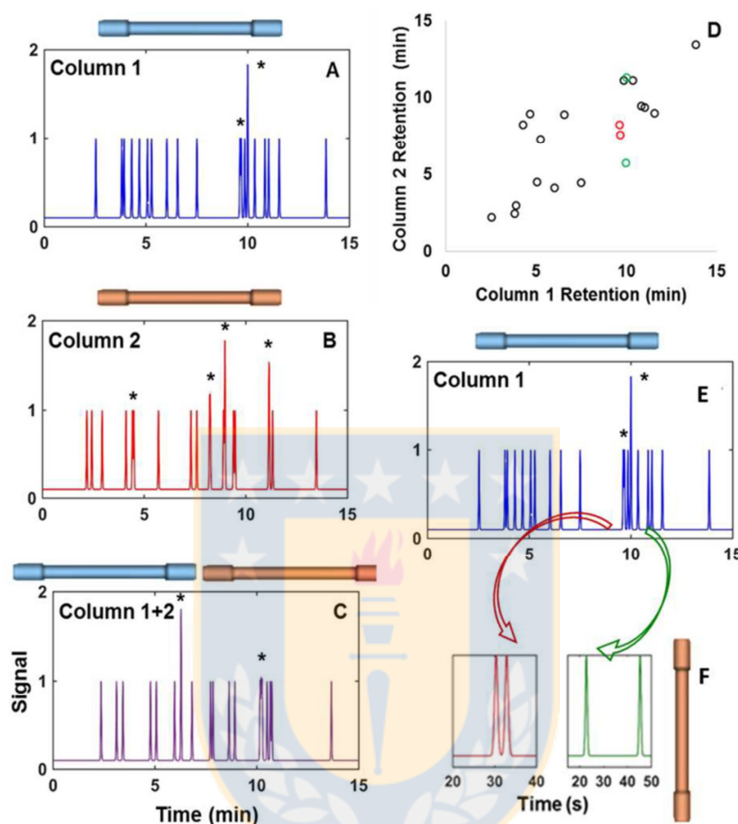


Figura 9: Representación esquemática de la separación a través de cromatografía bidimensional para una muestra de 20 compuestos, (*) son compuestos que coeluyen. **A** y **B** Cromatografía en una sola dimensión, **C** Separación en serie con las columnas usadas en **A** y **B**, **D** Separación bidimensional continua (LC x LC), **E** y **F** corresponden a cromatografía en donde se seleccionan las fracciones a llevar a una segunda dimensión (LC-LC). (Adaptado de Stoll et al., 2016).

La capacidad de peak es un parámetro usualmente empleado para medir la separación en cromatografía. Se refiere al número de peaks que caben en una ventana de tiempo definida.

Comunmente se considera como cuatro veces la desviación estándar del ancho del peak en la ventana de tiempo en cromatografía unidimensional (Neue 2008., Li et al., 2009). La capacidad de peak cobra relevancia en cromatografía bidimensional, como medida de la separación en ambas dimensiones, debido a que se puede perder separación cuando se transfiere de ¹D a ²D. Los rangos pueden ser amplios y no hay una gran dependencia de la capacidad de peak de ¹D. La productividad de la separación en la segunda dimensión (capacidad del peak por unidad de tiempo de gradiente en la segunda dimensión) debe ser maximizada para lograr una buena separación en cromatografía bidimensional (Li et al., 2009).

Las combinación RP-LC x RP-LC es la más usada en cromatografía bidimensional (32.3 %), mientras que HILIC-LC x RP-LC se utiliza en menor medida (21.8 %) (Li et al., 2015, Cacciola et al., 2017). HILIC-LC x RP-LC se ha utilizado para elucidar la composición (poli)fenólica de cocoa (Kalili et al., 2013), semillas de uva (Montero et al., 2013) y vino (Willemse et al., 2015). Esta combinación se caracteriza por separar en base a la hidrofobicidad y polaridad, posee una capacidad de peak alta (>2000) debido a la baja correlación de los mecanismos ($R^2 < 0.2$) (Cacciola et al 2017). La configuración HILIC-LC x RP-LC es adecuada para el análisis de procianidinas, separándolas de acuerdo a su incremento en DP en ¹D, siendo el solvente ocupado en ¹D en el gradiente compatible en ²D. A través de HILIC con una columna en una dimensión es posible separar procianidinas < 10 DP, mientras que en C18, sólo es posible separar hasta tetrameros. En semillas de uva, usando HILIC LC x RP LC, fue posible la separación de 46 polifenoles, incluyendo procianidinas hasta un DP de 7 sin pre-tratamiento de muestra (Montero et al., 2013).

Comparando la separación unidimensional RP-LC para procianidinas se obtiene una capacidad de peak de 300, pero coeluyen isómeros con igual DP. Empleando la

combinación HILIC LC x RP LC “on line” se obtuvo una capacidad de peak entre 200-300 para procianidinas de cocoa. Sin embargo, isómeros de procianidinas de igual grado de polimerización coeluyeron. En contraste, la capacidad de peak es mayor cuando se utilizan métodos “off line” (fuera de línea) o “stop flow” (flujo detenido), sin embargo la reproducibilidad es menor y el gasto de tiempo es mayor (Kalili et al., 2013).

La cromatografía bidimensional genera un alto volumen de datos. Se forma un set de datos multi- vías de acuerdo al orden del instrumento. La data cambia en cada una de dimensiones, de acuerdo con el tiempo, sumado a la dimensión espectral y finalmente por las réplicas de la muestra se puede generar un hipercubo de información (Matos et al 2012).



2. Hipótesis y Objetivos

En base a los antecedentes planteados y discutidos en la sección precedente, se plantea la siguiente hipótesis para la presente Tesis:

2.1. Hipótesis:

Los sarmientos contienen compuestos fenólicos (proantocianidinas y estilbenoides), destacando sus altos niveles de estilbenoides. Ambas familias tienen un interés potencial de aplicación, debido a su capacidad antioxidante y por su posible actividad antiproliferativa en células cancerosas.

El almacenamiento post-poda de los sarmientos incrementa sus niveles, especialmente (*E*)-resveratrol. Este incremento puede ocurrir por:

- Aumento de su biosíntesis gatillada por el stress inducido por la poda
- Envejecimiento de la madera y el concomitante incremento de la extractabilidad de estilbenos que estaban unidos a estructuras celulares.
- Una combinación de ambos procesos

2.2. Objetivo General:

Evaluar la incidencia de las condiciones de guarda (temperatura, humedad y tiempo) sobre las concentraciones o sobre la evolución de los niveles estilbenoides y proantocianidinas post poda y caracterizar los compuestos (poli)fenólicos estudiados mediante una plataforma analítica avanzada e integrada.

2.3. Objetivos específicos:

2.3.1. Implementar y validar un método cromatográfico que considere menor tiempo de análisis, consumo de fase móvil y detección en serie mediante HPLC-DAD y fluorescencia para la cuantificación de distintos compuestos (poli)fenólicos en sarmientos.

2.3.2. Aislar y caracterizar los estilbenoides en extracto de sarmientos a través de CPC, HPLC-semipreparativa, HPLC-DAD-QToF y RMN mediante CPC para obtener compuestos purificados para la calibración cuantitativa de cada uno y evaluar su actividad antiproliferativa en células cancerosas humanas.

2.3.3. Desarrollar una metodología cromatográfica bidimensional (LCxLC) para evaluar cuanto la combinación apropiada de dos fases estacionarias y móviles y mecanismos distintos de separación permiten resolver aún mejor mezclas muy complejas de (poli)fenoles presentes en extracto de sarmientos.

2.3.4. Evaluar la incidencia de las condiciones de guarda post-poda sobre los niveles de estilbenoides y proantocianidinas.

3. Estrategia analítica para el análisis de estilbenoides y procianidinas en sarmientos.

La estrategia analítica para dar cumplimiento al objetivo general, los específicos detallados en la sección precedente, se puede dividir en etapas, las cuales se ilustran en la figura 10.

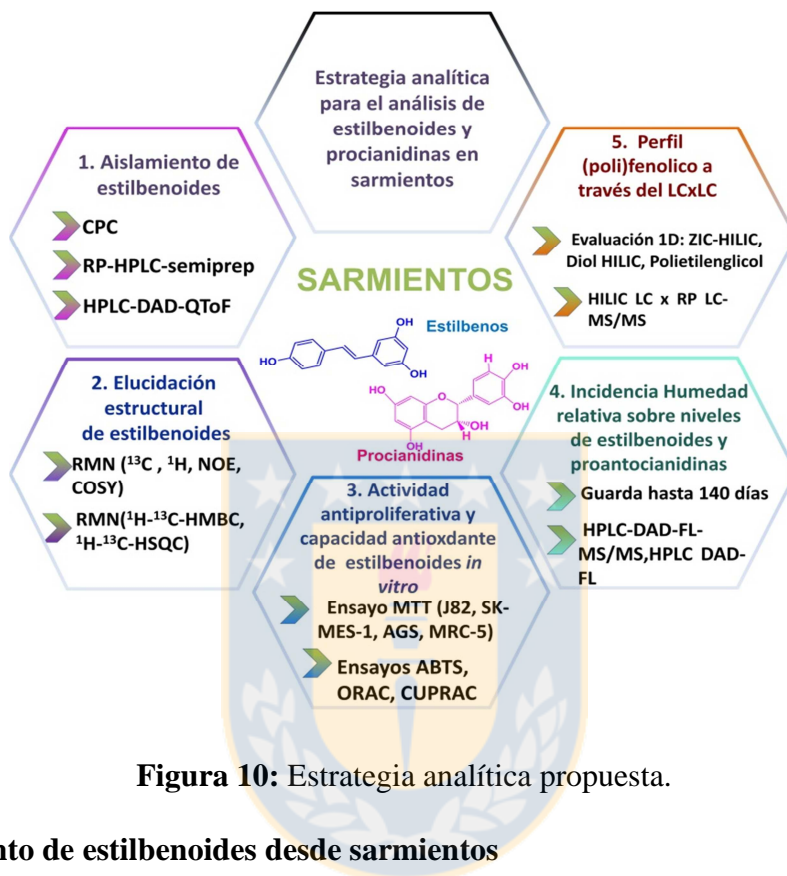


Figura 10: Estrategia analítica propuesta.

3.1. Aislamiento de estilbenoides desde sarmientos

Debido a la carencia de estándares y la falta de caracterización de los estilbenoides minoritarios, éstos se purificarán desde sarmientos. La variedad escogida es Pinot Noir, debido a los altos niveles reportados de estilbenoides para esta variedad, destacando sobre otras. Las técnicas cromatográficas preparativas como CPC o HPLC-semi preparativa serán empleadas, por lo que es imprescindible obtenerlos desde un extracto enriquecido como un extracto piloto. Se monitorearán las fracciones aisladas cuantificándolas por HPLC-DAD-FL, mientras que la caracterizará el extracto por HPLC-DAD-QToF. Las metodologías empleadas y los resultados obtenidos se explicitan en el Capítulo 2.

3.2. Caracterización y elucidación estructural de oligoestilbenoides

Los estilbenoides que serán aislados con alta pureza se elucidarán estructuralmente o se confirmará su identidad a través de RMN ^{13}C y ^1H (^1H - ^1H COSY, NOE), RMN bidimensional ^1H - ^{13}C -HMBC, ^1H - ^{13}C -HSQC. Se caracterizará el potencial antioxidante *in vitro* de los diversos oligoestilbenoides aislados a través de distintos ensayos de capacidad antioxidante en términos de capacidad protectora (ORAC-FL) y reductora (CUPRAC, ABTS).

3.3. Ensayos de actividad antiproliferante de estilbenoides en células cancerosas

Se evaluarán actividad antiproliferante de los estilbenoides aislados en mayor concentración a través del ensayo MTT en distintas líneas de células cancerosas humanas (adenocarcinoma gastrointestinal (AGS), células escamosas de cáncer de pulmón (SK-MES-1), carcinoma de vejiga (J82), además de una línea celular humana normal de fibroblasto de pulmón (MRC-5).

3.4. Determinación cuantitativa de estilbenoides y proantocianidinas en sarmientos: incidencia de condiciones en el proceso de guarda post-poda

Los sarmientos de diversas variedades se recolectarán inmediatamente después de la poda en los viñedos, una muestra de las variedades se mantendrán sin guarda a -20°C , mientras que las otras recolectadas se guardarán en dos condiciones distintas de humedad relativa para muestrear sucesivamente en el tiempo de guarda post-poda (12, 24, 45, 58, 77, 84, 98, 110, 124, 140 días luego del poda). Se implementará un método HPLC-DAD-FL-MS/MS para identificar los (poli)fenoles bioactivos en las muestras y se desarrollará y validará un método HPLC-DAD-FL para cuantificar los estilbenoides y proantocianidinas

simultáneamente, debido a la complejidad de la muestra se empleará la tecnología de núcleo sólido en las columnas.

3.5. Perfil de estilbenoides y procianidinas en sarmientos mediante LC x LC

La cromatografía bidimensional es una técnica poderosa para la separación de (poli)fenoles en matrices extremadamente complejas como son los sarmientos. Se optimizará e implementará un método LCxLC que combine HILIC con C18 para generar una herramienta para caracterizar el perfil de (poli)fenoles bioactivo presentes en los sarmientos de vides.



4. Referencias:

Abhijit, A & Destache, C. J. (2016). Natural polyphenols : potential in the prevention of sexually transmitted viral infections. *Drug Discovery Today*, 21(2), 333-341.

Amendola, D., Faveri, D. M. De, Egües, I., Serrano, L., Labidi, J., & Spigno, G. (2012). Bioresource Technology Autohydrolysis and organosolv process for recovery of hemicelluloses, phenolic compounds and lignin from grape stalks. *Bioresource Technology*, 107, 267–274.

Antionioli, A., Fontana, A. R., Piccoli, P., & Bottini, R. (2015). Characterization of polyphenols and evaluation of antioxidant capacity in grape pomace of the cv. Malbec. *Food Chemistry*, 178, 172–178.

Argun, H., & Onaran, G. (2015). Delignification of vineyard pruning residues by alkaline peroxide treatment. *Industrial Crops and Products*, 74, 697–702.

Barros, A., Gironés-vilaplana, A., Teixeira, A., Collado-González, J., Moreno, D. A., Gil-izquierdo, A., Rosa, E & Domínguez-perles, R. (2014). Evaluation of grape (*Vitis vinífera* L.) stems from Portuguese varieties as a resource of (poly)phenolic compounds : A comparative study. *Food Research International*, 65, 375–384.

Bavaresco, L, Mattivi, F, De Rosso, M., Flamini, R.(2012). Effects of elicitors, viticultural factors, and enological practices on resveratrol and stilbenes in grapevine and wine. *Mini Reviews in Medicinal Chemistry*, 12, 1366–1381.

Berman, A. Y., Motechin, R. A., Wiesenfeld, M. Y., & Holz, M. K. (2017). The therapeutic potential of resveratrol : a review of clinical trials. *Precision Oncology*, 35, 1- 9.

Billet, K., Houillé, B., Besseau, S., Mélin, C., Oudin, A., Papon, N., Courdavault, V., Clastre, M., Giglioli-Guivarch, N & Lanoue, A. (2018). Mechanical stress rapidly induces E-resveratrol and E-piceatannol biosynthesis in grape canes stored as a freshly-pruned byproduct. *Food Chemistry*, 240, 1022–1027.

Bisson, J., Poupard, P., Pawlus, A. D., Pons, A., Darriet, P., Mérillon, J. M., & Waffo-Téguo Pierre, P. (2011). Development of hybrid elution systems for efficient purification of stilbenoids using centrifugal partition chromatography coupled to mass spectrometry. *Journal of Chromatography A*, 1218(36), 6079–6084

Bojczuk, M., Zyzewicz, D & Hodurek, P.(2017). Centrifugal partition chromatography – A review of recent applications and some classic references. *Journal of Separation Sciences*, 40, 1597-1609.

Bonnefont-Rousselot, D. (2016). Resveratrol and Cardiovascular Diseases. *Nutrients*, 8, 250 1–24.

Boutegrabet, L., Fekete, A., Hertkorn, N., Papastamoulis, Y., Waffo-téguo, P., Mérillon, J. M., Jeandet, P., Régis, D & Schmitt-kopplin, P. (2011). Determination of stilbene derivatives in Burgundy red wines by ultra-high-pressure liquid chromatography. *Analytical and Bioanalytical Chemistry*, 401, 1513–1521.

Buratti, C., Barbanera, M., & Lascaro, E. (2015). Ethanol Production from Vineyard Pruning Residues with Steam Explosion Pretreatment. *Environmental Progress & Sustainable Energy*, 34(3), 802-809.

Cacciola, F., Farnetti, S., Dugo, P., Marriott, P. J., & Mondello, L. (2017). Comprehensive two-dimensional liquid chromatography for polyphenol analysis. *Journal of Separation Sciences*, 40, 7-24.

Carre, V., Latouche, G., & Poutaraud, A. (2017). Correlative Analysis of Fluorescent Phytoalexins by Mass Spectrometry Imaging and Fluorescence Microscopy in Grapevine Leaves. *Analytical Chemistry*, 89, 7099-7106.

Castell-auví, A., Cedó, L., Pallarès, V., Blay, M. T., Pinent, M., Motilva, M. J., Garcia-vallvé, S., Pujadas, G., Maechler, P & Ardévol, A. (2012). Procyanidins modify insulinemia by affecting insulin production and degradation. *Journal of Nutritional Biochemistry*, 23, 1565–1572.

Catalgol, B., Batirel, S., Taga, Y., & Ozer, N. K. (2012). Resveratrol: French paradox revisited. *Frontiers in Pharmacology*, 3, 1–18.

Çetin, E. S., Altinöz, D., Tarçan, E., & Göktürk Baydar, N. (2011). Chemical composition of grape canes. *Industrial Crops and Products*, 34(1), 994–998.

Chan, Chi., Trinité, B & Levy, D. Potent Inhibition of HIV-1 Replication in Resting CD4 T Cells by Resveratrol and Pterostilbene. *Antimicrobial Agents and Chemotherapy*, 61, 9, 1-16.

Chen, Z., Jin, K., Gao, L., Lou, G., Jin, Y., Yu, Y., & Lou, Y. (2010). Anti-tumor effects of bakuchiol , an analogue of resveratrol , on human lung adenocarcinoma A549 cell line. *European Journal of Pharmacology*, 643, 170–179.

Correddu, F., Nudda, A., Manca, M. G., Pulina, G., & Dalsgaard, T. K. (2015). Light-Induced Lipid Oxidation in Sheep Milk: Effects of Dietary Grape Seed and Linseed, Alone or in Combination, on Milk Oxidative Stability. *Journal of Agricultural and Food Chemistry*, 63, 3980-3986.

Cotana, F., Barbanera, M., Foschini, D., Lascaro, E & Buratti C. (2015). Preliminary optimization of alkaline pretreatment for ethanol production from vineyard pruning. *Energy Procedia*, 82, 389–394.

D' Attoma, A., Grivel, C., & Heinisch, S. (2012). On-line comprehensive two-dimensional separations of charged compounds using reversed-phase high performance liquid chromatography and hydrophilic interaction chromatography. Part I: Orthogonality and practical peak capacity considerations. *Journal of Chromatography A*, 1262, 148–159.

Das Neves Costa, F., & Leitão, G. G. (2010). Strategies of solvent system selection for the isolation of flavonoids by countercurrent chromatography. *Journal of Separation Science*, 33, 336–347.

De La Iglesia, R., Milagro, F. I., Campi3n, J., Boqu3, N., & Mart3nez, J. A. (2010). Healthy properties of proanthocyanidins. *BioFactors*, 36, 159–168.

Delgado-Torre, M. P., Ferreiro-Vera, C., Priego-Capote, F., P3rez-Juan, P. M., & Luque De Castro, M. D. (2012). Comparison of accelerated methods for the extraction of phenolic compounds from different vine-shoot cultivars. *Journal of Agricultural and Food Chemistry*, 60, 3051–3060.

Delgado de la Torre, M., Priego-Capote, F& Luque de Castro., M.D. (2015). Tentative identification of polar and mid-polar compounds in extracts from wine lees by liquid chromatography – tandem mass spectrometry in high-resolution mode. *Journal of Mass spectrometry*, 50,6,826–837.

Delmas, D., Aires, V., Limagne, E., Dutartre, P., Mazué, F., Ghiringhelli, F., & Latruffe, N. (2011). Transport, stability, and biological activity of resveratrol. *Annals of the New York Academy of Sciences*, 1215(1), 48–59.

Dimou, C., Kopsahelis, N., Papadaki, A., Papanikolaou, S., Kookos, I. K., Mandala, I., & Koutinas, A. A. (2015). Wine lees valorization: Biorefinery development including production of a generic fermentation feedstock employed for poly(3-hydroxybutyrate) synthesis. *Food Research International*, 73, 81–87.

Du, M., Zhang, Z., & Gao, T. (2017). Piceatannol induced apoptosis through up - regulation of microRNA-181a in melanoma cells. *Biological Research*, 50, 36, 1–10.

El-Seedi, H., El-Said, M.A, Khalifa, S., Göransson, U., Bohlin, L., Borg-Karlson, A.K & Verpoorte, R. (2012). Biosynthesis, Natural Sources, Dietary Intake, Pharmacokinetic Properties, and Biological Activities of Hydroxycinnamic Acids. *Journal of Agricultural of Food Chemistry*, 60, 10877–10895.

Esatbeyoglu, T., Ewald, P., Yasui, Y., Yokokawa, H., Wagner, A. E., Matsugo, S., Winterhalter, P & Rimbach, G. (2016). Chemical characterization, free radical scavenging, and cellular antioxidant and anti-inflammatory properties of a stilbenoid-rich root extract of *Vitis vinifera*. *Oxidative Medicine and Cellular Longevity*, 2016, 1-11.

Espinoza, J. L., & Inaoka, P. T. (2017). Gnetin-C and other resveratrol oligomers with cancer chemopreventive potential against cancer. *Annals of the New York academy of Sciences*, 1403, 5-14.

Ewald, P., Delker, U., & Winterhalter, P. (2017). Quantification of stilbenoids in grapevine canes and grape cluster stems with a focus on long-term storage effects on stilbenoid concentration in grapevine canes. *Food Research International*, 100, 326–331.

Fekete, S., Oláh, E., Fekete, J.(2012). Fast liquid chromatography : The domination of core – shell and very fine particles. *Journal of Chromatography A*, 1228, 57–71.

Fernández-Marín, M., Puertas, B., Guerrero, R.,García-Parrilla, M.,Cantos-Villar, E. (2014). Preharvest methyl jasmonate and postharvest UVC treatments: Increasing stilbenes in wine. *Journal of Food Sciences*, 79, C310–C317.

Fontana, A. R., Antonioli, A., & Bottini, R. (2016). Development of a high-performance liquid chromatography method based on a core – shell column approach for the rapid determination of multiclass polyphenols in grape pomaces. *Food Chemistry*, 192, 1–8.

Fu, J., Jin, J., Cichewicz, R., Hageman, S., Ellis, T., Xiang, L., Peng, Q., Jiang, M., Arbez, N., Hotaling, K., Ross, C & Duan W. Trans-(-)-ε-viniferina Increases Mitochondrial Sirtuin 3 (SIRT3), Activates AMP-activated Protein Kinase (AMPK), and Protects Cells in Model of Huntington Disease. *The Journal of Biological Chemistry*, 287(29), 24460-24472.

Gabaston, J., Cantos-villar, E., Biais, B., Waffo-Teguo, P., Renouf, E., Corio-Costet, M-F., Richard, T., & Mérillon, J-M. (2017). Stilbenes from *Vitis vinifera* L. Waste: A Sustainable

Tool for Controlling *Plasmopara Viticola*. *Journal of Agricultural and Food Chemistry*, 65, 2711-2718.

Gambini, J., Inglés, M., Olaso, G., Abdelaziz, K. M., Vina, J., & Borrás, C. (2015). Properties of Resveratrol : *In Vitro* and *In Vivo* Studies about Metabolism, Bioavailability, and Biological Effects in Animal Models and Humans. *Oxidative Medicine and Cellular Longevity*, 2015, 1-13.

Garrido, J., & Borges, F. (2013). Wine and grape polyphenols - A chemical perspective. *Food Research International*, 54(2), 1844–1858.

Giacobbo, A., Matos, J., Meneguzzi, A., Moura, A., Norberta, M., & Pinho, D. (2015). Microfiltration for the recovery of polyphenols from winery effluents. *Separation and Purification Technology*, 143, 12–18.

Giovannelli, L., Innocenti, M., Santamaria, A. R., Bigagli, E., & Pasqua, G. (2016). Antitumoural activity of viniferin-enriched extracts from *Vitis vinifera* L . cell cultures. *Natural Product Research*, 28 (22), 2006-2016.

González-Ruiz, V., Olives, A. I., & Martín, M. A. (2014). Core-shell particles lead the way to renewing high- performance liquid chromatography. *Trends in Analytical Chemistry*, 64, 17-28.

Gorena, T., Saez, V., Mardones, C., Vergara, C., Winterhalter, P., & Von Baer, D. (2014). Influence of post-pruning storage on stilbenoid levels in *Vitis vinifera* L. canes. *Food Chemistry*, 155, 256–263.

Gorena, T., Mardones, C., Vergara, C., Saez, V & Baer, D. von (2015). Evaluation of the Potential of Grape Canes as a Source of Bioactive Stilbenoids, chapter 22, 347-369., In Advances in Wine Research, American Chemical Society Symposium series.

Guerrero, R. F., Biais, B., Richard, T., Puertas, B., Waffo-teguo, P., Merillon, J., & Cantos-villar, E. (2016). Grapevine cane's waste is a source of bioactive stilbenes. *Industrial Crops & Products*, 94, 884–892.

Guo, Y., & Gaiki, S. (2011). Retention and selectivity of stationary phases for hydrophilic interaction chromatography. *Journal of Chromatography A*, 1218(35), 5920–5938.

Ha, D. T., Chen, Q. C., Hung, T. M., Youn, U. J., Ngoc, T. M., & Thuong, P. T. (2009). Stilbenes and Oligostilbenes from Leaf and Stem of *Vitis amurensis* and Their Cytotoxic Activity. *Archives of Pharmacal Research*, 32(2), 177–183.

Hayes, R., Ahmed, A., Edge, T., & Zhang, H. (2014). Core-shell particles: Preparation, fundamentals and applications in high performance liquid chromatography. *Journal of Chromatography A*, 1357, 36–52.

Hollands, W. J., Voorspoels, S., Jacobs, G., Aaby, K., Meisland, A., Garcia-villalba, R., Tomas-Barberan, F., Piskula, M., Mawson, D., Vovkg, I., Needs, P & Kroon, P. A. (2017). Development , validation and evaluation of an analytical method for the determination of monomeric and oligomeric procyanidins in apple extracts. *Journal of Chromatography A*, 1495, 46–56.

Houillé, B., Papon, N., Boudesocque, L., Bourdeaud, E., Besseau, S., Courdavault, V., Enguehard-Gueiffier, C., Delanoue, G., Guérin, L., Bouchara, J-Ph., Clastre, M., Giglioli-

Guivarc'h, N., Guillard, J & Lanoue, A. (2014). Antifungal activity of resveratrol derivatives against *Candida* Species. *Journal of Natural Products*, 77, 1658–1662.

Houillé, B., Besseau, S., Courdavault, V., Oudin, A., Glévarec, G., Delanoue, G., Delanoue, G., Guérin, L., Simkin, A.J., Papon, N., Clastre, M., Giglioli-Guivarc'h & Lanoue, A. (2015). Biosynthetic Origin of E-Resveratrol Accumulation in Grape Canes during Postharvest Storage. *Journal of Agricultural and Food Chemistry*, 63, 1631–1638.

Hümmer, W., & Schreier, P. (2008). Analysis of proanthocyanidins. *Molecular Nutrition and Food Research*, 52 (12), 1381–1398.

Jackson, R.S. (2000). Chemical Constituents of Grapes and Wine, chapter 6, 232-280., *Wine Science, principles and applications*, Academic Press, Third Edition, Elsevier.

Jeandet, P., Delaunois, B., Conreux, A., Donnez, D., Nuzzo, V., Cordelier, S., Clement, C & Courot, E. (2010). Biosynthesis, metabolism, molecular engineering, and biological functions of stilbene phytoalexins in plants. *BioFactors*, 36(5), 331–341.

Jungfer, E., Zimmermann, B. F., Ruttkat, A., & Galensa, R. (2012). Comparing Procyanidins in Selected *Vaccinium* Species by UHPLC-MS² regard to authenticity and healthy effects. *Journal of Agricultural and Food Chemistry*, 60, 9688-9696.

Karacabey, E., & Mazza, G. (2010). Optimisation of antioxidant activity of grape cane extracts using response surface methodology. *Food Chemistry*, 119, 343–348.

Khanal, R.C., Howard, L.R & Prior, R.L. (2009). Procyanidin Content of Grape Seed and Pomace, and Total Anthocyanin Content of Grape Pomace as Affected by Extrusion Processing. *Journal of Food Science*, 74 (6), 174-182.

Karaoglu, M. H., Zor, S & Mehmet, U. (2010). Biosorption of Cr (III) from solutions using vineyard pruning waste. *Chemical Engineering Journal*, 159, 98–106.

Katalinic, V., Mozina, S., Skroza, D., Generalic, I., Abramovic, H., Milos, M., Ljubenkovic, T., Piskernik, S., Pezo, I., Terpin, P & Boban, M. (2010). Polyphenolic profile , antioxidant properties and antimicrobial activity of grape skin extracts of 14 *Vitis vinifera* varieties grown in Dalmatia (Croatia). *Food Chemistry*, 119, 715–723.

Kalili, K. M., & Villiers, A. De. (2013). Systematic optimization and evaluation of on-line , off-line and stop-flow comprehensive hydrophilic interaction chromatography × reversed phase liquid chromatographic analysis of procyanidins , Part I: Theoretical considerations. *Journal of Chromatography A*, 1289, 58–68.

Keylor, M. H., Matsuura, B. S., & Stephenson, C. R. J. (2015). Chemistry and Biology of Resveratrol-Derived Natural Products. *Chemical Reviews*, 115(17), 8976–9027.

Kim, H., Bartley, G. E., Arvik, T., Lipson, R., Nah, S., Seo, K., & Yokoyama, W. (2014). Dietary Supplementation of Chardonnay Grape Seed Flour Reduces. *Journal of Agricultural and Food Chemistry*, 62, 1919 – 1925.

Mc Calley, D. V. (2017). Understanding and manipulating the separation in hydrophilic interaction liquid chromatography C18 Reversed- phase. *Journal of Chromatography A*, 1523, 49–71.

Maier, T., Schieber, A., Kammerer, D. R., & Carle, R. (2009). Residues of grape (*Vitis vinifera* L.) seed oil production as a valuable source of phenolic antioxidants. *Food Chemistry*, *112*(3), 551–559.

Mao, J. T., Xue, B., Smoake, J., Lu, Q., Park, H., Henning, S. M., Burns, W., Bernabei, A., Elashoff, D., Serio, K & Massie, L. (2016). Micro RNA-19a/b mediates grape seed procyanidin extract-induced anti-neoplastic effects against lung cancer. *Journal of Nutritional Biochemistry*, *34*, 118–125.

Mark, L., Nikfardjam, M. S., Avar, P., Ohmacht, R. (2005). A validated HPLC method for the quantitative analysis of trans-resveratrol and trans-piceid in Hungarian wines. *Journal of Chromatographic Sciences*, *43*, 445–449

Martinez-Micaelo, N., González-Abuín, N., Terra, X., Richart, C., Ardèvol, A., Pinent, M., & Blay, M. (2011). Omega-3 docosahexaenoic acid and procyanidins inhibit cyclooxygenase activity and attenuate NF- κ B activation through a p105/p50 regulatory mechanism in macrophage inflammation. *Biochemical Journal*, *441*, 653–663.

Matos, J. T. V, Duarte, R. M. B. O., & Duarte, A. C. (2012). Trends in data processing of comprehensive two-dimensional chromatography: State of the art. *Journal of Chromatography B*, *910*, 31–45.

Michel, T., Destandau, E., & Elfakir, C. (2014). New advances in countercurrent chromatography and centrifugal partition chromatography: focus on coupling strategy. *Analytical and Bioanalytical Chemistry*, *406* (4), 957–969.

Ministerio de Agricultura (2017). Boletín de vino: producción, precios y comercio exterior, <http://www.odepa.gob.cl/boletin/boletin-del-vino-febrero-de-2017/>

Montero, L., Herrero, M., Prodanov, M., Ibáñez, E., & Cifuentes, A. (2013). Characterization of grape seed procyanidins by comprehensive two-dimensional hydrophilic interaction \times reversed phase liquid chromatography coupled to diode array detection and tandem mass spectrometry. *Analytical and Bioanalytical Chemistry*, 405 (13) 4627–4638.

Moss, R., Mao, Q., Taylor, D., & Saucier, C. (2013). Investigation of monomeric and oligomeric wine stilbenoids in red wines by ultra-high-performance liquid chromatography/electrospray ionization quadrupole time-of-flight mass spectrometry. *Rapid Communications in Mass Spectrometry*, 27, 1815–1827.

Naziri, E., Glisic, S. B., Th, F., Tsimidou, M. Z., Nedovic, V., & Bugarski, B. (2016). The Journal of Supercritical Fluids Advantages of supercritical fluid extraction for recovery of squalene from wine lees. *The Journal of Supercritical Fluids*, 107, 560–565.

Neilson, A. P., O’Keefe, S. F., & Bolling, B. W. (2016). High-Molecular-Weight Proanthocyanidins in Foods: Overcoming Analytical Challenges in Pursuit of Novel Dietary Bioactive Components. *Annual Review of Food Science and Technology*, 7(1), 43-64.

Neue, U. D. (2008). Peak capacity in unidimensional chromatography. *Journal of Chromatography A*, 1184, 107–130.

Nivelle, L., Hubert, J., Courot, E., Jeandet, P., Aziz, A., Nuzillard, J., Renault, J-H., Clément, C., Martiny, L., Delmas, D & Tarpin, M. (2017). Anti-Cancer Activity of Resveratrol and Derivatives Produced by Grapevine Cell Suspensions in a 14 L Stirred Bioreactor. *Molecules*, 22, 474, 1-14.

Lambert, C., Richard, T., Renouf, E., Bisson, J., Waffo-Téguo, P., Bordenave, L., Ollat, N., Mérillon, J-M & Cluzet, S. (2013). Comparative analyses of stilbenoids in canes of major *Vitis vinifera* L. cultivars. *Journal of Agricultural and Food Chemistry*, 61, 11392–11399.

Lavelli, V., Torri, L., Zeppa, G., Fiori, L., & Spigno, G. (2016). Recovery of winemaking by-products. *Italian Journal of Food Science*, 28, 542–564.

Li, X., Stoll, D. R., & Carr, P. W. (2009). Equation for Peak Capacity Estimation in Two-Dimensional Liquid Chromatography. *Analytical Chemistry*, 81(2), 845–850.

Oliveira, M., & Duarte, E. (2016). Integrated approach to winery waste : waste generation and data consolidation, *10*(1), 168–176.

Organization Internationale de la Vigne et du Vin. OIV, World Vitiviniculture Situation. OIV Statistical Report on World Vitiviniculture, (2016) 16. <http://www.oiv.int/public/medias/5029/world-vitiviniculture-situation-2016.pdf>.

Ortega, N., Romero, M., Macia, A., Reguant, J., Angles, N., Morelló, J.R & Motilva, M. (2010). Comparative study of UPLC–MS/MS and HPLC–MS/MS to determine procyanidins and alkaloids in cocoa samples. *Journal of Food Composition and Analysis* 23, 298–305.

Ou, K., & Gu, L. (2014). Absorption and metabolism of proanthocyanidins. *Journal of Functional Foods*, 7(1), 43–53.

Papastamoulis, Y., Richard, T., Nassra, M., Badoc, A., Krisa, S., Harakat, D., Monti, J-P., Méryllon, J-M & Waffo-Teguo, P. (2014). Viniphenol A, a complex resveratrol hexamer from *Vitis vinifera* stalks: Structural elucidation and protective effects against amyloid- β -induced toxicity in PC12 cells. *Journal of Natural Products*, 77(2), 213–217.

Pavela, R., Waffo-Teguo, P., Biais, B., Richard, T & Méryllon, J-M- (2017). *Vitis vinifera* canes , a source of stilbenoids against *Spodoptera littoralis* larvae. *Journal of Pest science*, 90(3), 961–970.

Pawlus, A., Sahli, R., Bisson, J., Riviere, C., Delaunay, J., Richard, T., Gomes, E., Bordenave, L., Waffo-Teguo, P & Méryllon, J-M. (2013). Stilbenoid Profiles of Canes from *Vitis* and *Muscadinia* Species. *Journal of Agricultural and Food Chemistry*, 61, 501-511.

Pérez-bibbins, B., Torrado-agrasar, A., Salgado, J. M., Souza, R. P. De, & Domínguez, J.M. (2015). Potential of lees from wine, beer and cider manufacturing as a source of economic nutrients : An overview. *Waste Managment* 40, 72–81.

Piñeiro, Z., Guerrero, R. F., Fernández-Marin, M. I., Cantos-Villar, E., & Palma, M. (2013). Ultrasound-assisted extraction of stilbenoids from grape stems. *Journal of Agricultural and Food Chemistry*, 61, 12549–12556.

Pflieger, A., Teguo, P. W., Papastamoulis, Y., Subra, F., Munir, S., Delelis, O., Lesbats, P., Calmels, C., Andreola, M-L., Merillon, J-M., Auge-Gouillou., C &Parissi, V. (2013).

Natural Stilbenoids Isolated from Grapevine Exhibiting Inhibitory Effects against HIV-1 Integrase and Eukaryote MOS1 Transposase *In Vitro* Activities. *Plos One*, 8(11), 1-13.

Püssa, T., Floren, J., Kuldkepp, P., & Raal, A. (2006). Survey of grapevine *Vitis vinifera* stem polyphenols by liquid chromatography-diode array detection-tandem mass spectrometry. *Journal of Agricultural and Food Chemistry*, 54(20), 7488–7494.

Quiñones, M., Miguel, M & Aleixandre, A. (2013). Beneficial effects of polyphenols on cardiovascular disease. *Pharmacological Research*, 68, 125–131.

Rajha, H. N., Boussetta, N., Louka, N., Maroun, R. G., & Vorobiev, E. (2015). Electrical , mechanical , and chemical effects of high-voltage electrical discharges on the polyphenol extraction from vine shoots. *Innovative Food Science and emerging Technologies*, 31, 60–66.

Reis, G. M., Faccin, H., Viana, C., & Barcellos, M. (2017). *Vitis vinifera* L . cv Pinot noir pomace and lees as potential sources of bioactive compounds. *International Journal of Food Sciences and Nutrition*, 67 (7), 789-796.

Richard, T., Pawlus, A. D., Iglésias, M., Pedrot, E., Waffo-teguo, P, Mérillon, J-M & Monti, J-P. (2011). Neuroprotective properties of resveratrol and derivatives. *Annals of the New York Academy of Sciences*, 1215, 103–108.

Riss, T. L., Moravec, R. A., Niles, A. L., Duellman, S., Benink, H. A., Worzella, T. J., & Minor, L. (2013). Cell Viability Assays. *Assay Guidance Manual*, 114(8), 785–796.

Rivière, C., Pawlus, A. D., & Mérillon, J.-M. (2012). Natural stilbenoids: distribution in the plant kingdom and chemotaxonomic interest in Vitaceae. *Natural Product Reports*, 29, 1317-1333.

Rockenbach, I. I., Jungfer, E., Ritter, C., Santiago-Schübel, B., Thiele, B., Fett, R., & Galensa, R. (2012). Characterization of flavan-3-ols in seeds of grape pomace by CE, HPLC-DAD-MS and LC-ESI-FTICR-MS. *Food Research International*, 48(2), 848–855.

Romain, C., Gaillet, S., Carillon, J., Vidé, J., Ramos, J., Izard, J.-C., Cristol, J.-P., & Rounaet, J.-M. (2012). Vineatrol and Cardiovascular Disease: Beneficial Effects of a Vine-Shoot Phenolic Extract in a Hamster Atherosclerosis Model. *Journal of Agricultural and Food Chemistry*, 60, 11029-11036.

Romo Sánchez, S., Gil Sánchez, I., Arévalo-Villena, M & Briones Pérez, A. (2015). Production and immobilization of enzymes by solid-state fermentation of agroindustrial waste. *Bioprocess and Biosystems Engineering*, 38(3), 587–593.

San José, M., Alvarez, S., García, I., & Peñas, F. J. (2013). A novel conical combustor for thermal exploitation of vineyard pruning wastes. *Fuel*, 110, 178–184.

Sánchez-Gómez, R., Alonso, G., Salinas, M.-R., Zalacain, A. (2017). Reuse of Vine-Shoots Wastes for Agricultural Purposes. *Handbook of Grape Processing By-Products: sustainable Solution*, chapter 4, 79-104, Academic Press, editor: Galanakis, C.

Sánchez-Gómez, R., Garde-Cerdán, T., Zalacain, A., Garcia, R., Cabrita, M. J., & Salinas, M. R. (2016a). Vine-shoot waste aqueous extract applied as foliar fertilizer to

grapevines : Effect on amino acids and fermentative volatile content. *Food Chemistry*, 197, 132–140.

Sánchez-Gómez, R., Zalacain, A., Alonso, G. L., & Salinas, M. R.(2014). Vine-shoot waste aqueous extracts for re-use in agriculture obtained by different extraction techniques: Phenolic, volatile, and mineral compounds. *Journal of Agricultural and Food Chemistry*, 62(45), 10861–10872.

Sánchez-Gómez, R., Zalacain, A., Alonso, G. L., & Salinas, M. R. (2016b). Effect of vine-shoots toasting on the generation of high added value volatiles. *Flavour and Fragrance Journal*, 31(4),293–301.

Schnee, S., Queiroz, E. F., Voinesco, F., Marcourt, L., Dubuis, P. H., Wolfender, J. L., & Gindro, K. (2013). *Vitis vinifera* canes, a new source of antifungal compounds against *Plasmopara viticola*, *Erysiphe necator*, and *Botrytis cinerea*. *Journal of Agricultural and Food Chemistry*, 61, 5459–5467.

Schönnenbeck, C., Trouvé, G., Valente, M., Garra, P., & Brilhac, J. F. (2016). Combustion tests of grape marc in a multi-fuel domestic boiler. *Fuel*, 180, 324–331.

Sharma, A. K., & Kumar, R. (2015). Use of fine wine lees for value addition in ice cream. *Journal of Science and Technology*, 52, 592–596.

Shen, T., Wang, X., & Lou, H. (2009). Natural stilbenes : an overview. *Natural Product Report*, 26, 916–935.

Szkudelski, T., & Szkudelska, K. (2015). Resveratrol and diabetes : from animal to human studies. *Biochimica et Biophysica Acta*, 1852, 1145–1154.

Spigno, G., Maggi, L., Amendola, D., Dragoni, M., & Faveri, D. M. De. (2013). Influence of cultivar on the lignocellulosic fractionation of grape stalks. *Industrial Crops and Products*, 46, 283–289.

Spigno, G., Marinoni, L., & Garrido, G. D. (2017). *State of the Art in Grape Processing By-Products*, chapter 1, 1-28., *Handbook of Grape Processing By-Products*, editor: Galanakis, Elsevier Inc.

Spinelli, R., Nati, C., Pari, L., Mescalchin, E., & Magagnotti, N. (2012). Production and quality of biomass fuels from mechanized collection and processing of vineyard pruning residues. *Applied Energy*, 89, 374–379.

Stockert, J. C., Blázquez-Castro, A., Cañete, M., Horobin, R. W., & Villanueva, Á. (2012). MTT assay for cell viability: Intracellular localization of the formazan product is in lipid droplets. *Acta Histochemica*, 114(8), 785–796.

Stoll, D. R., & Carr, P. W. (2017). Two-Dimensional Liquid Chromatography: A State of the Art Tutorial. *Analytical Chemistry*, 89, 519- 531.

Tao, Y., Wu, D., Zhang, Q., & Sun, D. (2014). Ultrasonics Sonochemistry Ultrasound-assisted extraction of phenolics from wine lees : Modeling, optimization and stability of extracts during storage. *Ultrasonic Sonochemistry*, 21, 706–715.

Teixeira, A., Baenas, N., Dominguez-perles, R., Barros, A., & Rosa, E. (2014). Natural Bioactive Compounds from Winery By-Products as Health Promoters: A Review. *International Journal of Molecular Sciences*, 15(9), 15638–15678.

Timmers, S., Konings, E., Bilet, L., Houtkooper, R. H., van de Weijer, T., Goossens, G., Hoeks, J., van der Krieken, S., Ryu, D., Kersten, S., Moonen-Kornips, E., Hesselink, MC., Kunz, I., Schrauwen-Hinderling, V.B., Blaak, E., Auwerx, J & Schrauwen, P. (2014). Calorie restriction-like effects of 30 days of Resveratrol (resVida™) supplementation on energy metabolism and metabolic profile in obese humans. *Cell metabolism*, 14(5), 612-622.

Tyagi, A., Raina, K., Shrestha, S. P., Miller, B., Thompson, J. A., Wempe, M. F., Agarwal, R & Agarwal, C. (2014). Active Constituent of Grape Seed Extract , Induces Apoptosis in Human Prostate Cancer Cells Via Targeting NF- κ B , Stat3 , and AP1 Transcription Factors Constituent of Grape Seed Extract , Induces Apoptosis in Human Prostate Cancer Cells Via Targeting NF- κ B , Stat3 , and AP1 Transcription Factors. *Nutrition and Cancer*, 66 (4),736-746.

Vergara, C., Von Baer, D., Mardones, C., Wilkens, A., Wernekinck, K., Damm, A., Macke, S., Gorena, T & Winterhalter, P. (2012). Stilbene levels in grape cane of different cultivars in southern Chile: Determination by HPLC-DAD-MS/MS method. *Journal of Agricultural and Food Chemistry*, 60(4), 929–933.

Vinken, M., & Blaauboer, B. J. (2017). In vitro testing of basal cytotoxicity: Establishment of an adverse outcome pathway from chemical insult to cell death. *Toxicology in Vitro*, 39, 104–110.

Vrhovsek, U., Malacarne, G., Masuero, D., Zulini, L., Guella, G., Stefanini, M., Velasco, R & Mattivi, F.(2012). Profiling and accurate quantification of trans- resveratrol, trans-piceid, trans-pterostilbene and 11 viniferins induced by *Plasmopara viticola* in partially resistant grapevine leaves. *Australian Journal of Grape Wine Research*, 18, 11–19.

Willemse, Ch., Stander, M., Vestner, J., Tredoux, A & Villiers, A. De. (2015). Comprehensive Two-Dimensional Hydrophilic Interaction Chromatography (HILIC) × Reversed-Phase Liquid Chromatography Coupled to High-Resolution Mass Spectrometry (RP-LC-UV-MS) Analysis of Anthocyanins and Derived Pigments in Red Wine. *Analytical Chemistry*, (87), 24, 12006-12015.

Winterhalter, P., Kuhnert, S & Ewald, P. (2015). Bioactives from Side Streams of Wine Processing, chapter 21, 337-345. In *Advances in Wine Research*, American Chemical Society Symposium series.

Wu, L., Wang, X., Wang, H., Yang, H., Jia, A., & Ding, Q. (2010). Cytotoxic polyphenols against breast tumor cell in *Smilax china* L. *Journal of Ethnopharmacology*, 130, 460–464.

Xie, L., & Bolling, B. W. (2014). Characterisation of stilbenes in California almonds (*Prunus dulcis*) by UHPLC – MS. *Food Chemistry*, 148, 300–306.

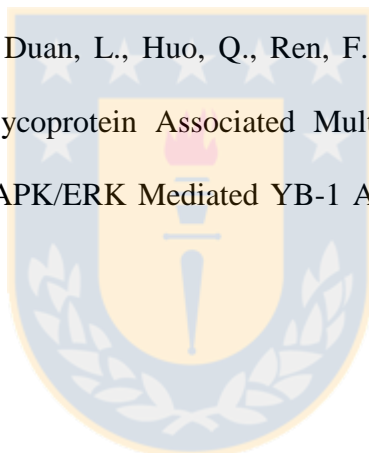
Xue, Y. Q., Di, J. M., Luo, Y., Cheng, K. J., Wei, X., & Shi, Z. (2014). Resveratrol oligomers for the prevention and treatment of cancers. *Oxidative Medicine and Cellular Longevity*, 2014, 1-9.

Yang, K., & Chan, C. B. (2017). Proposed mechanisms of the effects of proanthocyanidins on glucose homeostasis. *Nutrition Reviews*, 75 (8), 642-657.

Zga, N., Papastamoulis, Y., Toribio, a., Richard, T., Delaunay, J. C., Jeandet, P., Renault, P., Monti, J.P., Mérillon, J.M &Waffo-Téguo, P. (2009). Preparative purification of antiamyloidogenic stilbenoids from *Vitis vinifera* (Chardonnay) stems by centrifugal partition chromatography. *Journal of Chromatography B: Analytical Technologies in the Biomedical and Life Sciences*, 877, 1000–1004.

Zhang, A., Wan, L., Wu, C., Fang, Y., Han, G., Li, H., Zhang, Z &Wang, H. (2013). Simultaneous determination of 14 phenolic compounds in grape canes by HPLC-DAD-UV using wavelength switching detection. *Molecules*, 18(11), 14241–14257.

Zhao, B., Sun, Y., Wang, S., Duan, L., Huo, Q., Ren, F., & Li, G. (2013). Grape Seed Procyanidin Reversal of P-glycoprotein Associated Multi-Drug Resistance via Down-regulation of NF- κ B and MAPK/ERK Mediated YB-1 Activity in A2780 /T cells. *Plos One*, 8(8), e71071.



Capítulo 2:

Title:

Oligostilbenoids in Pinot Noir Grape Cane Extract: Isolation, Characterization, Antioxidant Capacity and *in vitro* Anti-proliferative Effect on Cancer Cells

Vania Sáez^a, Edgar Pastene^b, Carola Vergara^a, Claudia Mardones^a, Isidro Hermosín-Gutiérrez^c, Sergio Gómez-Alonso^c, M. Victoria Gómez^c, Cristina Theoduloz^d, Dietrich von Baer^{a*}.

^a Departamento de Análisis Instrumental, Facultad de Farmacia, Universidad de Concepción, P.O. Box 160-C, Concepción, Chile.

^b Laboratorio de Farmacognosia, Facultad de Farmacia, Universidad de Concepción, P.O. Box 160-C, 4070386, Concepción, Chile.

^c Instituto Regional de Investigación Científica Aplicada, Universidad de Castilla-La Mancha, Campus Universitario s/n 13071, Ciudad Real, Spain.

^d Laboratorio de Cultivo Celular, Facultad de Ciencias de la Salud, Universidad de Talca, P.O. Box 747, 3460000, Talca, Chile.

Corresponding author*

dvonbaer@udec.cl

Formato manuscrito, enviado el 03 de diciembre del 2017 a Food Chemistry.

Abstract

The following oligostilbenoids were isolated from extracts of Pinot Noir grape canes produced at a pilot-plant scale: (*E*)- ϵ -viniferin, (*E*)-resveratrol, (*E*)-piceatannol, ampelopsin A, vitisin B, pallidol, (*E*)- δ -viniferin, (*E*)- ω -viniferin, (*E*)-*trans-cis*-miyabenol C, isorhapontigenin, scirpusin A, and a new isomer named iso-scirpusin A. The antioxidant capacity of the isolated stilbenoids was studied by three different assays, and their 50% inhibition concentration (IC₅₀) against cancer cells was determined by MTT reduction assay. Pallidol and (*E*)-*trans-cis*-miyabenol C showed outstanding antioxidant capacity by ORAC-FL assay. The strongest antiproliferative effect was observed for (*E*)-piceatannol and ampelopsin A against the bladder cancer cell line J82. (*E*)-Piceatannol has inhibitory effect on human lung cancer SK-MES-1 cells. Moreover, the whole extract has antiproliferative effect on all tested cell lines. In conclusion, beside (*E*)-resveratrol, grape cane extract contains oligostilbenoids with potential health benefits. This underexploited viticultural residue has the potential to produce valuable phytochemicals or nutraceutical ingredients in functional foods.

Keywords: Grape cane, oligostilbenoids, (*E*)-resveratrol, antioxidant capacity, antiproliferative effect.

Chemical compounds studied in this article:

(*E*)-Resveratrol (PubChem CID 445154); (*E*)- ϵ -Viniferin (PubChem CID 5315233); (*E*)-Piceatannol (PubChem CID 667639); Ampelopsin A (PubChem CID 182999); Vitisin B (PubChem CID 71308302); (*E*)- ω -Viniferin (PubChem CID 72551484); (*E*)- δ -Viniferin

(PubChem CID 11487842); Pallidol (PubChem CID 484757); Scirpusin A (PubChem CID 5458896); Isorhapontigenin (PubChem CID 5318650)



1. Introduction

Stilbenoids are non-flavonoid phenols present in the grape family (*Vitaceae*), and they act as phytoalexins to protect the plant from pathogens. With (*E*)-resveratrol (*trans*-3,4',5-trihydroxystilbene) being their core structure, these stilbenoids are biosynthesized through the phenylpropanoid pathway, a common pathway shared with cinnamic acids and flavonoids. Oligostilbenoids are generated by the oligomerization of resveratrol units to form dimers to octamers with complex and diverse structures (Rivière, Pawlus & Mérillon, 2012). (*E*)-Resveratrol has been shown to have diverse health benefits in neurodegenerative diseases, chronic diseases such as diabetes, cardiovascular diseases (Catalogol, Batirel, Taga & Ozer, 2012), and as a chemopreventive agent in cancer by different cell death pathways (Delmas, Solary & Latruffe, 2011). However, less information is available about oligostilbenoids due to the unavailability or high price of commercial pure compounds. Nevertheless, oligostilbenoids have been reported to have *in vitro* effects against HIV-1 integrase and MOS 1 transposase (Pflieger, Teguo, Papastamoulis, Subra, Munir & Delelis, 2013), cytotoxic and anti-cancer activity (Xue, Di, Luo, Cheng, Wei & Shi, 2014; Wang & Yao, 2015), anti-inflammatory, anti-diabetic effects and antioxidant activity (Wang & Yao, 2015; Nopo-Olazabal, Hubstenberger, Nopo-Olazabal & Medina-Bolivar, 2013). These properties of stilbenoids could be utilized to develop new strategies to prevent (Xue et al., 2014) and treat diseases such as cancer. They could be either combined with cytotoxic agents (Delmas et al., 2011; Xu & Tao, 2015) with fewer side effects, or used as food complements (Vendrely, Peuchant, Buscail, Moranvillier, Rousseau & Bedel, 2017).

Grape (*Vitis vinifera*) wastes from the viticulture industry offer a complex and wide profile of oligostilbenoids from dimers to hexamers (Pawlus, Sahli, Bisson, Rivière, Delaunay & Richard, 2013; Gorena, Sáez, Mardones, Vergara, Winterhalter & von Baer, 2014;

Guerrero, Biais, Richard, Puertas, Waffo-Teguo & Merillon, 2016; Papastamoulis, Richard, Nassra, Badoc, Krisa & Harakat, 2014). The oligostilbenoid concentrations in root extracts is 223–302 g kg⁻¹ (Esatbeyoglu, Ewald, Yasui, Yokokawa, Wagner & Matsugo, 2016; Gabaston, Cantos-Villar, Biais, Waffo-teguo, Renouf & Corio-Coset, 2017), 351 mg g⁻¹ dry weight in the wood extract (Gabaston et al., 2017), 238–542 mg kg⁻¹ dry weight in stem residues (Piñeiro, Guerrero, Fernández-Marin, Cantos-Villar & Palma, 2013; Ewald, Delker & Winterhalter, 2017).

Grape canes are produced during the annual winter pruning of vines. They contain a relatively high amount (803–8485 mg kg⁻¹ dry weight) of oligostilbenoids (Vergara, von Baer, Mardones, Wilkens, Wernekinck & Damm 2012; Lambert, Richard, Renouf, Bisson, Waffo-Tégou & Bordenave, 2013; Gorena et al., 2014; Guerrero et al., 2016; Ewald et al. 2017). Besides containing significant levels of (*E*)-resveratrol (110–6533 mg kg⁻¹ dry weight) (Vergara et al., 2012; Houillé, Besseau, Courdavault, Oudin, Glévarec & Delanoue, 2015; Gorena et al., 2014; Guerrero et al., 2016) and (*E*)-piceatannol (190–1710 mg kg⁻¹ dry weight) (Lambert et al., 2013), this residue can be an interesting source of oligostilbenoids (Guerrero et al., 2016) such as (*E*)- ϵ -viniferin (967–3329 mg kg⁻¹ dry weight) (Lambert et al., 2013; Ewald et al., 2017). The profile also some minor oligostilbenoids, including hopeaphenol (287–1468 mg/kg) (Lambert et al., 2013), ampelopsin A (908–950 mg/kg) (Guerrero, 2016), miyabenol C (22–174 mg/kg) (Lambert, 2013), vitisin B (88–1116 mg/kg) (Lambert, 2013), isohopeaphenol, (*E*)-piceid, and (*E*)- ω -viniferin (Guerrero, 2016). The profile of oligostilbenoids in grape canes depends on the *Vitis* genus, the cultivar, and the growing conditions (Lambert et al., 2013; Guerrero et al., 2016). The highest levels of stilbenoids in canes were reported in Pinot Noir and Gewürztraminer cultivars (Gorena et al., 2015; Guerrero et al., 2016). Furthermore, their

concentration range in grape canes also depends on the storage/treatment of the canes after pruning (Gorena et al., 2015; Houillé et al., 2015; Billet, Houillé, Besseau, Mélin, Oudin & Papon, 2018). For example, the stilbenoid concentration can be increased up to 5–7 fold following at least 3 months of storage at room temperature after pruning (Gorena et al., 2014). Most of this change is attributed to (*E*)-resveratrol, whose concentration is significantly increased in the second month of storage (Vergara et al., 2012; Gorena et al., 2014). The storage temperature and size of canes also influenced this change (Houillé et al., 2015; Billet et al., 2018). The optimal temperature was 15–20 °C: among eight *Vitis* varieties, the (*E*)-resveratrol induction can increase to 106-fold at 20 °C after 6 weeks (Houillé et al., 2015). In Cabernet Franc canes, the key genes involved in the biosynthesis of (*E*)-resveratrol constitutively expressed transcriptional activity with 6 weeks of storage at 20 °C. Meanwhile, abundant transcripts of stilbene synthases (STS) were induced in the first month of storage, proving that the additional (*E*)-resveratrol is from *de novo* synthesis (Houillé et al., 2015). Very recently, the cutting size was also found to modify the time delay in which the stilbenoid levels rise up. If the cane is immediately cut to short pieces after pruning, the time needed to accumulate of stilbenoids is drastically shortened from 6 to 2 weeks, due to a transient expression of phenylalanine ammonia-lyase (PAL) and STS genes (Billet et al., 2018). On fresh canes after pruning at room temperature, the major stilbenoid is (*E*)- ϵ -viniferin (Gorena et al., 2014), and the concentrations of (*E*)-piceatannol increased with storage time in a fashion similar to (*E*)-resveratrol but to a lower extent (Houillé et al., 2015). Moreover, in grape canes, the oligomeric stilbenoids are accumulated during the growing season, whereas monomeric stilbenoids are mainly induced after cane pruning (Houillé et al., 2015).

The oligostilbenoids can be isolated from extracts of *Vitis* tissues by centrifugal partition chromatography (CPC) for stems (Zga, Papastamoulis, Toribio, Richard, Delaunay & Jeandet, 2009), canes (Pawlus et al., 2013; Houillé, Papon, Boudesocque, Bourdeaud, Besseau & Courdavault, 2014, Pavela, R., Waffo-Teguo, P., Benoît, B., Richard, T & Mérillon, J-M, 2017), and roots (Bisson, Poupard, Pawlus, Pons, Darriet & Mérillon, 2011). Therefore, while grape canes are commonly burned or incorporated into the soil, they could also be a source of diverse oligostilbenoids.

In the present study, purified oligostilbenoids were obtained from Pinot Noir extract at a pilot-plant scale, by combining CPC with HPLC. The compounds were further identified by HPLC-Q-Tof and NMR methods. The *in vitro* antioxidant capacity of the isolated oligostilbenoids, as well the viability of cancer cells lines in their presence were tested. The results contribute to increase the scientific background to promote the use of grape cane extracts in the nutraceutical field, thereby adding value to this underutilized residue.

2. Material and methods

2.1 Solvents and reagents

The following chemicals were provided by Merck (Darmstadt, Germany): acetonitrile (HPLC grade) and formic acid used for quantification and isolation of stilbenoids, methanol, ethanol, heptane, ethyl acetate, copper (II) chloride, ammonium acetate, potassium dihydrogen phosphate, and potassium hydrogen phosphate. Acetonitrile (HPLC grade), water (HPLC grade), and formic acid for identification of stilbenoids were purchased from Fisher Scientific (Pittsburg, PA, USA). Potable ethanol (98%) for the pilot extraction was obtained from Oxiquim S.A. (Concepción, Chile). Standards of (*E*)- ϵ -viniferin ($\geq 99.8\%$) were from Phytolab (Vestenbergsgreuth, Germany) and isorhapontigenin

(≥98%) from BOC Sciences (New York, USA). (*E*)-Resveratrol (≥99%), (*E*)-piceatannol (≥98%), neocuproine hemihydrate, 6-hydroxy-2,5,7,8-tetramethylchroman-2-carboxylic acid (Trolox), 2,2'-azino-bis(3-ethylbenzothiazoline-6-sulfonic acid) (ABTS), fluorescein sodium salt, 2,2'-azobis(2-methyl-propionamide)dihydro-chloride (AAPH), 3-(4,5-dimethylthiazol-2-yl)-2,5-diphenyltetrazolium bromide (MTT), and etoposide (E1383) were provided by Sigma (St. Louis, MO, USA).

2.2 Grape cane extract

Healthy Pinot Noir grape canes were pruned in the winter of 2014 at De Neira Vineyard, Bio-Bio region, Chile. After storage for at least 3 months at 20±2 °C, 67.2 kg of the grape canes was cut to 1 cm in length, and extracted in a 1000-L reactor with 672 L of mixed potable ethanol/water (80:20 v/v) at 80°C for 100 minutes. After solvent evaporation, 96.6 L of the extract was obtained. 450 mL of which was freeze-dried in darkness and stored at -20 °C for purification and isolation.

2.3 Purification of extract by centrifugal partition chromatography

The Arizona solvent systems L and K were chosen based on the available CPC methods (Zga et al., 2009; Pawlus et al., 2013; Houillé et al., 2014), the reported partition coefficients (Bisson et al., 2011), and the fact that grape canes with post-pruning storage contain (*E*)-resveratrol and (*E*)- ϵ -viniferin as the major stilbenoids.

The gradient for purification on an SCPC-250L system (Armen Glider, 56890 Saint-Avé, France) used the upper phase of the biphasic system L (2:3:2:3 v/v/v/v heptane: ethyl acetate: methanol: water) and K (1:2:1:2 v/v/v/v heptane: ethyl acetate: methanol: water) Arizona scale as follows: 142 min for L system in ascending mode at 1800 rpm, 20 min

with K system in ascending mode at 1800 rpm, then 25 min of extrusion at 1000 rpm. The flow rates were 6 and 25 ml min⁻¹ for the elution and extrusion steps, respectively. In each run, 3.5 g of freeze-dried extract was dissolved in 10 mL of the L biphasic solvent for injection. Peak detection was made at 306 and 280 nm (Armen Glider spot prep II liquid chromatograph, 56890 Saint-Avé, France). The eluted fractions were evaporated under reduced pressure below 40 °C, and then freeze-dried and stored at -20 °C.

2.4 Identity assignment by HPLC-DAD-QToF and quantification by HPLC-DAD-FL

Identity assignment was carried out using an HPLC-diode array detection (DAD) system (1260 series, Agilent Technologies, Santa Clara, CA, USA) coupled with a Q-ToF mass spectrometer (6545 series, Agilent Technologies, Santa Clara, CA, USA). The separation used an Ascentis Express C18 column (150 mm × 2.1 mm, 1.7 µm particle size, Sigma-Aldrich). The mobile phases consisted of water with 0.1% formic acid (A) and a mixture of methanol: acetonitrile (30:70 v/v) with 0.1% formic acid (B). The injection volume was 5 µL. The gradient was as follows: 0 min, 15% of B; 2 min, 20% of B; 20 min, 45% of B; 22 min, 100% of B; 26 min, 100% of B; 28 min, 15% of B; 30 min, 15% of B; post-time, 8 min. The oven temperature was set at 40°C, and the flow rate was 0.35 ml min⁻¹. The ion source used Agilent jet stream electro spray ionization (AJS ESI) in the negative mode, and the capillary voltage was set at 3750 V. Nitrogen was used as sheath gas (400 °C and flow rate of 12 L min⁻¹), drying gas (325 °C), and collision gas. The nebulizer was set at a pressure of 40 psi. Accurate mass acquisition was made between *m/z* 100 and 1200, and the isolation width was 4 *m/z*. The MS ToF conditions were set as follows: fragmentor, 150; skimmer, 45; and Oct1 RF Vpp, 750. The collision energy (CE) increased linearly in the range of 30–45 eV depending on the *m/z* range (100–1000).

The quantification of stilbenoids was made using a C-18 core-shell column (150 mm × 4.6 mm, 2.7 μm particle size, Halo, Advance Materials Technology) on a Shimadzu Nexera HPLC system (Kyoto, Japan). The injection volume was 15 μL, and the mobile phases were (A) 0.1% formic acid in water and (B) acetonitrile. The steps of the gradient are as follows: at 4 min the mobile phase B was increased from 20% to 35%, to 44% at 7.5 min, and to 100% at 8.5 min. Then, the column was washed with acetonitrile for 2 min, and re-equilibrated using 20% of B for 2 min. The column oven temperature was set at 40 °C, and the flow rate was 1.5 ml min⁻¹. The DAD detection was set at 306, 323, and 280 nm (SPD-M20A, Shimadzu, Kyoto, Japan), and fluorescence detection was carried out at 330 nm for excitation and 374 nm for emission (RF-20 AXS, Shimadzu, Kyoto, Japan).

2.5 Isolation of oligostilbenoids by semi-preparative HPLC-UV

Semi-preparative purification was performed on a C-18 column (10 mm × 250 mm, 5 μm particle size, Kromasil, Akzo Nobel, Bohus, Sweden) on a YL911S binary HPLC pump (Young Ling Instruments, Anyang-si, Gyeonggi-do, Korea). The mobile phase A was 0.1% formic acid in water, and B was acetonitrile. The flow rate was 2.5 ml min⁻¹, and the injection volume was 500 μL. The gradient program was described in the literature (Vergara et al., 2012). The detection was done at 306 and 280 nm with a YL9120S UV/VIS detector (Young Ling Instruments, Anyang-si, Gyeonggi-do, Korea). The isolated oligostilbenoids were stored at -20 °C after freeze drying.

2.6 Structural determination of isolated oligostilbenoids by NMR spectroscopy

For isolated oligostilbenoids, the proton (¹H) and carbon (¹³C) peaks were assigned using ¹H-NMR, ¹H-¹H-COSY, selective 2D experiments, ¹H-¹³C-HSQC, and ¹H-¹³C-HMBC

experiments in deuterated methanol or acetone. The NMR experiments were carried out using a Varian Inova 500 or VNMRS NMR spectrometer operating at 500 or 400 MHz for ^1H and 125 or 100 MHz for ^{13}C .

2.7 Antioxidant capacity of isolated oligostilbenoids

Three different antioxidant capacity assays (CUPRAC, ABTS, and ORAC-FL) were performed for the purified oligostilbenoids, as well as for isorhapontigenin and (*E*)-resveratrol as standards. The assays were made in a 96-well microplate reader (Synergy/HTX multi-mode reader, BioTeK, Winooski, Vermont, USA). CUPRAC and ABTS protocol assays were performed according to Ribeiro, Magalhães, Reis, Lima & Segundo (2011) and Ruiz, Hermosín-Gutierrez, Mardones, Vergara, Herlitz & Vega (2010) with modifications. An ABTS solution (7.5 mM) with $\text{K}_2\text{S}_2\text{O}_8$ (2.5 mM) was diluted with ethanol to obtain an absorbance of 0.7 at 734 nm. The Trolox calibration curve was determined from 2 to 180 μM in ethanol. Into each well was added 190 μL of diluted ABTS radical solution. After 5 minutes at 30 °C, the first read was done at 734 nm. The sample or Trolox calibration point (10 μL) was added, then the well-plate was incubated for 20 minutes at 30 °C. The ORAC-FL assay was realized according to Ou, Chang, Huang & Prior (2013). The Trolox calibration curve was from 1 to 70 μM . All assays were done in triplicate, and the oligostilbenoids were protected from light to avoid isomerizations.

2.8 Antiproliferative assay in human cell lines

The antiproliferative effect was determined by using 3-(4,5-dimethylthiazol-2-yl)-2,5-diphenyltetrazolium bromide (MTT). Four adherent human cell lines were obtained from the American Type Culture Collection (Manassas, VA, USA): MRC-5 normal lung

fibroblasts (ATCC ®, CCL-171TM), AGS gastric adenocarcinoma cells (ATCC®, CRL-1739TM), SK-MES-1 lung cancer cells (ATCC ®, HTB-58TM), and J82 bladder carcinoma cells (ATCC ®, HTB-1TM). MRC-5, J82, and SK-MES-1 cells were grown in Eagle's minimum essential medium that contained 2 mM L-glutamine, 1 mM sodium pyruvate, and 1.5 g L⁻¹ NaHCO₃. AGS cells were grown in Ham's F-12 medium containing 2 mM L-glutamine and 1.5 g L⁻¹ NaHCO₃. All media were additionally supplemented with 10% heat-inactivated fetal bovine serum, 100 IU/mL penicillin G, and 10 mg mL⁻¹ streptomycin. The cells were sub-cultured once a week, and the medium was changed every two days. For the assay, cells were plated in 96-well plates (100 µL/well) at a density of 50,000 cells mL⁻¹. One day after seeding, the cells were treated with the medium containing the compounds at concentrations ranging from 0 to 100 µg mL⁻¹. If compound to be tested was not completely soluble in culture medium, DMSO was added reaching a final concentration of 1%, diluted with complete medium, and incubated for 72 h in a humidified incubator with 5% CO₂ in the air at 37 °C. Untreated cells were used as 100% viability controls. Control cells were grown with complete medium with 1% DMSO. At the end of the incubation, the MTT reduction assay was performed as previously described (Rodriguez & Haun, 1999). The final concentration of MTT was 0.5 mg mL⁻¹, and etoposide (E1383) was used as reference compound. Each experiment was carried out in quadruplicate. The results were transformed to percentage of controls, and the IC₅₀ value was obtained by adjusting the dosage-response curve to a sigmoidal model.

3. Results and Discussion

3.1.Purification of grape cane extract by CPC

The purpose of this step is to obtain enriched fractions of the major stilbenoids and the minor oligostilbenoids in the same run in the shortest possible time. The Arizona solvent

scale offers a wide biphasic composition with different polarities and elution strengths. Systems L and K are suitable for the fractionation of oligostilbenoids from extracts of *Vitis* tissues (Zga et al., 2009; Bisson et al., 2011; Pawlus et al., 2013; Houillé et al., 2014).

In the 14.416 g of the extract injected successively for CPC, 5.6% corresponded to three major and known stilbenoids: (*E*)-resveratrol (1.7%), (*E*)- ϵ -viniferin (3.5%), and (*E*)-piceatannol (0.4%), as shown in the HPLC chromatogram of the whole extract (Figure 1).

By CPC, five stilbenoid-rich fractions were obtained (Table 1 and Figure 1 in Supplementary Material). Each pooled fraction had a predominant oligostilbenoid (Table 1, Supplementary Material). Fractions 1, 2, and 3 contained mainly (*E*)-resveratrol (64.9%), (*E*)- ϵ -viniferin (58.4%) and (*E*) piceatannol (16.9%), respectively.



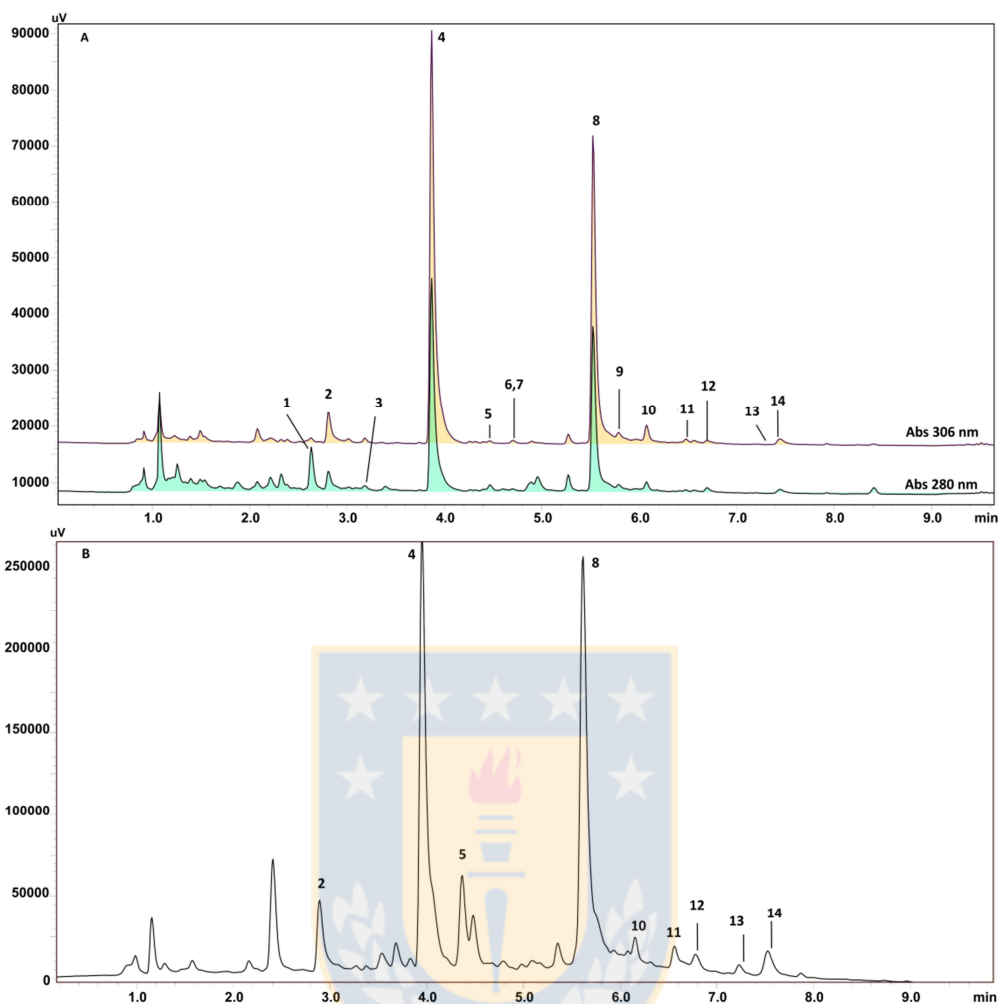


Figure 1: HPLC-DAD-FL chromatograms on the core-shell C18 column. (A): Scale-up extract at 280 and 306 nm. (B): Fluorescence detection at 330 and 374 nm for excitation and emission, respectively. For the peak numbers, see Table 1.

The low percentage of (*E*)-piceatannol is a consequence of the co-elution of (*E*)- ϵ -viniferin and (*E*)-piceatannol in Fraction 3 by CPC separation. This is critical for obtaining a fraction enriched in (*E*)-piceatannol compared to (*E*)- ϵ -viniferin, due to the low amount of the former stilbenoid in the initial pilot plant-scale extract. Fractions 4 and 5 corresponded to enriched fractions of two minor oligostilbenoids in the extract, namely vitisin B and ampelopsin A.

Since commercial standards are not available for both oligostilbenoids, they are quantified as resveratrol equivalents in this step, thereby underestimating the proportion of these minor oligostilbenoids (Lambert et al., 2013). The concentration of vitisin B in the extract is $1.3 \pm 0.1 \text{ mg g}^{-1}$ (expressed as (*E*)-resveratrol equivalents) and reached 2.5% in the fraction. Fraction 5 had 5.4% ampelopsin A and was collected in the extrusion mode, making it free of the co-eluting major stilbenoids. In the pilot plant extract, the concentration of ampelopsin A is low and considered as a trace. Ampelopsin A is a dimeric oligostilbenoid present in grape cane extract at low levels (Gorena et al., 2014; Guerrero et al., 2016). As shown in Table 1, in the different fractions obtained by CPC there were also some minor oligostilbenoids that required further purification. It is possible to tentatively assign the identity of oligostilbenoids based on the MS/MS literature data, although unequivocal identification requires the confirmation by NMR spectra. The minor monomeric stilbenoid isolated along with (*E*)-resveratrol from Fraction 1 has a deprotonated $[M-H]^-$ ion at m/z 257, and the most abundant fragment is m/z 241, which is probably formed for the neutral loss of a methyl radical (16 Da) (Fernández-Marín, Guerrero, García-Parrilla, Puertas, Richard & Rodríguez-Werner, 2012). Based on literature data, two isomeric stilbenoids were consistent with the obtained MS/MS data, namely rhapontigenin (3,3',5'-trihydroxy-4-methoxystilbene) and isorhapontigenin (3,4',5-trihydroxy-3'-methoxystilbene). They have similar UV-absorbance maxima near 325 nm (Hui, Li & Chen, 2011; Fernández-Marín et al., 2012).

Table 1: HPLC-DAD-QToF of oligostilbenoids in the different fractions of CPC separation.

Fraction	Peak	tR ₁ (min)	tR ₂ (min)	λ _{max}	[M-H] ⁻	Fragments	Assignment of oligostilbenoid identity
1	4	3.86	9.17	306, 318	227.0713	185.0606 , 143.0500	(<i>E</i>)-resveratrol
1	5	4.29	10.30	324	257.0828	241.0511 , 224.0485, 172.0532	Monomer (Rhapontigenin*, Isorhapontigenin*)
2	8	5.56	14.71	322	453.1349	411.1220, 359.0925, 347.0922 , 253.0521, 225.0555	(<i>E</i>)-ε-viniferin
2	10	6.07	17.62	323	453.1282	359.0928, 347.0924 , 225.0549, 197.0615	(<i>E</i>)-δ-viniferin*
2	12	6.51	18.73	322	453.1352	435.1241, 411.1234 , 385.1451, 369.1126, 359.0925	(<i>E</i>)-ω-viniferin*
3	2	2.80	6.57	323	243.0665	201.0555, 159.0451	(<i>E</i>)-Piceatannol
3	13	7.35	20.25	317, 332	905.2620	799.2191 , 359.0926	Tetramer

3	9	5.83	15.71	297, 323	679.1982	573.1550 , 451.1183, 345.0768	Miyabenol C*
4	6	4.77	12.04	323	469.1304	385.1091, 375.0851, 347.0925, 359.0931, 241.0511 , 333.1150, 253.0625, 227.0549	Dimer (Scirpusin A*)
4	7	4.87	12.79	327	469.1297	375.0955, 359.0931 , 347.0925 , 341.1125, 265.0497, 241.0502, 109.0292, 227.0713, 213.0562	Dimer (heterodimer)
4	11	6.48	18.38	294, 322	679.1992	573.1562 , 451.1194, 345.0779, 225.0718	Trimer
4	14	7.71	20.59	326	905.2619	799.2170, 451.1155, 359.0921	Vitisin B
5	1	2.65	6.07	280	469.1306	451.1191 , 423.1238, 375.0812, 345.0765	Ampelopsin A
5	3	3.33	8.10	280	453.1354	359.0929, 265.0509 , 93.0343	Pallidol*

tR₁: Retention time with HPLC-DAD-FL., tR₂: Retention time with HPLC-DAD-QToF., *Assignment of Identity based on literature data.

The identity assignments for dimeric oligostilbenoids with the molecular formula $C_{28}H_{22}O_6$ and deprotonated ion at m/z 453 were made according their MS/MS spectra (Table 1). The homodimeric stilbenoid forms based on resveratrol may have two different rings in their structure: an indane ring or a 2,3-dihydrobenzofuran ring (Moss et al., 2013). Pallidol is a symmetrical oligostilbenoid with an indano ring, whose MS/MS data agrees with that for the minor oligostilbenoid in Fraction 5 (Moss et al., 2013). Ampelopsin A and pallidol do not have an olefinic double bond, so they are detectable at 280 nm in the absorbance mode but not in the fluorescence mode.

Two homodimeric stilbenoids were identified as (*E*)- ω -viniferin and (*E*)- δ -viniferin based on their MS/MS spectral data (Moss et al., 2013; Gabaston et al., 2017). The neutral loss of water (18 Da), phenol (94 Da), 4-methylenecyclohexa-2,5-dienone (106 Da), or C_2H_2O (42 Da) generates fragments for these homodimers with m/z 435, 359, 347, and 411. (Kong et al., 2011; Moss et al., 2013). Two heterodimers were isolated from Fraction 4 (Table 1). The MS/MS data of one fits with scirpusin A (Moss et al., 2013). For the other heterodimer, it was not possible to assign a tentative identity with the DAD and MS/MS data. One of the trimers could possibly be (*E*)-miyabenol C (Moss et al., 2013; Gabaston, 2017), which exhibits fragments at m/z 573, 451, and 345. This fits with the fragment pathway described by Moss et al. (2013). However, there exist at least three stereoisomers of miyabenol C: (*E*)-*trans-cis*-miyabenol C, (*E*)-*cis-cis*-miyabenol C, and (*E*)-*cis-trans*-miyabenol C (Papastamoulis, Bisson, Tamsamani, Richard, Marchal & Mérillon, 2015).

3.2. Purification of the major and minor oligostilbenoids by semi-preparative HPLC-UV

The amounts of (*E*)-resveratrol isolated by semi-preparative HPLC-UV purification were 81.7 mg from Fraction 1 and 20.1 mg from Fraction 2 with 99% purity. Their combined yield of (*E*)-resveratrol in the initial pilot extract was 40.7%. In addition, 197.2 mg of (*E*)- ϵ -viniferin was isolated, 182.3 mg (98% purity) of which from Fraction 2 and 14.9 mg (94% purity) from Fraction 4. The total yield of (*E*)- ϵ -viniferin, calculated as its content in the pilot plant extract, was 39.4%. In the case of (*E*)-piceatannol, 13.4 mg was isolated by semi-preparative HPLC, of which 10.9 mg (93.9%) was from Fraction 3 and 2.5 mg came from Fraction 4. The recovery of (*E*)-piceatannol from the starting material was 23.6%.

Vitisin B (14.8 mg, purity 94.4%) and ampelopsin A (17.5 mg, purity 94.2%) were isolated from Fractions 4 and 5. Their identities were corroborated with the ^1H and ^{13}C NMR data. In the case of ampelopsin A, it was fundamental to use the data obtained by HMBC experiment (Supplementary data, Table 2).

The identities of the minor oligostilbenoids were confirmed by NMR. Isorhapontigenin was isolated and confirmed as the minor stilbenoid that co-eluted with (*E*)-resveratrol in Fraction 1. Despite the low amount isolated (<1 mg), it was possible to confirm the identity through ^1H -NMR (Supplementary Material, Table 3). Isorhapontigenin had been detected in wine grapes (Fernández-Marín et al., 2012) and stems of Sauvignon Blanc vines (19.8 mg/kg dry weight) collected after destemming process for winemaking (Piñeiro et al., 2013). To the best of our knowledge, isorhapontigenin has not been previously reported and isolated from grape cane extracts.

The homodimers were isolated from CPC Fractions 2 and 5: 3.3 mg of (*E*)- δ -viniferin, 1.1 mg (*E*)- ω -viniferin, and 2.13 mg of pallidol with purities of 90%. Their identities were

unequivocally corroborated by ^1H and ^{13}C NMR and HMBC experiments (Supplementary Material, Tables 4 and 5). (*E*)- ω -Viniferin was reported in leaves of hybrid *Vitis vinifera* (Merzling x Teroldego) infected with *Plasmopara viticola* (Mattivi et al., 2011). Later, it was reported and quantified in canes of Muscadinia grape species (65–365 mg/kg dry weight), and just detected but not quantified in a Cabernet Sauvignon cane extract (Pawlus et al., 2013). (*E*)- δ -Viniferin was reported in stressed leaves of *Vitis* (Pezet, Perret, Jean-Denis, Tabacchi, Gindro & Viret, 2003) and also in wine (Moss, 2013). Recently, (*E*)- δ -viniferin, (*E*)- ω -viniferin, and pallidol were reported in extracts from viticulture residues like wood, roots, and grape cane extract (Gabaston et al., 2017). In contrast to pallidol and (*E*)- ω -viniferin, (*E*)- δ -viniferin was detected but could not be quantified in these extracts due the low concentration.



Table 2: ^1H , ^{13}C and HMBC data for scirpusin A and its structural isomer in acetone- d_6 and methanol- d_4 .

	Scirpusin A*				Iso-scirpusin A*				Iso-scirpusin A**			
	$\delta^1\text{H}$ (ppm)	$J_{\text{H,H}}$ (Hz)	$\delta^{13}\text{C}$ (ppm)	HMBC	$\delta^1\text{H}$ (ppm)	$J_{\text{H,H}}$ (Hz)	$\delta^{13}\text{C}$ (ppm)	HMB C	$\delta^1\text{H}$ (ppm)	$J_{\text{H,H}}$ (Hz)	$\delta^{13}\text{C}$ (ppm)	HMBC
Benzenic A₁			134.9	H-5a; H-7a; H-8a			147.8	H-8a			134.0	H-3a,5a; H-8a
2a	6.83 d	2.0	113.4	H-6a; H-7a	7.20 d	8.8	127.6	H-7a	7.13 d	8.7	128.2	H-7a
3a			146.0	H-5 ^a	6.83 d	8.8	115.8		6.76 d	8.8	116.1	
4a			145.9	H-2a; H-6a			157.9	H- 2a,6a			158.3	H-2a,6a
5a	6.80 d	7.8	116.0		6.83 d	8.8	115.8		6.76 d	8.8	116.1	
6a	6.70 dd	7.8; 2.0	118.1	H-2a; H-7a	7.20 d	8.8	127.6	H-7a	7.13 d	8.7	128.2	H-7a
Dihydropyran A												
7a	5.36 d	4.9	93.9	H-2a; H-6a; H-8a	5.42 d	5.4	64.1		5.34 d	5.9	94.7	H-2a,6a; H-8a
8a	4.45 d	4.9	57.1	H-7 ^a	4.47 d	5.4	57.4	H- 10a,1 4a	4.34 d	5.9	57.8	H- 10a,14a
Benzenic A₂												
9a			147.6	H-7a; H-8a			147.5	H-7a			147.5	H-7a; H- 8a
10a	6.23 brs		106.9	H-12a; H-8a	6.25 d	2.0	106.6	H- 12a;	6.14 d	1.9	107.3	H-12a; H-8a

11a			159.8	H-10a,14a; H-12a				H-8a			159.8	H-12a
12a	6.23 brs		102.0	H-10a,14a	6.22 t	2.0	101.9	H-10a,14a	6.17 brt	1.9; 2.5	102.1	H-10a,14a
13a			159.8	H-10a,14a; H-12a							159.8	H-12a
14a	6.23 brs		106.9	H-12a; H-8a	6.25 d	2.0	106.6	H-12a; H-8a	6.14 d	1.9	107.3	H-12a; H-8a
Benzenic B₁												
1b			130.1	H-8b; H-3b,5b			130.5	H-8b; H-5b; H-6b			130.9	H-5b; H-8b
2b	7.19 d	8.3	128.7	H-7b	6.89 d	1.5	113.7	H-7b	6.69 d	1.9	113.9	H-7b; H-6b
3b	6.73 d	8.3	116.3								146.5	H-5b
4b			158.2	H-2b,6b; H-3b,5b							146.5	H-2b; H-6b
5b	6.73 d	8.3	116.3		6.69-6.71 m		104.1		6.63 d	8.3	116.1	H-7b
6b	7.19 d	8.3	128.7	H-7b	6.69-6.71 m		115.8		6.57 dd	8.3; 2.0	119.9	H-7b; H-2b
Olefin B												
7b	6.91 d	16.6	129.9	H-	6.85 d	16.6	115.8		6.76 d	16.2	130.8	H-2b

8b <i>Benzenic B₂</i> 9b	6.72 d	16.6	123.4	2b,6b H-14b	6.68 d	16.0	119.6	H-14b	6.53 d	16.6	123.9	H-14b
			136.4	H-7b; H-8b; H-14b							137.0	H-7b
10b			119.8	H-8b; H-8a; H-12b; H-14b			134.2	H-8a			119.7	H-14b; H-8b; H- 8a
11b			162.5	H-12b; H-7a; H-8a			130.5	H-8b			162.5	H-8a
12b 13b	6.32 d	2.0	96.7	H-14b	6.32 d	2.0	96.5		6.24 d	2.5	96.7	H-14b
14b	6.72 d	2.0	104.1	H-8b; H-12b	6.69- 6.71 m		104.1		6.62 d	2.4	104.4	H-8b
											ND	

* data acquired in acetone-d₆ and ** methanol-d₄. ND: not detected, brs: broad singlet

Additionally, two stilbenoid heterodimers were isolated from CPC Fraction 4. One of them was confirmed to be scirpusin A (2.8 mg, 92.4% purity) by ^1H -, ^{13}C -NMR and HMBC data (Table 2). Scirpusin A was previously described and isolated from stems of wine grapes (Kong et al., 2011), Merlot stalks (Pflieger et al., 2013; Papastamoulis et al., 2014), and canes of *V. rotundifolia* (Pawlus et al., 2013). The unknown heterodimer (1.0 mg, 93.4% of purity) has a MS/MS fragmentation pattern similar to scirpusin A (Table 1). ^{13}C - and ^1H -NMR data obtained in deuterated acetone (Table 2) suggest that this oligostilbenoid has the same structural core skeleton as scirpusin A: a double *trans* bond, a benzohydropyran ring, and three phenolic rings in concordance with MS/MS data. When the solvent is changed to deuterated methanol (Table 2), the ^1H NMR spectra confirmed the core structure, and it was possible to avoid the overlapping of some signals as observed in the spectra recorded in acetone- d_6 . The data indicate that this oligostilbenoid is a scirpusin A structural isomer (Figure 2). The HMBC experiments confirmed that the phenol rings A_1 and A_2 are bound to a benzohydropyran ring in position 7a (correlation with H-2a, 6a; H-8a) and 8a (correlation with H-10a, 14a). The HMBC data also confirmed that B_2 and B_1 rings are joined through an olefin. The key is the long-range coupling of H-8b with C-1b, C-10b, and C-14 b. The stereochemistry of this structural isomer of H-7a and H-8 could not be resolved, despite the $J_{\text{H-H}}$ values for H-7 and H-8 for scirpusin A (4.9 Hz) and the isomer (5.4 Hz) are closer for the analogous nucleus in the spectrum acquired in acetone- d_6 . NOESY experiments could resolve the uncertainty of isomer stereochemistry, but they were not possible here due to the low quantity of the isolated compound. Nevertheless, evidence of this kind of heterodimer was provided by accurate MS/MS (Moss et al., 2013). These authors discussed the possibility of an unreported isomer of scirpusin A, since the fragmentation of both dimers is similar to or perhaps is ampelopsin A.

Based on the fragmentation pathway proposed for homodimers (Kong et al., 2011; Moss et al., 2013), a fragmentation pathway for heterodimers is proposed and shown in Figure 2. Iso-scirpusin A has intensity for the fragments at m/z 375 and m/z 359, which very likely correspond to the losses of phenol (94 Da) and resorcinol (110 Da), respectively. However, for both heterodimers these fragments are characteristic, as well as the fragment at m/z 347. The fragment at m/z 265 observed for iso-scirpusin A could be caused by the loss of phenol (94 Da) and resorcinol (110 Da), and is consistent with that proposed by Moss et al. (2013). The fragment at m/z 241 is characteristic for scirpusin A, but not for its isomer. This is due to the neutral loss of resveratrol (228 Da), as well the fragment at m/z 333 due to the successive neutral loss of 94 Da (C_6H_6O) and 42 Da (C_2H_2O). The fragment at m/z 385 may be formed by the elimination of 84 Da (two C_2H_2O). A structural isomer of scirpusin A was reported only in red wine (Moss et al., 2013). To the best of our knowledge, it is the first time that such isomer of scirpusin A is reported in grape cane or other parts of grapevines. The identity of (*E*)-miyabenol C (6.2 mg, 90.4% purity) was confirmed by ^{13}C -, 1H -NMR and HMBC data (Supplementary data, Table 6). It corresponds to (*E*)-*trans-cis*-miyabenol C according to the NMR data reported for this oligostilbenoid isolated from Merlot grapevine stalks (Papastamoulis et al., 2015). In *Vitis* tissues, (*E*)-miyabenol C was reported and identified in *V. vinifera* root extract (Esatbeyoglu et al., 2016; Gabaston et al., 2017), wood (Gabaston et al., 2017), and extract from a mixture of Cabernet Sauvignon and Merlot canes (Gabaston et al., 2017). However, most of these studies did not specify the stereoisomer. An unknown trimer (1.4 mg) and a tetramer (6.8 mg) were also isolated in the present work (Peaks 11 and 13 in Figure 1), but it was not possible to elucidate their structures due the low quantity for the trimer and the instability of the purified tetramer.

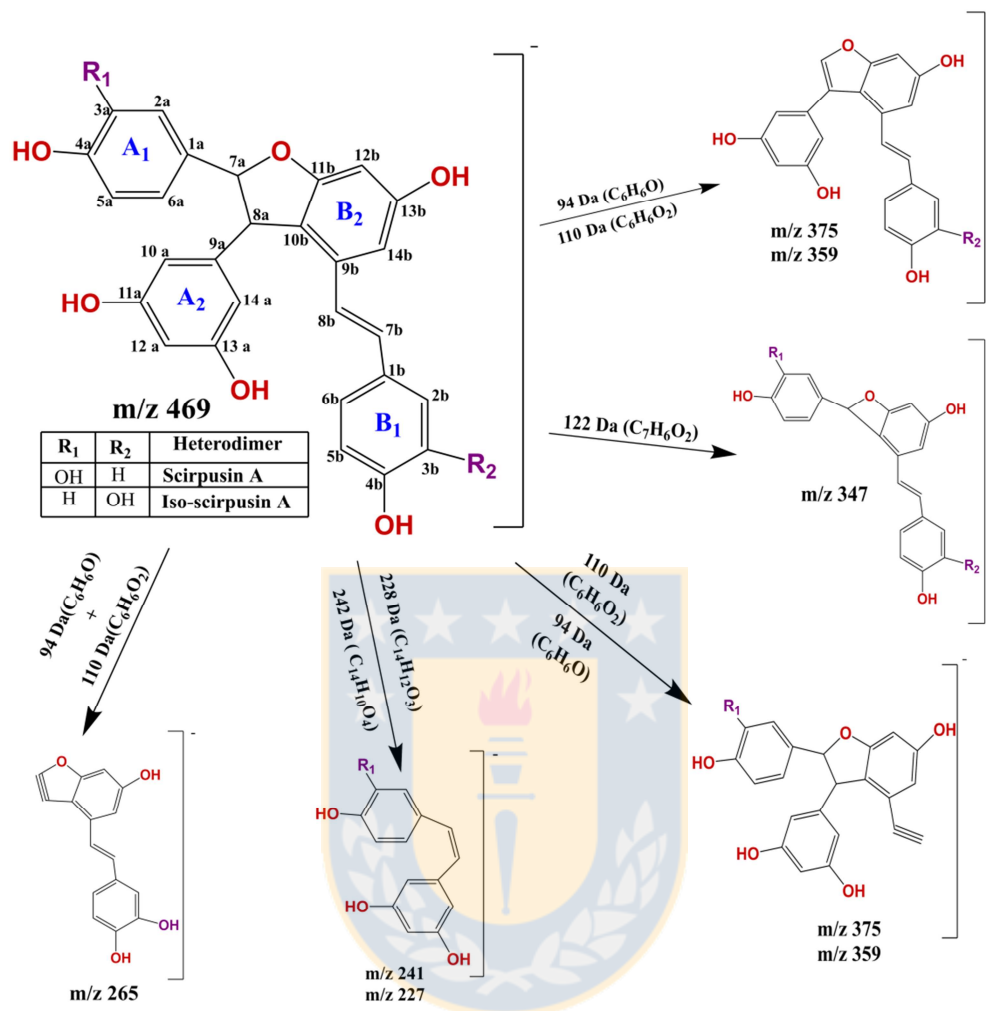


Figure 2: Chemical structures of heterodimers isolated from the pilot plant extract of Pinot Noir grape canes, and the proposed fragmentation pathways.

3.3 Antioxidant capacity of stilbenoids

The *in vitro* antioxidant capacity of isolated oligostilbenoids was determined by three different assays (Table 3). They measure the radical antioxidant scavenging potential (ABTS^{•+}), the Cu²⁺ reducing power (CUPRAC), and protective effect against oxidation produced by a radical generator (ORAC-FL).

ABTS and CUPRAC are considered electron-transfer (ET) based methods with similar characteristics and closer reduction potential, while ORAC-FL is considered a hydrogen atom-transfer (HAT) method. The antioxidant capacity was evaluated by increasing the concentrations of purified oligostilbenoids (Supplementary data, Figure 3). As shown in Table 3, the purified oligostilbenoids exhibited a stronger antioxidant capacity than (*E*)-resveratrol by ORAC-FL. Pallidol and (*E*)-*trans-cis*-miyabenol C showed similar and the greatest antioxidant capacity among the isolated oligomers, while those of ampelopsin A and (*E*)- δ -viniferin were also similar. There is no relationship between the number of hydroxyl groups in the structure of oligostilbenoids and their antioxidant capacity. This fits with data reported recently by Rodríguez-Bonilla, Ganía-Herrero, Matencio, García-Carmona & López-Nicolás (2017).



Table 3: TEAC_{CUPRAC, ABTS} and ORAC-FL for oligostilbenoids isolated.

Oligostilbenoid	ABTS	CUPRAC	ORAC-FL
	TEAC	TEAC	TEAC
	(μ M)	(μ M)	(μ M)
<i>(E)</i> -resveratrol	24.89 \pm 3.85	17.28 \pm 0.95 _a	5.40 \pm 0.37 _a
Isorhapontigenin	51.62 \pm 4.12 _a	24.88 \pm 1.28	11.08 \pm 0.32
<i>(E)</i> -piceatannol	73.00 \pm 9.28 _{a,b,c,d}	24.22 \pm 2.29	6.63 \pm 0.09 _a
<i>(E)</i> - ϵ -viniferin	46.56 \pm 8.55 _b	18.72 \pm 0.78 _a	9.93 \pm 0.20 _{c,d}
<i>(E)</i> - δ -viniferin	60.89 \pm 3.47	19.90 \pm 0.87	14.04 \pm 2.52 _c
<i>(E)</i> - ω -viniferin	<LoQ	<LoQ	8.00 \pm 0.50 _b
Ampelopsin A	56.33 \pm 1.67 _c	19.43 \pm 0.20	14.29 \pm 0.66 _d
Scirpusin A	25.85 \pm 4.04	23.12 \pm 2.26	16.46 \pm 0.84
Pallidol	32.57 \pm 6.23	10.90 \pm 1.25	25.56 \pm 1.57
<i>(E)</i> - <i>trans-cis</i> -miyabenol C	34.00 \pm 5.15	25.06 \pm 2.43	27.68 \pm 5.84
Unknown Tetramer	45.38 \pm 3.29 _d	25.26 \pm 1.75	12.30 \pm 5.62
Vitisina B	43.95 \pm 3.59	26.17 \pm 1.06	8.49 \pm 0.18 _b

TEAC: Trolox equivalent antioxidant capacity. The data presented are the mean \pm standard deviation (SD) of three replicates, TEAC_{ABTS, CUPRAC} for oligostilbenoid at 10 μ M. For ORAC-FL at 1 μ M. LoQ: limit of quantification. Lower letters indicated significant differences ($P < 0.05$).

In a quantitative structure-antioxidant activity study of diverse stilbenoids based on the density functional theory, Mikulski & Molski (2010) concluded that these compounds are capable of scavenging radicals mainly by HAT and less by ET mechanism. This was confirmed by the present results (Table 3), in which a higher antioxidant capacity was observed with the ORAC-FL test based on HAT, compared to those tests based on ET.

If the oligostilbenoid radical has a planar stilbenoid moiety and a quinone or semi-quinone form, then it contributes favorably to scavenging radicals (Mikulski & Molski, 2010). Pallidol has a symmetrical structure, differing from the other tested stilbenoids. The absence of the typical resveratrol core in pallidol can help to explain its high antioxidant capacity by ORAC-FL assay. Previous theoretical studies showed that the octane skeleton bends in the radical form, and the planar *trans*-stilbene moiety is lacking. However, the symmetric geometry gives similar stability to all hydroxyl bonds, therefore the hydroxyl groups have similar reactivity to scavenge radicals in biological systems (Mikulski & Molski, 2010). Results of the present work are in agreement with the high efficiency of pallidol to scavenge free radicals. The assays for vitisin B had to be repeated, because a HPLC-DAD-MS/MS reanalysis revealed the presence of a second tetramer after purification, freeze drying, and storage at $-20\text{ }^{\circ}\text{C}$ in darkness. To eliminate this new tetramer, which affected the antioxidant capacity (Supplementary data, Table 8), vitisin B was re-purified and its antioxidant capacity immediately determined (Table 3).

For ABTS and CUPRAC assays (Table 4), the antioxidant capacity was measured at $10\text{ }\mu\text{M}$ for each compound. In both assays, (*E*)-resveratrol exhibited one of the lowest antioxidant capacities compared with other tested stilbenoids, whereas (*E*)-piceatannol ($73.0 \pm 9.3\text{ }\mu\text{M TEAC}$) and (*E*)- δ -viniferin ($60.9 \pm 3.5\text{ }\mu\text{M TEAC}$) showed the strongest antioxidant capacity in ABTS assay. (*E*)-Piceatannol and (*E*)- ϵ -viniferin have higher antioxidant capacity than (*E*)-resveratrol with the ABTS method, in agreement with data reported by Nopo-Olazabal et al. (2013). (*E*)-Resveratrol ($24.8 \pm 3.8\text{ TEAC }\mu\text{M}$) and scirpusin A ($25.8 \pm 4.0\text{ TEAC }\mu\text{M}$) have the lower values.

In the case of CUPRAC assay, the higher values of TEAC were observed for (*E*)-*trans-cis*-miyabenol C and vitisin B. Differing from the other stilbenoids, (*E*)- ω -viniferin did not

exhibit any appreciable antioxidant capacity when measured in the ET methods, in contrast with the other homodimers having a similar skeleton.

3.4 Antiproliferative assay in human cell lines

The *in vitro* antiproliferative activity of stilbenoids on four different cell lines (MRC-5, AGS, SK-MES-1, and J82) was determined by means of the MTT reduction assay. The results are expressed as IC₅₀ (µg mL⁻¹), defined as the concentration that inhibits the cell growth by 50%. As shown in Table 4, for normal MRC-5 cells, no significant difference was observed between ampelopsin A and (*E*)-ε-viniferin, whereas (*E*)-resveratrol had the lowest IC₅₀. It was not possible to obtain the IC₅₀ for (*E*)-piceatannol, which is less active in MRC-5 cells.

(*E*)-Resveratrol was more active in the inhibition of gastric adenocarcinoma cells (AGS) than the oligostilbenoids tested. In previous studies with these cell lines, (*E*)-resveratrol is postulated as a possible gastric cancer chemopreventive agent. It suppressed the cell proliferation by the stimulation of caspase 3 and cytochrome oxidases, the breakdown of nuclear proteins, and also the loss of cell viability and increased cell senescence (Zulueta, Caretti, Signorelli & Ghidoni, 2015). The whole pilot plant extract could also suppress the proliferation of AGS cells, which can be attributed mainly to its high resveratrol content.

As shown in Table 4, for the human squamous cell lung carcinoma (SK-MES-1), (*E*)-piceatannol showed a significantly lower IC₅₀ than (*E*)-ε-viniferin. The whole pilot plant extract showed an intermediate activity, whereas (*E*)-resveratrol and ampelopsin A showed no appreciable effect. Contrasting with these results, previous publications reported inhibitory effects (by MTT assay) on these cells treated with pterostilbene (*trans*-3,5-dimethoxy-4-hydroxystilbene), a dimethylated analog of (*E*)-resveratrol, although no data

has been reported for (*E*)-resveratrol with this cell line. Pterostilbene is an antiproliferative agent by caspase-dependent apoptosis (Schneider, Alosi, McDonald & McFadden et al., 2010).

In the case of piceatannol, it has to be pointed out that while in the present work it was more active in inhibiting SK-MES-1 cells, for another lung cancer cell line (non-small cell type, A549) it also enhanced the cytotoxic and apoptotic effects of gemcitabine. This synergistic combination increased the expression of the Bcl-2 pro apoptotic protein family. However, there is no evidence of the alterations in cytochrome c expression and the caspases for the apoptotic process in A549 cancer cells (Xu & Tao, 2015).

For the J82 cell line of bladder cancer, the lowest IC_{50} values were observed for (*E*)-piceatannol and ampelopsin A. Surprisingly, the whole pilot plant extract showed the lowest growth inhibiting concentration with J82 cells. This trend was not observed for the other tested cell lines, indicating that J82 is more susceptible to the whole pilot plant extract. In 2017, more than 70000 new cases of bladder cancer and 16870 associated deaths are expected in the USA alone (Cancer facts & figures, 2017). As far as we know, this study is the first one on this cell line treated with stilbenoids. The mechanism and signaling pathway for the current inhibiting effects are unknown, and therefore further study is needed for the potential applications. However, the antiproliferative activity of the oligostilbenoids is lower on all tested cancer cells than the synthetic drug etoposide used as positive control.

Table 4: IC₅₀ values for isolated stilbenoids, whole cane extract and synthetic etoposide on different cell lines expressed in µg mL⁻¹ and µM (in parenthesis).

Stilbenoid	Cell lines			
	MRC-5	AGS	SK-MES-1	J82
<i>(E)</i> -resveratrol*	10.1 ± 0.6^a (44.6 ± 2.9)	4.29 ± 0.1^a (18.8 ± 0.8)	> 22.8 (>100)	10.1 ± 0.6^a (44.5 ± 2.9)
<i>(E)</i> -ε-viniferin	22.6 ± 1.3^b (49.9 ± 3.0)	19.3 ± 0.7^b (42.6 ± 1.7)	35.8 ± 1.4^a (78.8 ± 3.3)	25.7 ± 0.5^b (56.7 ± 1.2)
<i>(E)</i> -piceatannol	> 45.4 (>100)	10.8 ± 0.7^c (44.4 ± 3.2)	7.64 ± 0.5^b (31.3 ± 2.1)	6.7 ± 0.3^c (27.7 ± 1.4)
Ampelopsin A	21.0 ± 1.3^b (44.8 ± 2.9)	22.7 ± 2.1^d (48.3 ± 4.6)	> 47 (>100)	14.1 ± 1.0^d (30.0 ± 2.3)
Whole extract **	57.5 ± 2.5^e	23.3 ± 1.3^f	45.0 ± 3.6^g	9.6 ± 0.7^h
Etoposide	2.2 ± 0.1 (3.9 ± 0.2)	0.23 ± 0.0 (0.4 ± 0.0)	1.5 ± 0.0 (2.6 ± 0.1)	1.6 ± 0.1 (2.8 ± 0.2)

MRC-5: normal lung fibroblast.

AGS: human gastric adenocarcinoma.

SK-MES-1: human lung cancer.

J82: human bladder carcinoma.*(*E*)-resveratrol standard. In each column for isolated stilbenoids in upper letters indicated the significant difference (p<0.001) by Tukey-Kramer multiple comparison test, after one-way ANOVA. **For the whole extract the significance test was made between the different cell lines

4. Conclusions

Grape canes could be a source of valuable, high-purity oligostilbenoids that have prominent antioxidant capacity and antiproliferative activity in cancer cell lines. From a Pinot Noir grape cane extract were isolated mainly (*E*)- ϵ -vinifera, (*E*)-resveratrol, (*E*)-piceatannol, and also ampelopsin A and vitisin B. Additionally, some minor oligostilbenoids, such as (*E*)- δ -viniferin, (*E*)- ω -viniferin, pallidol, scirpusin A, isorhapontigenin, and (*E*)-*trans-cis*-miyabenol C were isolated. Furthermore, a new heterodimer and structural isomer of scirpusin A, named iso-scirpusin A, was isolated.

Pallidol and (*E*)-*trans-cis*-miyabenol C showed a remarkably high antioxidant capacity in the ORAC-FL assay, in which all other oligostilbenoids performed better than (*E*)-resveratrol. The whole extract has antiproliferative effect by MTT assay in three human cancer cell lines, with the strongest effect against J82. To the best of our knowledge, it is the first time that the J82 bladder cancer cell line is treated with stilbenoids. (*E*)-Piceatannol and ampelopsin A also showed better antiproliferative effects on J82 cells than (*E*)-resveratrol and (*E*)- ϵ -viniferin. Interestingly, (*E*)-piceatannol affects the SK-MES-1, AGS, and J82 cancer cell lines, but showed no appreciable effect on the MRC-5 normal lung fibroblast cells. Therefore, the grape cane extract, as well as the oligostilbenoids isolated from it, can have potential applications in the nutraceutical field.

Acknowledgments

This work received financial support from FONDECYT Grant 1150721, FONDEQUIP Grant EQM150025, PhD scholarship, and PFB-27 Grant (all from CONICYT, Chile); and CORFO Grant 14 IDL2-30156.

References:

1. Billet, K., Houillé, B., Besseau, S., Mélin, C., Oudin, A., Papon, N., Courdavault, V., Clastre, M., Giglioli-Guivarc'h, N., & Lanoue, A. (2018). Mechanical stress rapidly induces *E*-resveratrol and *E*-piceatannol biosynthesis in grape canes stored as a freshly-pruned byproduct. *Food Chemistry*, 240 (July 2017), 1022–1027.
2. Bisson, J., Poupard, P., Pawlus, A. D., Pons, A., Darriet, P., Mérillon, J. M., & Waffo-Téguo (2011). Development of hybrid elution systems for efficient purification of stilbenoids using centrifugal partition chromatography coupled to mass spectrometry. *Journal of Chromatography A*, 1218(36), 6079–6084.
3. Cancer facts & figures 2017. <https://www.cancer.org/research/cancer-facts-statistics/all-cancer-facts-figures/cancer-facts-figures-2017.html> Accessed: 29.10.2017
4. Catalgol, B., Batirel, S., Taga, Y., & Ozer, N. K. (2012). Resveratrol: French paradox revisited. *Frontiers in Pharmacology*, 3 JUL(July), 1–18.
5. Delmas, D., Solary, E., & Latruffe, N. (2011). Resveratrol, a phytochemical inducer of multiple cell death pathways: apoptosis, autophagy and mitotic catastrophe. *Current Medicinal Chemistry*, 8(18) 1100–1121.
6. Esatbeyoglu, T., Ewald, P., Yasui, Y., Yokokawa, H., Wagner, A. E., Matsugo, S., Winterhalter, P., & Rimbach, G. (2016). Chemical characterization, free radical scavenging, and cellular antioxidant and anti-inflammatory properties of a stilbenoid-rich root extract of *Vitis vinifera*. *Oxidative Medicine and Cellular Longevity*, 2016, 1–11.

7. Ewald, P., Delker, U., & Winterhalter, P. (2017). Quantification of stilbenoids in grapevine canes and grape cluster stems with a focus on long-term storage effects on stilbenoid concentration in grapevine canes. *Food Research International*, *100*(August), 326–331.
8. Fernández-Marín, M. I., Guerrero, R. F., García-Parrilla, M. C., Puertas, B., Richard, T., Rodriguez-Werner, M. A., Winterhalter P., Monti, J. P., & Cantos-Villar, E. (2012). Isorhapontigenin: A novel bioactive stilbene from wine grapes. *Food Chemistry*, *135*, 1353–1359.
9. Gabaston, J., Cantos-villar, E., Biais, B., Waffo-Teguo, P., Renouf, E., Corio-Coset M.F., Richard, T., & Mérillon, J. M. (2017). Stilbenes from *Vitis vinifera* L. waste: A sustainable tool for controlling *Plasmopara viticola*. *Journal of Agricultural and Food Chemistry*, *65*, 2711-2718.
10. Gorená, T., Saez, V., Mardones, C., Vergara, C., Winterhalter, P., & Von Baer, D. (2014). Influence of post-pruning storage on stilbenoid levels in *Vitis vinifera* L. canes. *Food Chemistry*, *155*, 256–263.
11. Guerrero, R. F., Biais, B., Richard, T., Puertas, B., Waffo-teguo, P., Merillon, J., & Cantos-villar, E. (2016). Grapevine cane's waste is a source of bioactive stilbenes. *Industrial Crops & Products*, *94*, 884–892.
12. Hui, Y., Li, X., & Chen, X. (2011). Assessment for the light-induced *cis* – *trans* isomerization of rhapontigenin and its glucoside rhaponticin by capillary electrophoresis and spectrometric methods. *Journal of Chromatography A*, *1218*, 5858–5866.

13. Houillé, B., Papon, N., Boudesocque, L., Bourdeaud, E., Besseau, S., Courdavault, V., Enguehard-Gueiffier, C., Delanoue, G., Guérin, L., Bouchara, J-P., Clastre, M., Giglioli-Guivarc'h, N., Guillard, J., & Lanoue, A. (2014). Antifungal activity of resveratrol derivatives against *Candida* Species. *Journal of Natural Products*, 77, 1658–1662.
14. Houillé, B., Besseau, S., Courdavault, V., Oudin, A., Glévarec, G., Delanoue, G., Guérin, L., Simkin, A.J., Papon, N., Clastre, M., Giglioli-Guivarc'h, N., & Lanoue, A. (2015). Biosynthetic origin of *E*-resveratrol accumulation in grape canes during postharvest storage. *Journal of Agricultural and Food Chemistry*, 63, 1631–1638.
15. Kong, Q. J., Ren, X. Y., Hu, N., Sun, C. R., & Pan, Y. J. (2011). Identification of isomers of resveratrol dimer and their analogues from wine grapes by HPLC/MSⁿ and HPLC/DAD-UV. *Food Chemistry*, 127(2), 727–734.
16. Mattivi, F., Vrhovsek, U., Malacarne, G., Masuero, D., Zulini, L., Stefanini, M., Moser, C., Velasco, R., & Guella, G. (2011). Profiling of resveratrol oligomers, important stress metabolites, accumulating in the leaves of hybrid *Vitis vinifera* (Merzling × Teroldego) genotypes infected with *Plasmopara viticola*. *Journal of Agricultural and Food Chemistry*, 59, 5364–5375.
17. Mikulski, D., & Molski, M. (2010). Quantitative structure-antioxidant activity relationship of trans-resveratrol oligomers, trans-4,4'-dihydroxystilbene dimer, trans-resveratrol-3-O-glucuronide, glucosides: *Trans*-piceid, *cis*-piceid, *trans*-astringin and trans-resveratrol-4'-O-β-D-glucoopyranoside. *European Journal of Medicinal Chemistry*, 45(6), 2366–2380.

18. Moss, R., Mao, Q., Taylor, D., & Saucier, C. (2013). Investigation of monomeric and oligomeric wine stilbenoids in red wines by ultra-high-performance liquid chromatography/electrospray ionization quadrupole time-of-flight mass spectrometry. *Rapid Communications in Mass Spectrometry*, 27(May), 1815–1827.
19. Nopo-Olazabal, C., Hubstenberger, J., Nopo-Olazabal, L., & Medina-Bolivar, F. (2013). Antioxidant activity of selected stilbenoids and their bioproduction in hairy root cultures of muscadine grape (*Vitis rotundifolia* mich x.). *Journal of Agricultural and Food Chemistry*, 61(48), 11744–11758.
20. Lambert, C., Richard, T., Renouf, E., Bisson, J., Waffo-Téguo, P., Bordenave, L., Ollat, N., Mérillon, J-M., & Cluzet, S. (2013). Comparative analyses of stilbenoids in canes of major *Vitis vinifera* L. cultivars. *Journal of Agricultural and Food Chemistry*, 61, 11392–11399.
21. Ou, B., Chang, T., Huang, D., & Prior, R. (2013). Determination of total antioxidant capacity by oxygen radical absorbance capacity (ORAC) using fluorescein as the fluorescence probe: first action. *Journal of AOAC International*, 96 (6), 1372–1376.
22. Papastamoulis, Y., Richard, T., Nassra, M., Badoc, A., Krisa, S., Harakat, D., Monti, J-P., Mérillon, J-M., & Waffo-Teguo, P. (2014). Viniphenol A, a complex resveratrol hexamer from *Vitis vinifera* stalks: Structural elucidation and protective effects against amyloid- β -induced toxicity in PC12 cells. *Journal of Natural Products*, 77(2), 213–217.
23. Papastamoulis, Y., Bisson, J., Tamsamani, H., Richard, T., Marchal, A., Mérillon J-M, & Waffo-Téguo, P. (2015). New *E*-miyabenol isomer isolated from grapevine

- cane using centrifugal partition chromatography guided by mass spectrometry. *Tetrahedron*, 71, 3138–3142.
24. Pavela, R., Waffo-Teguo, P., Benoît, B., Richard, T & Mérillon, J-M. (2017). *Vitis vinifera* canes , a source of stilbenoids against *Spodoptera littoralis* larvae. *Journal of Pest Science*, 90, 961-970.
25. Pawlus. A., Sahli. R., Bisson. J., Rivière C., Delaunay, C., Richard, T., Gomès, E., Bordenave, L., Waffo-Téguo. P., & Mérillon. J-M. (2013). Stilbenoid profiles of canes from *Vitis* and *Muscadinia* species. *Journal of Agricultural and Food Chemistry*, 61, 501–511.
26. Pezet, R., Perret, C., Jean-Denis, J., Tabacchi, R., Gindro, K., & Viret, O. (2003). δ -Viniferin, a resveratrol dehydrodimer: one of the major stilbenes synthesized by stressed grapevine leaves. *Journal of Agricultural and Food Chemistry*, 51(18), 5488–5492.
27. Pflieger, A., Teguo, P. W., Papastamoulis, Y., Subra, F., Munir, S., Delelis, O., Lesbats, P., Calmels, C., Andreola, M-L., Merillon, J-M., Auge-Gouillou, C., & Parissi, V. (2013). Natural stilbenoids isolated from grapevine exhibiting inhibitory effects against HIV-1 integrase and eukaryote MOS1 transposase *in vitro* activities. *PLOS ONE*, 8(11), 1–13.
28. Piñeiro, Z., Guerrero, R. F., Fernández-Marin, M. I., Cantos-Villar, E., & Palma, M. (2013). Ultrasound-assisted extraction of stilbenoids from grape stems. *Journal of Agricultural and Food Chemistry*, 61, 12549–12556.
29. Ribeiro, J. P. N., Magalhães, L. M., Reis, S., Lima, J. L. F. C., & Segundo, M. A. (2011). High-throughput total cupric ion reducing antioxidant capacity of biological

- samples determined using flow injection analysis and microplate-based methods. *Analytical Sciences: The International Journal of the Japan Society for Analytical Chemistry*, 27(5), 483–488.
30. Rivière, C., Pawlus, A. D., & Mérillon, J.-M. (2012). Natural stilbenoids: distribution in the plant kingdom and chemotaxonomic interest in Vitaceae. *Natural Product Reports*, 29, 1317-1333.
31. Rodríguez-Bonilla, P., Gandía-Herrero, F., Matencio, A., García-Carmona, F., & López-Nicolás, & J. M. (2017). Comparative study of the antioxidant capacity of four stilbenes using ORAC, ABTS+, and FRAP techniques. *Food Analytical Methods*, 10(9), 2994–3000.
32. Rodríguez., J & Haun, M. (1999). Cytotoxicity of trans-dehydrocrotonin from *Croton cajucara* on V79 cells and rat hepatocytes. *Planta Medica* 1999; 65(6): 522-526.
33. Ruiz, A., Hermosín-Gutierrez, I., Mardones, C., Vergara, C., Herlitz, E., Vega, M., Dorau, C., Winterhalter, P., & von Baer, D. (2010). Polyphenols and antioxidant activity of calafate (*Berberis microphylla*) fruits and other native berries from southern Chile. *Journal of Agricultural and Food Chemistry*, 58, 6081–6089.
34. Schneider, J. G., Alosi, J. A., McDonald, D. E., & McFadden, D. W. (2010). Pterostilbene inhibits lung cancer through induction of apoptosis. *Journal of Surgical Research*, 161(1), 18–22.
35. Vendrely, V., Peuchant, E., Buscail, E., Moranvillier, I., Rousseau, B., Bedel, A., Brillac, A., de Verneuil, H., Moreau-Gaudry, F., & Dabernat, S. (2017). Resveratrol and capsaicin used together as food complements reduce tumor growth and rescue

- full efficiency of low dose gemcitabine in a pancreatic cancer model. *Cancer Letters*, 390, 91–102.
36. Vergara, C., Von Baer, D., Mardones, C., Wilkens, A., Wernekinck, K., Damm, A., Macke, S., & Winterhalter, P. (2012). Stilbene levels in grape cane of different cultivars in southern Chile: Determination by HPLC-DAD-MS/MS method. *Journal of Agricultural and Food Chemistry*, 60(4), 929–933.
37. Wang, X., & Yao, C. (2015). Naturally active oligostilbenes. *Journal of Asian Natural Products Research*, 6020, 1–30.
38. Xu, B., & Tao, Z. (2015). Piceatannol enhances the antitumor efficacy of gemcitabine in human. *Oncology Research*, 22, 213–217.
39. Xue, Y. Q., Di, J. M., Luo, Y., Cheng, K. J., Wei, X., & Shi, Z. (2014). Resveratrol oligomers for the prevention and treatment of cancers. *Oxidative Medicine and Cellular Longevity*, 2014. doi:10.1155/2014/765832
40. Zga, N., Papastamoulis, Y., Toribio, A., Richard, T., Delaunay, J. C., Jeandet, P., Renault, J.H., Monti, J.P., Mérillon, J.M., & Waffo-Téguo, P. (2009). Preparative purification of antiamyloidogenic stilbenoids from *Vitis vinifera* (Chardonnay) stems by centrifugal partition chromatography. *Journal of Chromatography B: Analytical Technologies in the Biomedical and Life Sciences*, 877 (10), 1000–1004.
41. Zulueta, A., Caretti, A., Signorelli, P., & Ghidoni, R. (2015). Resveratrol: A potential challenger against gastric cancer. *World Journal of Gastroenterology*, 21(37), 10636–10643.

Supplementary material:

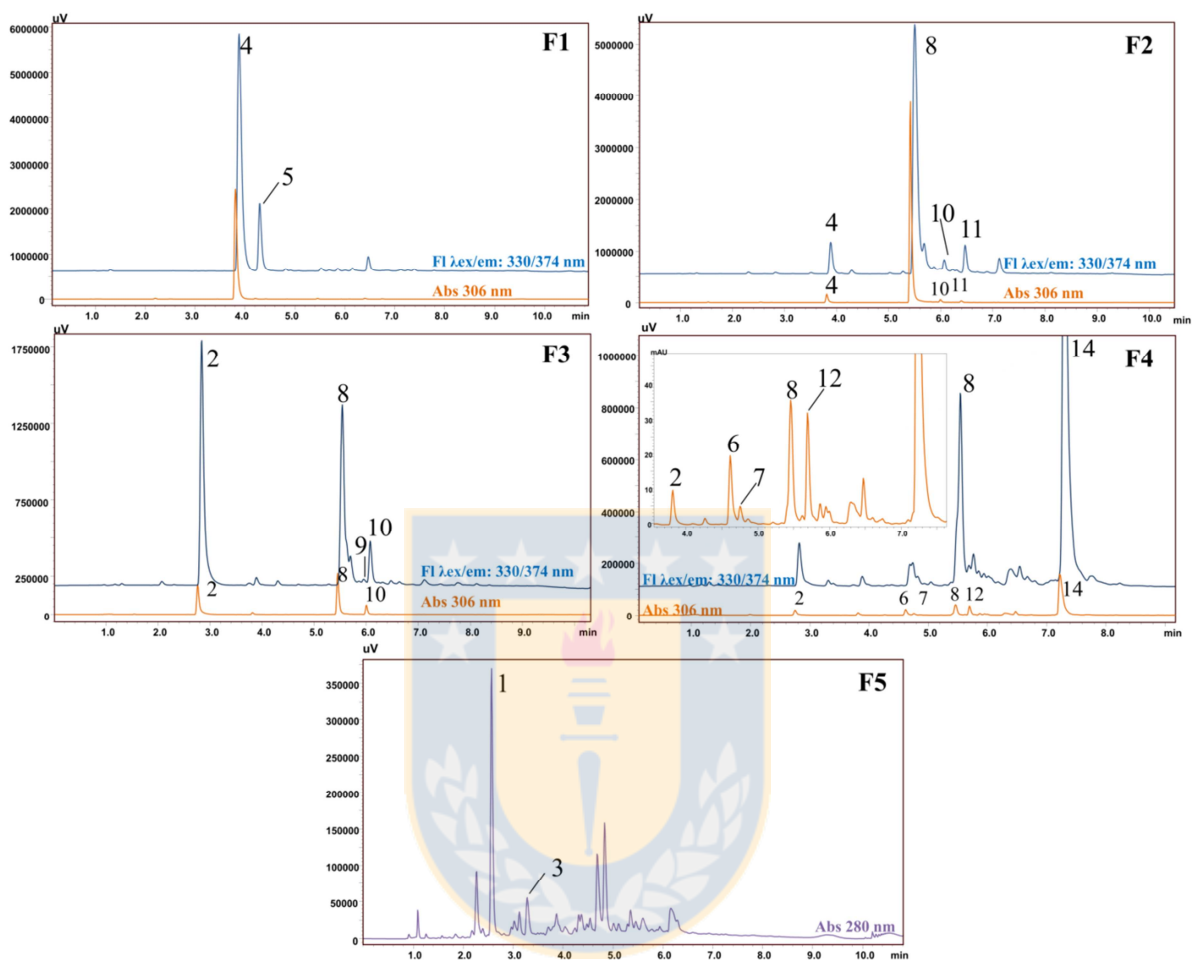


Figure S.1: HPLC-DAD-FL chromatogram on core shell C18 column. Pooled fractions by CPC: Fraction 1 (F1), Fraction2 (F2), Fraction 3 (F3), Fraction 4 (F4) and Fraction 5 (F5).

Peak number are indicated in table 1

Table S.1: Collected fractions by CPC of oligostilbenoids from 14 grams of Pinot Noir grape cane extract.

Fraction	Major stilbenoid	λ_{\max} (nm)	mg	Stilbenoid (%)
		280, 306,		
1	(<i>E</i>)-resveratrol	318	187.6	64.9 ± 0.7
2	(<i>E</i>)- ϵ -viniferin	289, 336	518.0	58.4± 0.3
3	(<i>E</i>)-piceatannol	329	171.7	16.9 ±0.3
4	Vitisin B	329	103.9	2.58±0.1*
				5.48± 0.1
5	Ampelopsin A	280	332.0	*

* The Percentage was calculated as (*E*)-resveratrol equivalents.



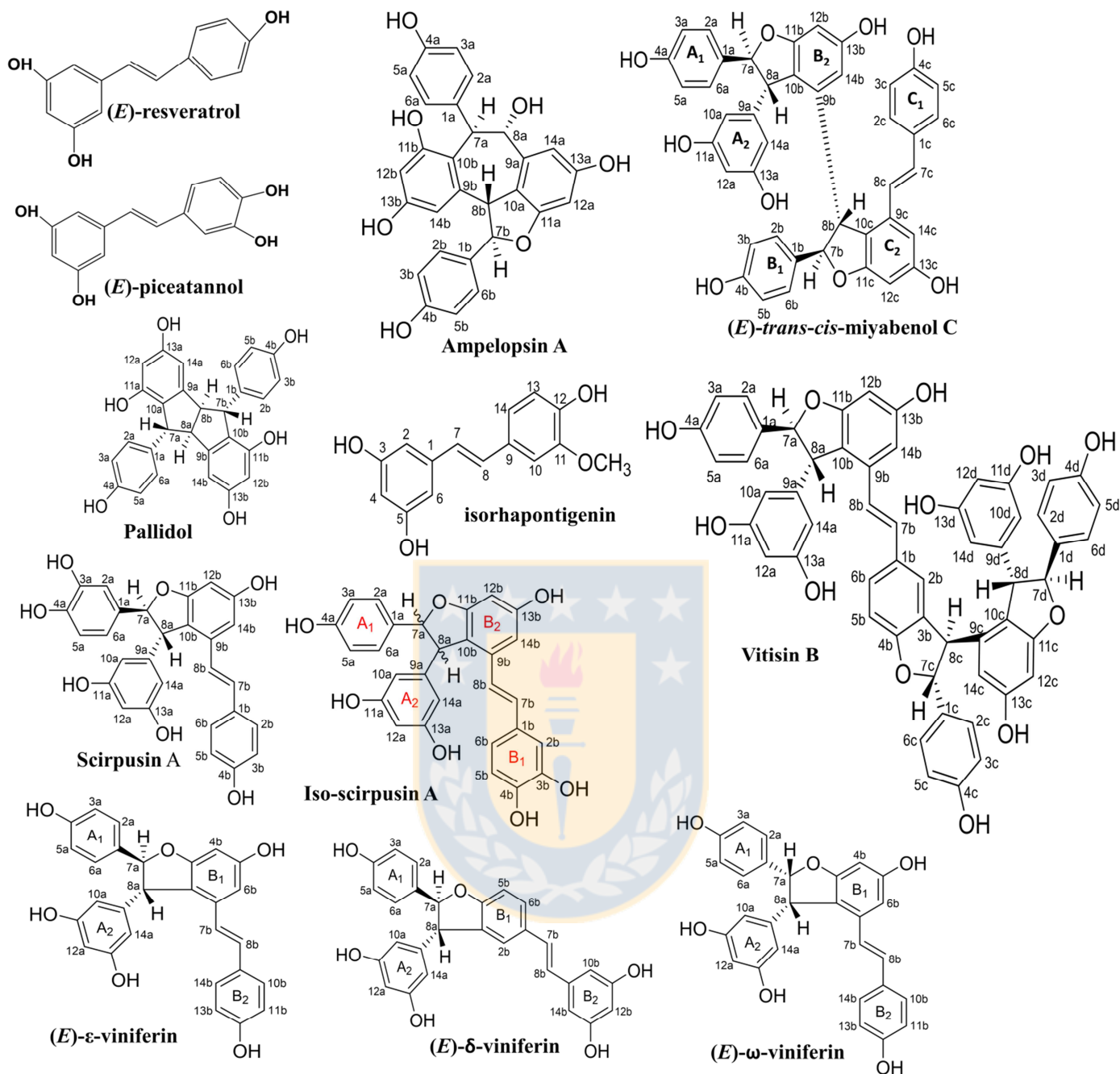


Figure S.2: Chemical structure of stilbenoids isolated from grape canes.

Table S.2: NMR data in acetone d6 for vitisin B 500 MHz and ampelopsin A at 500 MHz.

Vitisin B			Ampelopsin A				
$\delta^1\text{H}$ (ppm)	$J_{\text{H,H}}$ (Hz)		$\delta^1\text{H}$ (ppm)	$J_{\text{H,H}}$ (Hz)	$\delta^{13}\text{C}$ (ppm)	HMBC	
<i>Benzenic A₁</i>			<i>Benzenic A₁</i>				
2a	7.26 d	8.3	1a		130.1	H-3a,5a; H-7a	
3a	6.91 d	8.3	2a	6.88 d	8.8	127.9	H-7a
5a	6.91 d	8.3	3a	6.63 d	8.8	114.6	H-2a,6a
6a	7.26 d	8.3	4a		155.2	H-2a,6a; H-3a,5a	
<i>Pyran A</i>			5a	6.63 d	8.8	114.6	H-2a,6a
7a	5.41 d	4.4	6a	6.88 d	8.8	127.9	H-7a
8a	4.54 d	4.4	<i>Cycloheptan</i>				
<i>Benzenic A₂</i>			7a	5.44 d	4.8	43.0	H-2a,6a; H-8a
10a	6.12 d	2.0	8a	5.40 d	4.4	70.3	H-14a; H-7a
12a	6.19 d	1.9	<i>Benzenic A₂</i>				
14a	6.12 d	2.0	9a		139.6	H-7a; H-8b	
<i>Benzenic B₁</i>			10a		117.5	H-8a; H-14a; H-12a	
2b	6.85 brs		11a		159.3	H-12a; H-8b	
5b	6.76 d	7.8	12a	6.14 d	2.4	96.2	H-14a
6b	7.14 dd	8.3; 1.5	13a		158.0	H-14a	
<i>Olefin B</i>			14a	6.60 d	2.0	109.6	H-8a; H-12a

7b	6.64 d	16.4	Benzenic B₁				
8b	6.77 d	17.0				H-3b,5b; H-7b; H-8b	
1b					131.8		
Benzenic B₂							
2b	7.11 d	8.8	129.1			H-7b	
12b	6.32 brs		3b	6.76 d	8.3	115.1	H-2b,6b
14b	6.66 d	2.0	4b			157.6	H-2b,6b; H-3b,5b
Benzenic C₁			5b	6.76 d	8.3	115.1	H-2b,6b
2c	6.62 d	8.3	6b	7.11 d	8.8	129.1	H-7b
3c	6.58 d	8.8	Hydropyran B				
5c	6.58 d	8.8	7b	5.75 d	11.2	87.6	H-8b
6c	6.62 d	8.3	8b	4.15 d	11.7	48.7	H-14b; H-7b
Pyran C			Benzenic B₂				
7c	5.53 d	4.9	9b			142.2	H-7a; H-7b; H-8b
8c	4.32 d	4.9	10b			118.0	H-8a; H-12b; H-14b; H-8b
Benzenic C₂			11b			158.0	H-7a; H-8b
12c	6.32 brs		12b	6.42 d	2.4	100.6	H-14b
14c	6.21 brs		13b	6.22 brd		156.4	H-12b; H-14b
Benzenic D₁			14b			104.6	H-12b; H-8b
2d	7.20 d	8.3					
3d	6.83 d	8.3					

5d 6.83 d 8.3

6d 7.20 d 8.3

Pyran D

7d 5.42 d 5.4

8d 4.46 d 5.4

***Benzenic
D₂***

10d 6.21 brs

12d 6.23 brt

14d 6.21 brs



Table S.3: H-NMR data in acetone-d₆ for isorhapontigenin at 500 MHz.

	$\delta^1\text{H}$ (ppm)	$J_{\text{H,H}}$ (Hz)
1		
2	6.52 d	1.9
3		
4	6.25 d	1.9
5		
6	6.52 d	1.9
7	6.91 d	16.1
8	7.00 d	15.6
9		
10	7.20 brs	
11		
12		
13	6.99 d	8.4
14	6.79 d	8.3
OCH₃	3.88 d	

Table S.4: NMR data for (*E*)- δ -viniferin at 500 MHz and (*E*)- ω -viniferin at 400 MHz in acetone- d_6 .

	<i>(E)</i> - δ -viniferin					<i>(E)</i> - ω -viniferin			
	$\delta^1\text{H}$ (ppm)	$J_{\text{H,H}}$ (Hz)	$\delta^{13}\text{C}$ (ppm)	2D- HMBC	NOE	$\delta^1\text{H}$ (ppm)	$J_{\text{H,H}}$ (Hz)	$\delta^{13}\text{C}$ (ppm)	2D-HMBC
<i>Benzenic A₁</i>									
1a			132.15	H-3a; H-5a				129.3	H-8a
2a	7.24	8.3	128.55		B; C; F	7.21 (7.22)	8.7	127.9 (128.6)	
3a	6.85	8.8	116.10			6.74 (6.74)	8.7	115.5 (116.1)	
4a			158.38	H-2a; H-6a				158.5	H-2a; H-6a
5a	6.85	8.8	116.10			6.74 (6.74)	8.7	115.5 (116.1)	
6a	7.24	8.3	128.55		B; C; F	7.21 (7.22)	8.7	127.9 (128.6)	
<i>Dyhydropyran A</i>									
7a	5.45	8.3	94.02		A; C; E	5.85 (5.86)	8.2	89.8 (90.1)	
8a	4.46	8.3	57.83		B; D; E	4.68 (4.70)	8.2	52.1 (53.3)	
<i>Benzenic A₂</i>									
9^a			145.18	H-7a; H-8a				143.0	H-8a; H-7a
10^a	6.19	2.5	107.34		A; D; F	5.81 (5.80)	3.0	108.0 (108.4)	

11^a			159.71	H-10a; H-14a			159.0	
12^a	6.28	1.7	102.29			5.96 (5.96)	3.0	101.3 (101.4)
13^a			159.71	H-10a; H-14a				159.0
14^a	6.19	2.5	107.34		A; D; F	5.81 (5.80)	3.0	108.0 (108.4)
<i>Benzenic B₁</i>								
1b			131.73	H-8b				122.2 H-8a; H-8b
2b	7.26	brs	123.90		I; J			124.3 H-4b; H-7b
3b			132.50	H-8a				162.4 H-8a
4b			160.58	H-2b; H- 6b		6.71 (6.72)	2.1	104.5 (104.3)
5b	6.87	9.0	110.12					136.5 H-7b
6b	7.43	8.3; 2.0	128.59		I; J	6.36 (6.32)	2.5	96.4 (96.9)
<i>Olefin B</i>								
7b	7.06	16.1	129.07		G; J	6.94 (6.94)	16.6	129.6 (130.4)
8b	6.90	16.6	127.21		H; I	6.75 (6.76)	16.6	122.8 (123.6)
<i>Benzenic B₂</i>								
9b			140.74	H-7b				129.3 H-10b; H-14b; H-7b
10b	6.53	2.0	105.63		G; H	7.02 (7.03)	8.7	128.1 (128.8)
11b			159.51	H-10b; H-14b		6.61 (6.60)	8.7	114.5 (114.9)

12b	6.25	2.2	102.63				157.21	H-10b; H-14b
13b			159.51	H-10b; H-14b	6.61 (6.60)	8.7	114.5 (114.9)	
14b	6.53	2.0	105.63	G; H	7.02 (7.03)	8.7	128.1 (128.8)	



Table S.5: NMR data for pallidol at 500 MHz in acetone-d₆.

	$\delta^1\text{H}$ (ppm)	$J_{\text{H,H}}$ (Hz)	$\delta^{13}\text{C}$ (ppm)	2D-HMBC
<i>Benzenic A₁</i>				
1a			139.9	H-3,5; H-7; H-8
2a	6.98 d	8.8	128.7	
3a	6.71 d	8.3	115.4	
4a			156.3	H-2,6; H-3,5
5a	6.71 d	8.3	115.4	
6a	6.98 d	8.8	128.7	
<i>Cyclopentane A</i>				
7a	4.57 brs		53.6	
8a	3.82 brs		60.2	
<i>Benzenic A₂</i>				
9a			150.6	H-7; H-12
10a			123.3	H-7; H-8; H-12; H-14
11a			155.3	H-7; H-8
12a	6.19 d	1.9	102.1	
13a			159.4	H-12; H-14
14a	6.62 d	2.0	103.1	
<i>Benzenic B₁</i>				

1b			139.9	H-3,5; H-7; H-8
2b	6.98 d	8.8	128.7	
3b	6.71 d	8.3	115.4	
4b			156.3	H-2,6; H-3,5
5b	6.71 d	8.3	115.4	
6b	6.98 d	8.8	128.7	

Cyclopentane
B

7b	4.57 brs	brs	53.6	
8b	3.82 brs	brs	60.2	

Benzenic B₂

9b			150.6	H-7; H-12
10b			123.3	H-7; H-8; H-12; H-14
11b			155.3	H-7; H-8
12b	6.19 d	1.9	102.1	
13b			159.4	H-12; H-14
14b	6.62 d	2.0	103.1	

Table S.6: NMR data for (*E*)-*trans*-*cis*-miyabenol C at 500 MHz.

	$\delta^1\text{H}$ (ppm)	$J_{\text{H,H}}$ (Hz)	$\delta^{13}\text{C}$ (ppm)	2D-HMBC
<i>Benzenic A₁</i>				
1a			133.4	H-3a,5a; H-8a
2a	7.15 d	8.8	127.8	H-7a
3a	6.80 d	8.8	116.4	
4a			158.2	H-2a,6a; H-3a,5a
5a	6.80 d	8.8	116.4	
6a	7.15 d	8.8	127.8	H-7a
<i>Dihydropyran A</i>				
7a	5.37 d	5.3	94.5	H-2a,6a
8a	4.62 d	5.3	57.1	H-10a,14a
<i>Benzenic A₂</i>				
9a			147.6	H-7a; H-8a
10a	6.15 d	2.0	106.9	H-12a
11a			160.3	H-12a
12a	6.20 t	1.9; 2,5	102.5	H-10a,14a
13a			160.3	H-12a
14a	6.15 d	2.0	106.9	H-12a
<i>Benzenic B₁</i>				
1b			133.3	H-3b,5b; H-8b
2b	6.49 d	8.7	127.4	H-7b
3b	6.54 d	8.8	115.6	
4b			157.5	H-2b,6b; H-3b,5b

5b	6.54 d	8.8	115.6	
6b	6.49 d	8.7	127.4	H-7b
<i>Dihydropyran B</i>				
7b	5.19 d	0.9	92.2	H-2b,6b
8b	4.30 d	1.4	51.0	H-14b
<i>Benzenic B₂</i>				
9b			143.4	H-7b; H-8b
10b			118.6	H-8b; H-12b; H-14b
11b			162.3	H-8a
12b	6.28 d	1.9	96.3	H-14b
13b			162.1*	H-12b
14b	6.06 d	2.0	107.6	H-12b
<i>Benzenic C₁</i>				
1c			129.3	H-3c,5c; H-8c
2c	7.11 d	8.8	128.7	H-7c
3c	6.72 d	8.8	116.6	
4c			158.3	H-2c,6c; H-3c,5c
5c	6.72 d	8.8	116.6	
6c	7.11 d	8.8	128.7	H-7c
<i>Olefin C</i>				
7c	6.87 d	16.1	131.1	H-2c,6c
8c	6.60 d	16.1	122.8	H-14c
<i>Benzenic C₂</i>				
9c			136.0	H-7c
10c			121.2	H-8c; H-12c; H-14c

11c			162.1*	H-8b; H-7b
12c	6.33 d	2.0	97.1	H-14c
13c			159.5**	
14c	6.65 d	1.4	104.3	H-8c



Table S.7: Calibration curves for TEAC_{cuprac}, TEAC_{abts} and ORAC-FL using TROLOX

Antioxidant capacity assay	Equation	R ²	LOD (μM)	LOQ (μM)	Trolox Range (μM)
ABTS	Y=0.0007X+0.0492	0.990	3.96	11.9	[1-180]
CUPRAC	Y=0.0037X+0.1354	0.998	1.82	6.07	[1-150]
ORAC-FL	Y=22.34X+765.52	0.996	1.39	4.33	[1-70]



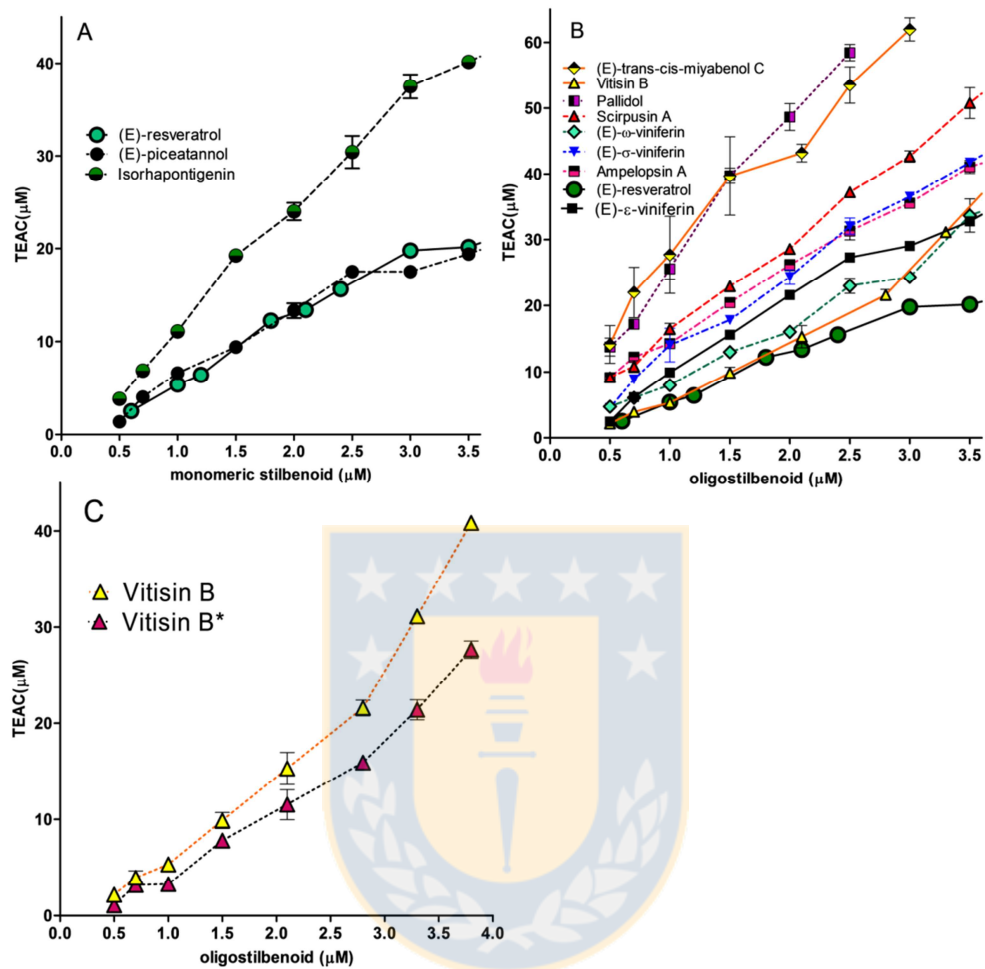
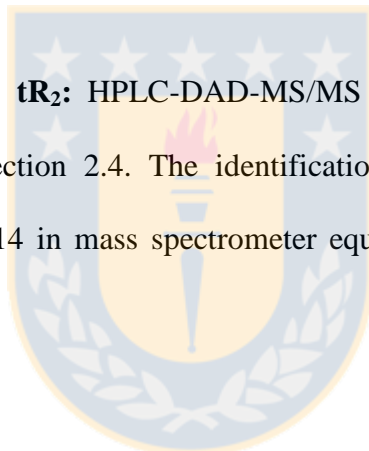


Figure S.3: Antioxidant capacity measured by ORAC-FL assay for increased concentrations of oligostilbenoids isolated from grape cane extract: monomeric stilbenoids (A), oligostilbenoids (B), comparison between vitisin B after isolation and vitisin B with presence of second tetramer (C).

Table S.8: HPLC-DAD-MS/MS for isolated vitisin B after freeze drying and storage at -20°C in darkness and compared with vitisin B repurified.

tR (min)	λ máx	tR (min)	[M-H]⁻	fragments	Stilbenoid
6.7	284	20.3	905	888, 812, 800 , 781, 705, 690, 676, 569, 546 , 528, 451, 439, 434, 392, 359, 347 , 345, 333 , 317, 240	Unknow tetramer
7.7	325	22.7	905	888, 870, 812, 800 , 781, 705, 676, 572, 545, 528, 451, 439, 359, 345, 333, 303 , 279, 241, 197	Vitisin B

tR₁: HPLC-DAD-FL method, **tR₂**: HPLC-DAD-MS/MS method. The chromatographic conditions as described in section 2.4. The identification was made under conditions described by Gorena et al 2014 in mass spectrometer equipped with a triple cuadrupole (Applied Biosystem).



Capítulo 3: Sección 1

Title:

C18 core-shell column with in-series absorbance and fluorescence detection for simultaneous monitoring of changes in stilbenoid and proanthocyanidin concentrations during grape cane storage

Vania Sáez^a, Camila Gayoso^a, Sebastián Riquelme^b, Julie Pérez^a, Carola Vergara^a, Claudia Mardones^a, and Dietrich von Baer^{a*}

^aFacultad de Farmacia, Departamento de Análisis Instrumental, Universidad de Concepción, Chile

^bUnidad de Desarrollo Tecnológico (UDT), Universidad de Concepción, Coronel, Chile

*Corresponding author: Dietrich von Baer

E-mail: dvonbaer@udec.cl



Formato manuscrito aceptado el 22 de diciembre del 2017 a Journal of Chromatography B.

DOI:10.1016/j.chromb.2017.12.028

Abstract

Grape canes, the residues from the annual pruning of vines, contain high levels of inducible (*E*)-resveratrol and also oligomeric stilbenoids and proanthocyanidins. These two families of phenolic compounds are bioactive, but to quantify them in a single chromatographic run using only ultraviolet detection is a difficult task. To overcome this limitation, a chromatographic method was developed using a core shell column for separation, an ultraviolet-visible diode array detector (DAD) and a fluorescence (FL) detector connected in series for quantification, with an electrospray ionization interface (ESI) and a triple quadrupole mass spectrometric detector (MS/MS) added for identification of the analytes. The proanthocyanidins (+)-catechin, (–)-epicatechin, procyanidins B1, B2, and C1, an unknown dimer and trimer, two prodelfphin dimers, and monogallate procyanidin dimers were detected in the tested grape cane samples. The stilbenoids detected were (*E*)-resveratrol, (*E*)-piceatannol, (*E*)-piceid, (*E*)- ϵ -viniferin, vitisin B, a glycosylated monomer, three oxidized dimers, an unknown dimer and a tetramer, pallidol, hopeaphenol, (*E*)- δ -viniferin, and (*E*)- ω -viniferin. However, this method required 60 min for each analysis. A faster and more efficient method for quantitative analysis was developed based on HPLC-DAD-FL, reducing the time required to 24 min for the simultaneous quantification of proanthocyanidins and stilbenoids in Cabernet Sauvignon, Pinot Noir, and Tintorera grape canes stored at controlled temperatures and relative humidities for 134 days after pruning. To the best of our knowledge, this is the first time a prodelfphin dimer has been quantified in grape canes. The incorporation of fluorescence detection in series with DAD not only allowed the quantification of proanthocyanidins, it also improved the detectability of some minor stilbenoids present in the canes, such as (*E*)-piceid. The (*E*)-resveratrol and (*E*)-piceatannol levels increased significantly during cane storage, while those of (*E*)- ϵ -viniferin

and ampelopsin A did not show significant increases. The relative humidity had a determining effect on the levels of (*E*)-resveratrol and (*E*)-piceatannol in the canes of all varieties studied; their concentrations were higher at a relative humidity of 60% than at 70%. This is the first time that the proanthocyanidin profiles of canes stored after pruning were monitored. The concentration of (–)-epicatechin decreased during storage under both relative humidities. Furthermore, the levels of proanthocyanidin B1 and the prodelphinidin dimer also decreased to a certain extent.

Keywords: stilbenoids, proanthocyanidins, core-shell column, DAD detection, fluorescence detection, grape cane.



1. Introduction

Grape canes, the residues from the pruning of vineyards, have diverse (poly)phenolic profiles, comprising stilbenoids [1-5] phenolic acids [1,6-7], flavonols [6], and proanthocyanidins such as procyanidins [1,6-8], and prodelfinidins [8]. Stilbenoids belong to the nonflavonoid family of phenolic compounds present in plants. (*E*)-resveratrol is the metabolic precursor and structural core of the stilbenoids present in Vitaceae. Resveratrol monomers form oligomers consisting of 2–8 units [9]. Furthermore, it has been reported that stilbenoids, mainly (*E*)-resveratrol, have a range of health benefits, including anti-inflammatory, cardioprotective, anticancer, and antidiabetic properties [10]. This is due to their capacity to interfere with signal transduction cascades and epigenetic pathways in cells, rather than having any particular enzyme target or specific mechanism [9].

Proanthocyanidins are formed by the oligomerization of flavan-3-ol units linked through interflavan bonds. Proanthocyanidins also have health-promoting properties. For instance, they can help prevent complications arising from type-2 diabetes, cardiovascular disease, and bacterial infections, [11] and exhibit anti-inflammatory activities [12].

Stilbenoids and proanthocyanidins are synthesized by the phenylpropanoid pathway. Phenylalanine, a product of the shikimate pathway, undergoes a series of enzymatic reactions resulting in secondary metabolites, such as proanthocyanidins and stilbenoids (Fig. 1). The (poly)phenolics generated by the shikimate pathway have p-coumaroyl-CoA as a central metabolite in their pathway [9,13]. Stilbenoids are generated by an enzymatic reaction through stilbene synthase (STS). The STS gene encoding is transcribed only when induced by stimuli, such as ultraviolet (UV) radiation, pathogen invasion, or physical trauma [9].

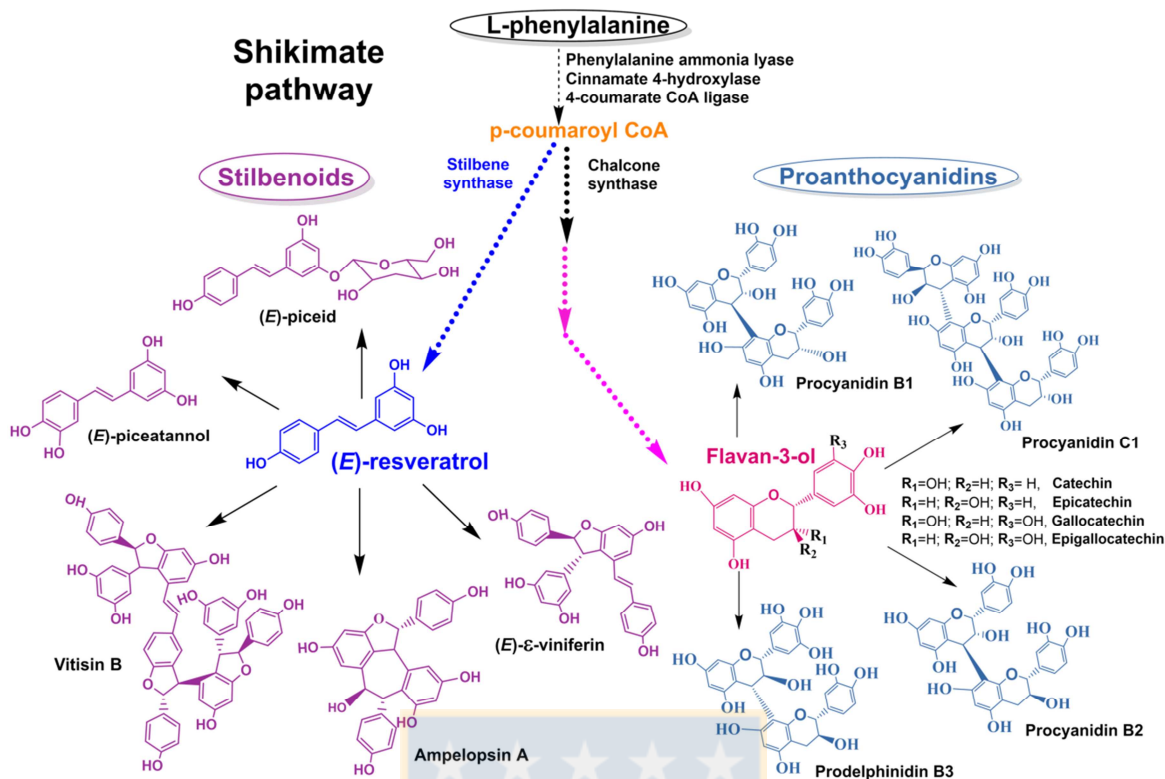


Fig. 1: Schematic diagram illustrating the formation of stilbenoids and proanthocyanidins derived from the phenylpropanoid pathway. Adapted from references 9, 13, 27 and 28.

The high levels of stilbenoids (2858–8485 mg/kg) [14] present in this viticultural residue have, until now, been the main the focus of diverse studies into grape cane as a source of bioactive stilbenoids with potential biotechnological applications [2-5,7,14]. To revalorize this residue, it is necessary to know also the contents of the other phenolic compounds present in it, including (+)-catechin (76–1000 mg/kg) and (-)-epicatechin (62–1300 mg/kg), which exhibit significantly high concentrations [6-7, 15].

Even a few months after pruning, grape canes remain metabolically active. Following the pruning process, the canes undergo modifications in terms of their stilbenoid composition, with increasing levels of (*E*)-resveratrol. This increment can be as high as a hundred-fold [16]. The increases in the levels of (*E*)-piceatannol and (*E*)-resveratrol during storage have biosynthetic origin and are attributable to STS induction. The temperature during storage

plays a key role, with the optimal temperature range being 15–20 °C [16]. On the other hand, the effect of relative humidity (RH) on the levels of inducible stilbenoids in pruned grape canes has not been studied. Furthermore, there are no data on how the proanthocyanidin content is affected during storage after pruning. This is relevant given the potential of grape cane extract for use in the formulation of nutritional supplements as well as in cosmetics and the biotechnology industry.

Due to their structural complexity, it is only possible to separate proanthocyanidins by hydrophilic interaction liquid chromatography (HILIC) according their degree of polymerization, or by reverse-phase chromatography; however, some of them coelute. It is possible to separate 81 bioactive (poly)phenols, including proanthocyanidins and stilbenoids, in 81 min by comprehensive bi-dimensional chromatography, using a diol stationary phase in the first dimension and a C18 stationary phase in the second dimension [8].

Core-shell column technology allows for the fast separation of complex samples over short times using high-performance liquid chromatography (HPLC) [17]. A core-shell column contains solid silica core particles (0.9–3.7 µm in diameter) covered with a chemically modified porous coat on the solid nucleus to generate together a spherical particle. The porosities and sizes of the particles influence chromatographic behavior; each core-shell particle has a solid core to reduce longitudinal diffusion and mass-transfer resistance without any dramatic increase in backpressure, even with small particles, when compared to alternative porous ultra-high-performance liquid chromatography (UHPLC) particles used to obtain better resolution. Compared to porous columns, the reduced porous region of each core-shell particle helps to increase permeability and is associated with a high thermal conductivity, which contributes to reducing band broadening [17,18].

In the case of procyanidins, the primary detection system used for quantification is based on fluorescence, as it is more selective and provides a stronger signal than UV absorption [19]. In the case of stilbenoids, detection is usually through a diode array detector (DAD) or mass spectrometry/mass spectrometry (MS/MS). The fluorescence-based detection of stilbenoids such as (*E*)-piceatannol is more sensitive than photometric detection. Furthermore, signal interference is weaker in the former case [20], allowing for the quantification of stilbenoids at low concentrations. In the present work, a rapid chromatographic method is developed that combines the advantages of core-shell particle technology with serial absorbance and fluorescence detection for monitoring the changes in the levels of these bioactive and antioxidant phenolic compounds during grape cane storage under different RH conditions.

2. Materials and methods

2.1 Chemicals used

Acetonitrile, water, formic acid, and ethanol were purchased from Merck (Darmstadt, Germany). (*E*)- ϵ -Viniferin ($\geq 99.8\%$), procyanidin B2 (96%), procyanidin B1 (93%), and procyanidin C1 (91%) were provided by Phytolab (Vestenbergersreuth, Germany). (+)-catechin hydrate ($\geq 98\%$), (-)-epicatechin ($\geq 90\%$), (*E*)-resveratrol ($\geq 99\%$), and piceatannol ($\geq 98\%$) were supplied by Sigma (St. Louis, MO, USA). Ampelopsin A (94%) and vitisin B (94%) were isolated from a pilot-scale plant extract of Pinot Noir grape canes. Hopeaphenol was provided by the research group of Prof. Dr. Peter Winterhalter (Institute of Food Chemistry, Technical University Braunschweig, Germany).

2.2 Plant material used

Grape cane samples were collected during the vine-pruning season in July-August 2016. Three red grape cultivars were sampled in vineyards of the Itata Valley, Bío-Bío Region in South Chile. Cabernet Sauvignon (CS) and Pinot Noir (PN) canes were collected at Viña Chillán in Bulnes and those of Tintorera (TN), a teinturier grape cultivar that accumulates anthocyanins in the grape skin and pulp, were pruned at the De Neira Vineyard. In each case, were collected randomly around 2 kg of canes from 5 different rows in the same vineyard as one composed sample. Immediately after pruning, canes were cut into pieces 25 cm in length. One representative fraction of each variety (approx. 250 g) was kept under cold conditions (4 °C) and then stored at -20°C in plastic bags (0 days after pruning). Two other randomly selected fractions of each variety were promptly stored under two different RH conditions (1 kg for each variety), namely at 20 ± 2 °C and 70% RH (Mettler HPP 110 constant climate chamber), and at 21 ± 2 °C and 60% RH (Clima Veneta, AXO 10 constant climate chamber); these two RH conditions represent the range commonly observed during cane storage practice. Every 2 weeks, 6–7 pieces of cane (30–40 g) were removed from the controlled ambient chamber, frozen, stored at -20°C, and subsequently subjected to extraction.

2.3 Extraction method used

The extraction was performed as described by Vergara et al. in 2012 [2] and Gorena et al. in 2014 [3]. Before extraction, frozen canes were cut into 2-cm-long pieces, freeze-dried and ground. A 2-g sample of the milled cane was extracted over 5 min with 16 mL of an 80:20 (v/v) ethanol/water mixture using an ultrasonic bar at 50 Hz (Cole Parmer, CPX 130). The extraction process was repeated four times for each sample and successive

fractions were pooled together. An aliquot of this pooled extract was diluted with a mixture composed of 90% mobile phase A (0.1% formic acid in water) and 10% mobile phase B (70:30 (v/v) acetonitrile:water) and filtered (PES, 0.22 μm).

2.4 Identification of analytes using HPLC-DAD-FL-ESI-MS/MS

The phenolic compounds in the extract were identified using an HPLC system coupled in series to a DAD, a fluorescence detector (FL), and finally, a triple-quadrupole mass spectrometer. The overall sequence of the system was as follows: SIL-30 AC Nexera Autosampler, an LC-30 AD Nexera liquid chromatograph, a CTO 20 AC column oven, a SPD M 20 A Prominence DAD, a RF 20Axs Prominence FL detector, and a CBM 20A communication bus (all from Shimadzu, Kyoto, Japan). The mass spectra were acquired using a QTrap3200 LC/MS/MS system (Applied Biosystems/MDS Sciex, Framingham, MA, USA). A C-18 core-shell particle column (150 \times 4.6 mm i.d. with 2.7 μm particles; Halo, Advanced Materials Technology, Inc., Wilmington, DE, USA) was used. Mobile phases A and B, described in part 2.3 (above), were used at 30 $^{\circ}\text{C}$ and at a flow rate 0.4 mL/min. The injection volume was 10 μL . The following gradient was used: 0.1 min 10% B, 3 min 15% B, 6 min 20% B, 11 min 28% B, 16 min 30% B, 25 min 35% B, 28 min 38%, 33 min 40% B, 43 min 70% B, 48 min 100% B. Next, the %B value was kept constant for 5 min and subsequently changed at 53 min to 10% B for 7 min. Detection using the DAD was performed at 306 nm and 280 nm. FL detection was performed in two different channels. The excitation and emission wavelengths were 230 nm and 320 nm for the proanthocyanidins and 330 nm and 374 nm for the stilbenoids. To improve the detection of oligostilbenoids, the emission and excitation spectra of ampelopsin A and vitisin B were measured using a detector (RF-20 Axs Prominence FL detector, Shimadzu,

Japan). Identities were assigned by comparing the retention times and mass spectra of the analytes with those of reference compounds when these compounds were available, and by comparison with literature data otherwise. The mass spectrometer employed electrospray ionization (ESI) and was operated in negative mode. The source temperature was set to 450 °C, the nebulizer gas pressure to 2.7 bar, and the auxiliary gas pressure to 3.4 bar. The m/z mass range was set to 100–1200.

2.5 HPLC-DAD-FL conditions for quantitative determination of analytes

A C-18 column (150 × 4.6 mm) packed with 2.7- μ m fused-core particles (Halo, Advanced Materials Technology, Inc., Wilmington, DE, USA) with 1.7 μ m nucleus and carbon load of 7.7% was used to separate the stilbenoids and proanthocyanidins. An 8.0 μ L aliquot of the sample was injected and analyzed at a flow rate of 1.4 mL/min at a column temperature of 30 °C. The gradient used was: from 10 to 15% of phase B increased in 0.25 min, reaching 20% at 1.8 min, 27% at 2.6 min, 29% at 6.0 min, 32% at 8.0 min, 38% at 8.6 min, 40% at 10.6 min, and 65% at 14 min. The column was then washed with 100% B for 4 min and equilibrated for 6 min with 10% B. A second C-18 core-shell column was tested for its chromatographic efficiency to rapidly quantify proanthocyanidins and stilbenoids (Supplementary Material).

2.6 Calculations

The plate number (N), plate height (H), and retention factor (K) values were calculated as specified by the instrument manufacturer while the peak resolution between the neighboring peaks was calculated as follows [21]:

$$R_s = 1.18 \times \left(\frac{t_{R2} - t_{R1}}{W_{h2} + W_{h1}} \right) \quad (1)$$

On the other hand, the limit of detection and limit of quantification values were calculated by estimating the typical error using the least-squares method from a low-concentration calibration curve [22-23].

3. Results and discussion

3.1 Identification of analytes using HPLC-DAD-FL-ESI-MS/MS

The low-mobile-phase-flow-rate (0.4 mL/min) method described in section 2.4 was used to identify the 30 phenolic compounds detected in Pinot Noir grape canes subjected to storage for 14 weeks. The obtained results are summarized in Table 1. By combining three different detectors in series, 11 proanthocyanidins could be separated and identified. These included procyanidin B1, C1, and B2, (+) catechin, (-) epicatechin, an unknown procyanidin dimer and a procyanidin trimer, two prodelphinidin dimers, and two monogallate procyanidin dimers. The respective chromatograms are available in the Supplementary Material (Fig. S1). The stilbenoids identified were ampelopsin A, (*E*)-resveratrol, (*E*)-piceatannol, (*E*)- ϵ -viniferin, vitisin B, and hopeaphenol. Pallidol, (*E*)- δ -viniferin, and (*E*)- ω -viniferin were tentatively identified based on a comparison of the measured data with the MS/MS data reported in the literature [3,5,24]. Two glycosylated stilbenoid monomers were also detected, one of which corresponded to (*E*)-piceid [3,24]. The other glycosylated stilbenoid monomer exhibited a fragment corresponding to (*E*)-resveratrol (m/z of 227) as well as (*E*)-piceid but exhibited high-intensity m/z peaks at 269 and 241 (Table 1). This suggests that this compound is possibly a structural isomer or perhaps (*Z*)-piceid. An unknown stilbenoid dimer, a tetramer, a methoxy-stilbenoid monomer with an m/z peak at 258, and three

oxidized dimers, each with an m/z peak at 471, were also detected. It is known that oxidized stilbenoid dimers undergo fragmentation [24], exhibiting fragments at m/z values of 349 and 255. Compounds 12 and 21 exhibited the same fragments but showed different intensities, which indicates that they may be isomers. On the other hand, compound 17 had a more complex fragmentation pattern. Similar oxidized dimers have been reported in the case of wine [24] and grape skin [25]. To the best of our knowledge, this is the first instance where oxidized dimers have been detected in grape canes. Finally, based on the MS/MS data, the two flavonols were tentatively identified as quercetin pentoside and quercetin hexoside.



Table 1: Identity assignation of phenolic compounds in grape cane extract using HPLC-DAD-FL-MS/MS

peak	t _R ^a (min)	λ _{max} (nm)	t _R ^b (min)	λ _{exc/em} (nm)	[M-H] ⁻	Fragments	Phenolic compound
1			5.95	230/320	593	423, 407 , 339, 289 , 245, 177, 161, 125	Prodelfphinidin dimer
2			10.02	230/320	593	467, 423, 407 , 305 , 289 , 273, 245, 217, 177 , 137, 125	Prodelfphinidin dimer
3			11.48	230/320	577	559, 451, 425, 407 , 381, 339, 289 , 245, 205, 161, 151, 125	Procyanidin B1*
4			12.51	230/320	577	559, 451, 425, 407 , 381, 339, 289 , 273, 245, 205, 161, 151, 125	Procyanidin Dimer
5	13.13	279	13.33	230/320	289	245 , 205, 137	(+)-Catechin*
6			14.52	230/320	577	451, 425, 407 , 339, 329, 289 , 245, 203, 161, 125	Procyanidin B2*
7	15.56	279	15.76	230/320	289	245 , 205, 179, 137	(-)-Epicatechin
8			16.67	230/320	865	577, 543, 525, 449, 425, 407 , 381, 339, 289 , 261, 245, 175, 161, 137, 125	Procyanidin C1*
9	16.87	283, 320	17.08	330/374	389	281, 269 , 251, 241 , 227, 163, 147	Glycosilated stilbenoid monomer
10			17.37	230/320	865	587, 577, 525, 447, 407 , 425, 341, 289, 261, 243, 175, 161, 125, 137	Procyanidin trimer
11	17.98	311,358			433	300 , 283	Quercetin-pentoside
12			18.55	230/320	471	349, 255	Oxidized stilbenoid dimer
13	18.33	279			729	603, 451, 437, 407 , 381, 363, 339, 299, 289 , 271, 245, 187, 161, 125	Procyanidin dimer monogallate
14	18.766	286			729	433, 407 , 389, 323, 305, 289 , 271, 253, 187, 161, 125	Procyanidin dimer monogallate
15	19.97	304, 315	20.19	330/374	389	227 , 175, 147	(<i>E</i>)-piceid
16	20.73	330			463	300 , 243, 175, 159	Quercetin-hexoside
17	20.80	283, 305	21.50	330/374	471	453, 349 , 287, 219, 201, 153 , 121	Oxidized stilbenoid dimer

18	21.78	288, 322 329			509	463 , 331	n.i.
19	23.35	280	23.57	230/320	469	451 , 407, 375, 357, 316, 301, 229	Ampelopsin A*
20	24.10	324	24.33	330/374	243	225, 201, 159, 147	(<i>E</i>)-piceatannol*
21			27.15	230/320	471	349 , 255	Oxidized stilbenoid dimer
22		280			453	359, 265	Pallidol
23	32.20	306	32.43	330/374	227	199, 185, 143	(<i>E</i>)-resveratrol*
24	34.80	324	34.93	330/374	258	241 , 224, 172	Metoxy monomer of stilbenoid
25	35.82	320	35.95	330/374	287	269, 241	n.i.
26	43.81	280	44.92	230/320	905	811 , 717 , 649, 481, 451 , 423, 359 , 345 , 329 , 265 ,	Hopeaphenol*
27	44.18	324	44.42	330/374	453	411 , 359, 347 , 333, 253, 225 , 199, 119	(<i>E</i>)- ϵ -viniferin*
28	45.55	324	45.78	330/374	453	435 , 359 , 347, 345, 305, 255, 225	(<i>E</i>)- δ -viniferina
29	46.47	324	46.70	330/374	453	435 , 411 , 343, 333, 317	(<i>E</i>)- ω -viniferina
30	47.05	324	47.26	330/374	453	369, 359	Stilbenoid dimer
31	47.89	326	48.10	330/374	905	887, 869, 811, 799 , 793, 705, 692, 637, 557, 545, 451, 439, 359 , 347, 333, 265	Stilbenoid tetramer
32	48.51	326	48.75	330/374	905	887, 811, 799 , 726, 665, 611, 571, 545, 451, 439, 359 , 347 , 333	(<i>E</i>)-Vitisin B*

t_R^a : DAD detector, t_R^b : fluorescence detector, * confirmed by MS/MS data and standard; n.i.: not identified. Fragments presented in bold indicated those that were the most intense.

3.2 Chromatographic separation

Under the conditions described in the preceding section, the proanthocyanidins and stilbenoids could be separated even though a single run took approximately 60 min. To quantify the evolution of the analytes in the grape cane samples stored for different durations, a faster HPLC-DAD-FL method was developed. For this method the flow rate was increased from 0.4 to 1.4 mL/min, which resulted in an increase in the pressure drop from 90 to 360 bar. The gradient was optimized and the chromatographic parameters were calculated using the cane extract of Pinot Noir grapes stored for three methods after pruning; the extract was injected three times (Table 2) and the chromatograms obtained are shown in Fig. 2. The critical peak pairs correspond to (+)-catechin and procyanidin B2, which were detected in fluorescence mode, and for the stilbenoids ampelopsin A and (*E*)-piceatannol, which were detected at 280 nm in absorbance mode. The most critical separation is in (+) catechin from procyanidin B2 ($R_s = 1.50$), is possible to separate these proanthocyanidins using another core-shell C18 column with similar characteristic and different gradient (Table 1 and figure 2, Supplementary Data). However, it was not possible to resolve with it all stilbenoids. The backpressure of the developed method was 360 bar; a pressure this low is advantageous for core-shell particle technology. The method is suitable for the quantification of major proanthocyanidins and it resolves dimers and trimers, even dimers of prodelphinidins; it also enables the quantification of major and minor stilbenoids.

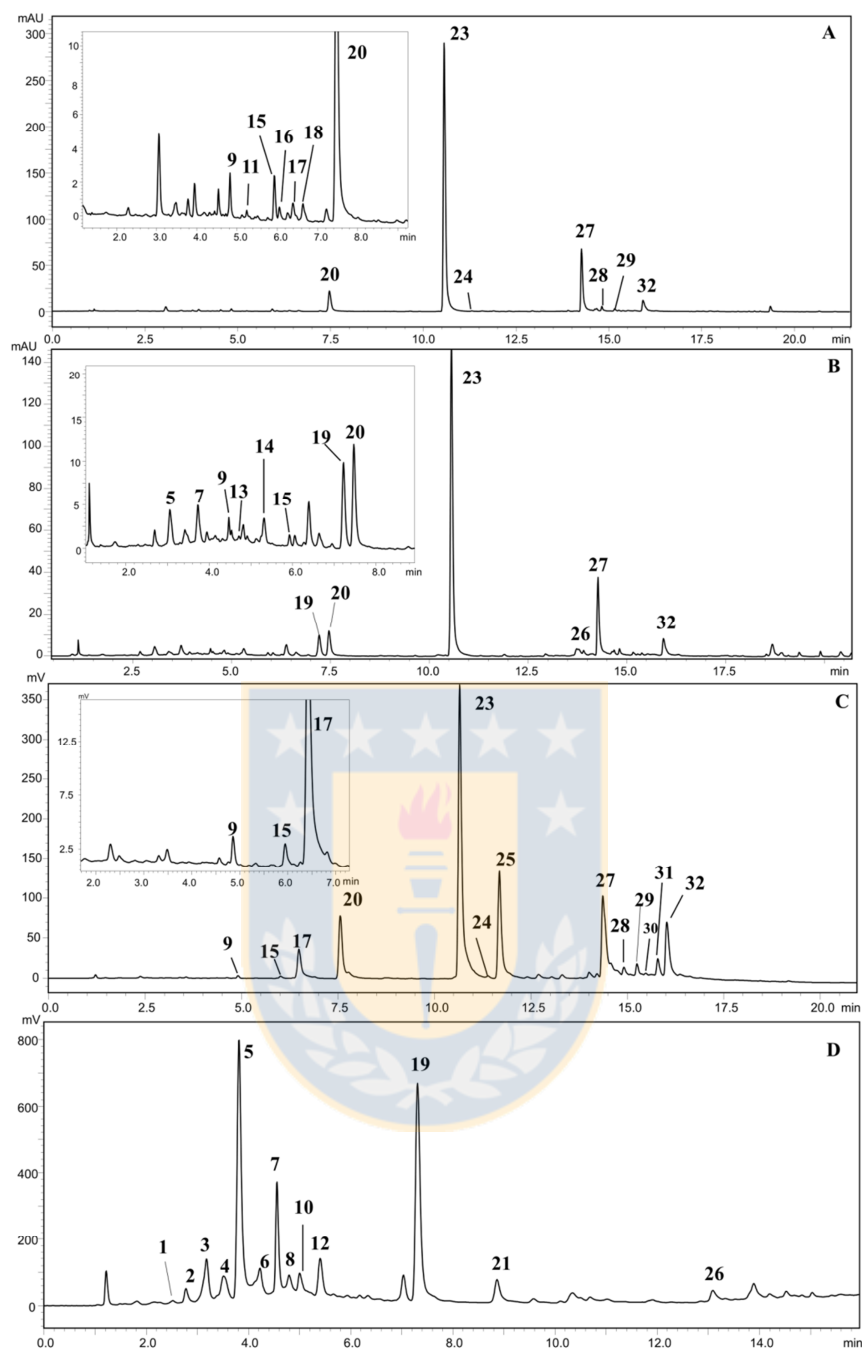


Fig. 2: HPLC-DAD-FL quantitative chromatograms for grape cane extracts. Peak numbers are as listed in Table 1. (A) Absorbance at 306 nm, (B) absorbance at 280 nm, (C) fluorescence detection at 330 and 374 nm, and (D) fluorescence detection at 230 and 320 nm.

Table 2: Chromatographic parameters calculated for development method in core shell column.

Critical peak pairs	t_R' (min)	Rs	N	H (μm)	k
(+)-Catechin	2.53 ±0.02		6170 ±157	24.31± 0.43	2.09± 0.01
Procyanidin B2	2.95 ± 0.01	1.50 ± 0.14	6735 ± 198	22.27± 0.65	2.45± 0.00
Ampelopsin A	6.06 ± 0.05		50205 ±1062	2.99± 0.12	5.37± 0.00
(E)-picetannol	6.31 ±0.05	1.93 ± 0.05	50928± 1033	2.94± 0.11	5.59 ±0.08

N: number of theoretical plates; HETP: Height Equivalent to a Theoretical Plate (μm), k: retention factor.

3.3 Quantification of proanthocyanidins and stilbenoids in grape canes

The linearity of the method was evaluated using an external calibration curve for stilbenoids and proanthocyanidins obtained in the fluorescence and absorbance modes using the DAD. Calibration was performed at the wavelengths indicated in Table 3 at the maximal of absorbance of each compound. The coefficient of regression was 0.994–0.999, indicating good linearity. For the stilbenoids, the sensitivity of the fluorescence mode was higher than that of the absorbance mode. The primary stilbenoids, namely, (*E*)-resveratrol, (*E*)-piceatannol, and (*E*)-ε-viniferin, were quantified in absorbance mode, as it allowed for a comparison of the results with previously reported data [3-4,16]. However, in the case of the stilbenoids with lower concentrations, quantification was performed in fluorescence mode. The fluorescence spectra of vitisin B and ampelopsin A were acquired (Fig. S3, Supplementary Material). In contrast to the other stilbenoids, it was not possible to detect ampelopsin A in fluorescence mode using the excitation and emission wavelengths

typically used for the other stilbenoids. This was also the case for hopeaphenol. The absence of olefin bonds in both oligostilbenoids may be the reason for the difference in the fluorescence behavior. To quantify ampelopsin A, excitation and emission wavelengths of 230 and 320 nm, respectively, are more appropriate, which are the same as those used to detect the proanthocyanidins; the latter exhibit very low absorptions at 280 nm.

The intraday and interday repeatabilities (on three different days) were evaluated based on the relative standard deviation (RSD) of three proanthocyanidins and four stilbenoids using Pinot Noir grape cane extract (Table 4). The RSD was less than 7% for all analytes, which is considered acceptable for the proposed method (including the extraction process and chromatographic analysis), because the biological variability of the analyzed material, as observed in previous studies, is greater than the variability of the analytical method [2,3].

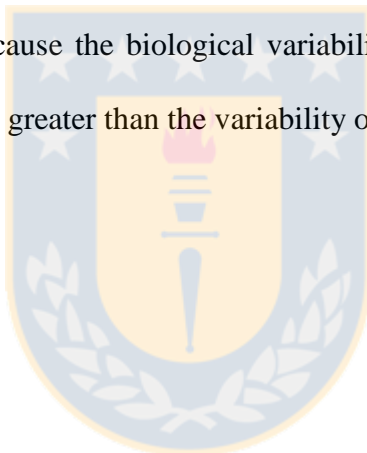


Table 3: Calibration curves and limits of detection (LOD) and quantification (LOQ) for stilbenoids and proanthocyanidins using DAD and fluorescence detection.

Phenolic compound	DAD detection					Fluorescence detection				
	λ_{\max} (nm)	Equation ^a	R ²	LOD mg/kg	LOQ mg/kg	$\lambda_{\text{Exc/Em}}$ (nm)	Equation ^a	R ²	LOD mg/kg	LOQ mg/kg
(E)-Resveratrol	306	y=22048 x-8657.2	0.999	2.13	7.08	330/374	y = 41065 x -11609	0.999	1.38	4.59
(E)-ϵ-Viniferin	323	y=9313.8 x-9340.3	0.998	5.84	19.46	330/374	y =20401 x-11671	0.998	4.07	13.55
(E)-Piceatannol	323	y=21358x-28861	0.994	3.83	12.77	330/374	y=78290x-87641	0.995	2.69	8.96
Ampelopsin A	280	y=2052.7x-641.8	0.999	6.06	20.19	230/321	y= 192924x-73015	0.998	4.43	14.76
Vitisin B	326	y= 3820.5 x-2338.3	0.997	5.94	19.80	330/374	y=22363x-18365	0.999	5.12	17.08
Hopeaphenol	280	y=1526.7x-528.61	0.999	8.18	27.27	230/321	y=13408x-7582.7	0.998	6.24	20.80
(+)-Catechin	280	y=1977.3x+6.0826	0.998	6.81	22.71	230/323	y= 447075x+360402	0.998	4.35	14.50
(-)-Epicatechin	280	y= 2040.2x+250.41	0.999	3.88	12.94	230/323	y=385616x+ 379016	0.997	2.81	9.35
Procyanidin B 1						230/323	y=114508x+19915	0.996	2.22	7.39
Procyanidin B 2						230/323	y=229244x+59657	0.998	1.47	4.90
Procyanidin C 1						230/323	y=183588x+20946	0.998	2.39	7.95

^a: x: mg L⁻¹; y: area units.

Table 4: Interday and intraday repeatability for stilbenoid and procyanidin concentrations in Pinot Noir grape canes (n= 3).

Phenolic compound	Inter-day		Intra-day	
	Average (mg/kg)	RSD %	Average (mg/kg)	RSD %
Procyanidin B1	636.1	1.6	635.2	2.4
(+) Catechin	782.9	1.4	795.9	0.9
(-) Epicatechin	187.9	2.0	190.9	2.4
Ampelopsin A	204.5	0.7	207.0	1.4
(E)-Piceatannol	374.1	5.5	376.0	6.4
(E)-Resveratrol	3655.3	4.3	3703.9	3.2
(E)-ε-Viniferin	1445.4	1.0	1473.9	1.0

RSD: relative standard deviation.

3.4. Effect of relative humidity during post-pruning storage on stilbenoid concentrations

As illustrated in Fig. 3A (*E*)-resveratrol, the main stilbenoid present in grape canes during storage at 60% RH, increased from 75 ± 2 mg/kg dry weight (DW) in fresh pruned Pinot Noir canes to 5453 ± 24 mg/kg after 75 days of storage. This implies that storage increases the (*E*)-resveratrol level by up to a factor of 68. In the case of Cabernet Sauvignon, the increase at 60% RH was a factor of 42 while for the Tintorera canes, it was a factor of 49. However, at an 70% RH (Fig. 3B), the increase in the (*E*)-resveratrol levels for Pinot Noir and Tintorera was approximately only half that observed at an RH of 60%, whereas for Tintorera, it was less than one-third, suggesting that for (*E*)-resveratrol, storage at 60% RH is more favorable for inducing biosynthesis after pruning than is storage at 70% RH. These results confirm the findings of Gorena (2014) [3] and Houillé (2015) [16] who reported that increases in (*E*)-resveratrol concentration during storage are variety dependent; however, they did not evaluated the effect of RH.

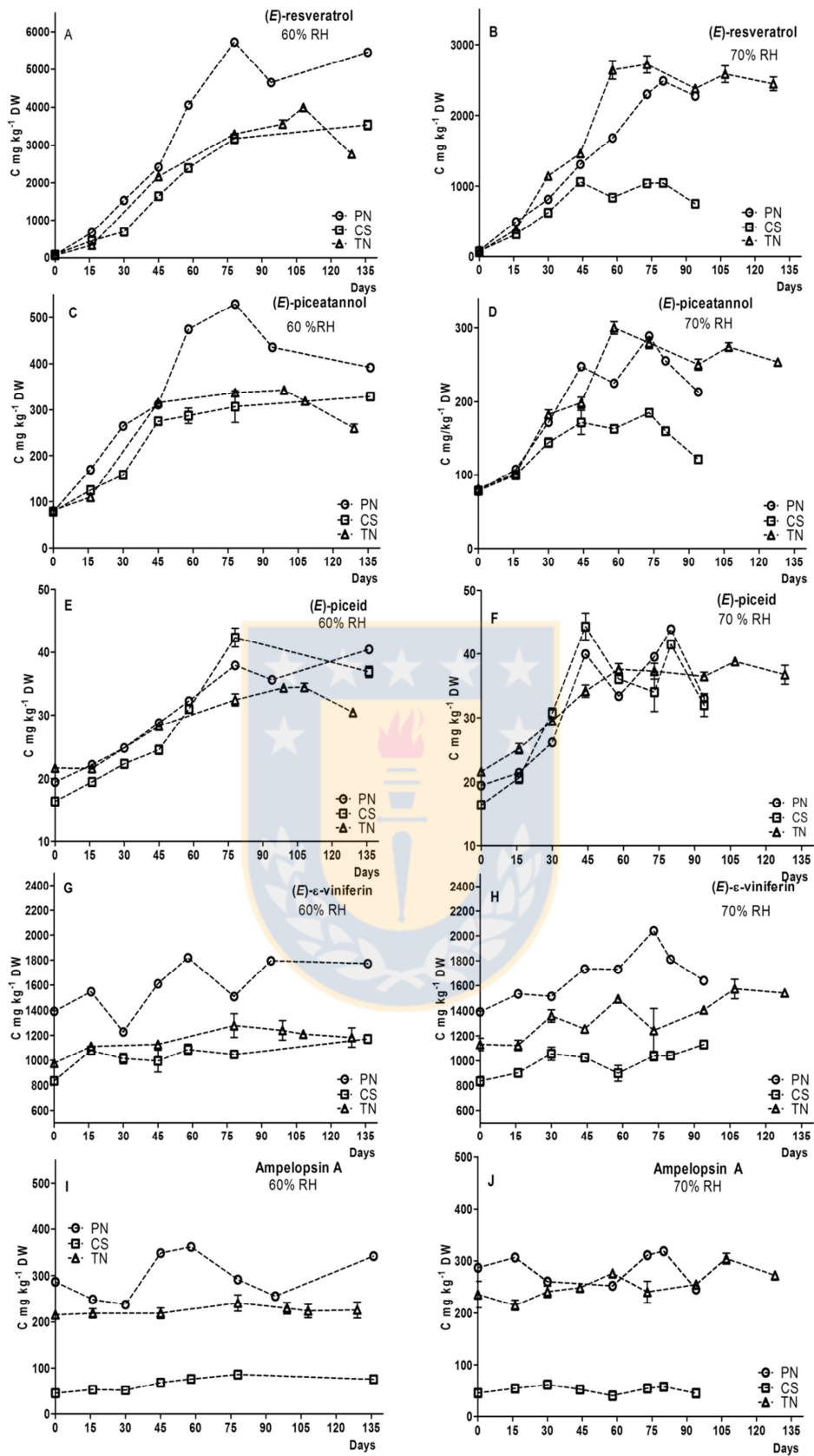


Fig. 3: Stilbenoid levels (mg/kg dry weight) as functions of time during grape cane

storage at 60% and 70% relative humidity (RH). Grape varieties: PN: Pinot Noir; CS: Cabernet Sauvignon; TN: Tintorera. Concentrations of (*E*)-piceid as (*E*)-resveratrol equivalents. Error bars correspond to analytical standard deviations.

The concentration of (*E*)-piceatannol also increased during storage of canes under both RH conditions. This increase for the canes stored at 60% RH was higher (Fig. 3C) than those for the canes stored at 70% RH; concentrations increased by factors of 6.8, 3.5, and 4, respectively, in the cases of Pinot Noir, Cabernet Sauvignon, and Tintorera after storage at 60% RH.

The concentrations of the two compounds, namely, (*E*)-resveratrol and (*E*)-piceatannol, increased after pruning and then plateaued. In the case of (*E*)-resveratrol, the plateauing occurred approximately 58 to 75 days after pruning when the canes were stored at 60% RH, whereas for Tintorera and Cabernet Sauvignon, it occurred between 45 and 75 days at 70% RH. Hence, there is good evidence to support the conclusion that the observed increases in concentrations were due of *de novo* biosyntheses. After pruning, the stilbene synthase transcription gene is induced in grape canes [16]. The known variables responsible for the increase in the (*E*)-resveratrol and (*E*)-piceatannol levels are the duration of storage after pruning [3] and the temperature [16]. Very recently, it was reported that mechanical stress on freshly pruned canes overinduces the biosyntheses of (*E*)-resveratrol and (*E*)-piceatannol [26] within a short period after pruning. When fresh canes are cut at small lengths (1 cm), the storage period after which increase in the stilbenoid levels plateaus is reduced from 42 days to 14 days [26]. Our data suggest that a new variable must be considered with respect to the formation of stilbenoids in canes, namely, the RH. The humidity of the environment in which canes are stored determines the levels of (*E*)-piceatannol and (*E*)-resveratrol. A difference of only 10 percentage

points in the RH can increase the concentration for the same variety significantly, with the concentrations of the stilbenoids at 60% RH being higher than those at 70% RH. To develop a strategy for maximizing the levels of inducible stilbenoids more quickly, it is necessary consider the relative humidity, along with the length of the cut, the temperature, and the storage period following pruning.

The change in the concentration of (*E*)-piceid during post-pruning storage has not been reported before. In this study, its concentration during the post-pruning storage of canes did not increase as much as those of (*E*)-resveratrol (by a factor of 100) and (*E*)-piceatannol (by a factor of 10), changing 19–21 mg/kg to 32–44 mg/kg as (*E*)-resveratrol equivalent ($p < 0.05$) at both RH for all the studied varieties (Fig. 3E and F); the highest level was observed at 44 days after pruning when stored at 70% RH, and at 78 days after storage at 60% RH.

In contrast to the previously mentioned monomeric stilbenoids, the oligomeric stilbenoids (*E*)- ϵ -viniferin (Fig. 3G, 3H) and ampelopsin A (Fig. 3J, 3I) did not exhibit significant increases in their levels during cane storage after pruning; this was irrespective of RH during storage. This confirms that these oligostilbenoids are not biosynthesized after pruning, consistent with the results of Gorena (2014) [3] and Houillé (2015) [16].

In addition to the stilbenoids discussed above, a glycosylated monomer and an oxidized dimer were also observed after storage; however, they could not be further identified. The oxidized dimer (compound 17) was present in noticeable concentrations in the Pinot Noir canes (up to 868 ± 14 mg/kg DW as (*E*)- ϵ -viniferin equivalent) but not in the other varieties.

The induction of stilbenoid biosynthesis in pruned canes is triggered by stress. Canes activate an intricate defense strategy in response to a stress stimulus. In addition to (*E*)-

resveratrol, (*E*)-piceatannol, and (*E*)-piceid, a few other stilbenoids may also be involved in the responses of canes to stress. The induction of glycosylated and oxidized stilbenoids that act as phytoalexins has been reported [27]. The accumulation of (*E*)-piceid in *in-vitro*-grown *Vitis* cells induced by an elicitor such as methyl jasmonate has also been reported [27], as has the glycosylation and peroxidation of phenolic compounds to yield phytoalexins as part of a defense mechanism [27].

3. 5. Changes in proanthocyanidin levels in canes during post-pruning storage

The change in the concentration of flavan-3-ol units during the post-pruning storage of grape canes differ in their levels in canes after pruning (Fig. 4). While the concentration of (–)-epicatechin showed a distinct decrease after 15 days of storage at 60% RH in all the varieties (Fig. 4A), there was a certain delay in this decrease in the case of storage at 70% RH (Fig 4B). The level of (+)-catechin in Tintorera, the teinturer variety, was much higher than those in the other varieties, with slight variations in the level observed during storage. On the other hand, the other varieties contained (+)-catechin in lower levels, with the level decreasing in some cases.

The concentration of procyanidin B1 also varied at 60% RH (Fig. 4E), with no distinct trend being observed. On the other hand, at 70 % RH, initially, the concentration increased after 15 days of storage and then decreased (Fig. 4 F). However, the final concentrations in both cases were similar.

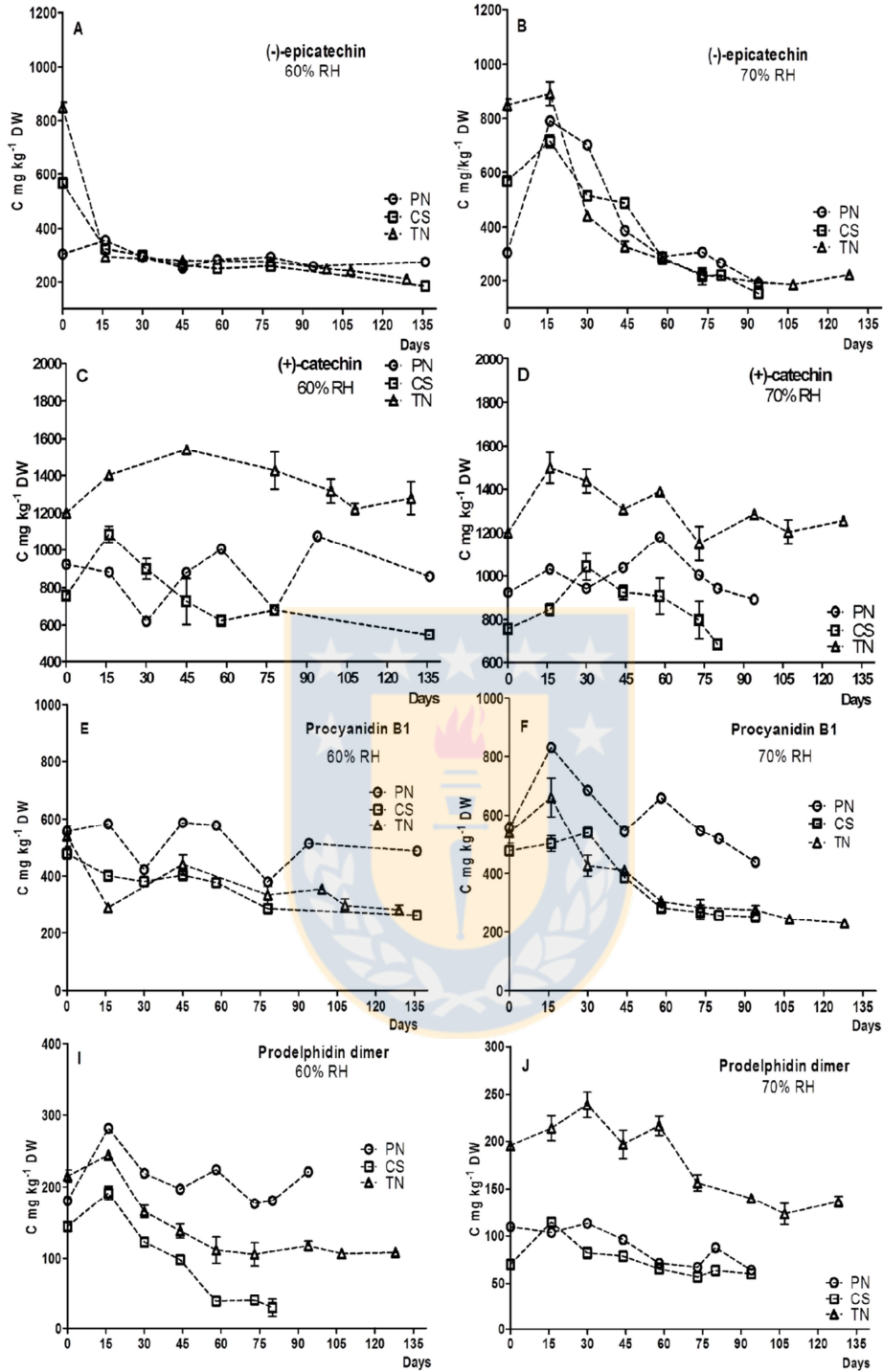


Fig. 4: Proanthocyanidin levels (mg/kg dry weight) as functions of time during grape cane storage at 60% and 70% relative humidity (RH). Grape varieties: PN: Pinot Noir; CS: Cabernet Sauvignon; TN: Tintorera. Concentrations of prodelphinidin dimer as procyanidin B1 equivalents. Error bars correspond to analytical standard deviations.

A prodelphinidin dimer was quantified for the first time in grape canes. The highest concentration observed for this dimer in the studied varieties was 288 ± 4 mg/kg as procyanidin B1 equivalents, while that for procyanidin B1 was 829 ± 18 mg/kg and that for the procyanidin dimer (compound 4) was 281 ± 14 mg/kg as procyanidin B1 equivalents. The concentration of the latter decreased slightly during storage in some cases (Fig. 4I and 4J).

A decrease in the proanthocyanidin level and a parallel increase in the stilbenoid levels has been reported for winegrape skins subjected to dehydration [28]. In these skins, the flavan-3-ol levels were measured under both fast and slow dehydration. (-)-epicatechin was depleted after slow dehydration but not after rapid dehydration. Furthermore, when the amount of water lost was low, the level of (-)-epicatechin increased [28]. The present data show that the levels of (-)-epicatechin in the grape canes stored at higher RH (70%) increased, probably because the amount of water lost over this period (15 days of storage) was low. On the other hand, the level decreased significantly after longer storage.

4. Conclusions

In this study, HPLC-DAD-FL-MS/MS was used to identify stilbenoids such as (*E*)-resveratrol, (*E*)-piceatannol, (*E*)- ϵ -viniferin, (*E*)-piceid, ampelopsin A, and (*E*)-vitisin B, and hopeaphenol in pruned grape canes stored for periods of up to three months. The compounds tentatively identified were pallidol, (*E*)- ω -viniferin, and (*E*)- δ -viniferin. In addition, a glycosylated stilbene monomer, a methoxy monomer, and three oxidized dimers were also detected. Flavan-3-ol units such as (+)-catechin, (-)-epicatechin, and the proanthocyanidins procyanidin B1, B2, and C1, as well as an unknown procyanidin

dimer, a trimer, two prodelfidin dimers, and monogallate procyanidin were also identified.

The proposed chromatographic method, which is shorter and faster, allows for the simultaneous quantification of the primary proanthocyanidins and stilbenoids present in grape canes within 24 min using an HPLC column based on core-shell particle technology. The combined use of a DAD and a FL detector in series helped to improve sensitivity for (*E*)-piceid and proanthocyanidins.

Using the developed method, we observed that the concentrations of monomeric stilbenoids among the canes stored at 60% RH were around twice that of those stored at 70% RH. We conclude, therefore, that the relative humidity has an inducing effect on the biosyntheses of monomeric stilbenoids during cane storage. On the other hand, the levels of (–)-epicatechin, and to a smaller extent those of procyanidin B1 and the prodelfidin dimer, decreased progressively during cane storage. At 70% RH, the concentration of (–)-epicatechin first increased and then decreased, with the overall concentration being lower than that observed at 60% RH.

Hence, these results confirm that the proposed quantitative HPLC-DAD-FL method is suitable for monitoring changes in the concentrations of proanthocyanidins and stilbenoids in stored canes owing to its high sensitivity. Furthermore, because it allows for the simultaneous quantification of proanthocyanidins and stilbenoids, it can also be used to quantify these two types of antioxidants in other matrices.

Acknowledgements

This work was supported by CONICYT Chile: (FONDECYT 1150721, Basal Project PFB-27 and Doctorate Fellowship. The authors thank Viña De Neira and Viña Chillán for allowing grape cane samples to be collected from their vineyards and to Editage for English editing of the manuscript.

References

- [1] E.S. Çetin, D. Altinöz, E. Tarçan, N. Göktürk Baydar, Chemical composition of grape canes, *Ind. Crops Prod.* 34 (2011) 994–998.
- [2] C. Vergara, D. von Baer, C. Mardones, A. Wilkens, K. Wernekinck, A. Damm, S. MacKe, T. Gorena, P. Winterhalter, Stilbene levels in grape cane of different cultivars in southern Chile: Determination by HPLC-DAD-MS/MS method, *J. Agric. Food Chem.* 60 (2012) 929–933.
- [3] T. Gorena, V. Sáez, C. Mardones, C. Vergara, P. Winterhalter, D. Von Baer, Influence of post-pruning storage on stilbenoid levels in *Vitis vinifera* L. canes, *Food Chem.* 155 (2014) 256–263.
- [4] R.F. Guerrero, B. Biais, T. Richard, B. Puertas, P. Waffo-Teguo, J.M. Merillon, E. Cantos-Villar, Grapevine cane's waste is a source of bioactive stilbenes, *Ind. Crops Prod.* 94 (2016) 884–892.
- [5] J. Gabaston, E. Cantos-villar, P. Wa, E. Renouf, T. Richard, J. Me, Stilbenes from *Vitis vinifera* L. Waste: A Sustainable Tool for Controlling *Plasmopara Viticola*. 65 (2017), 2711-2718.
- [6] A. Zhang, L. Wan, C. Wu, Y. Fang, G. Han, H. Li, Z. Zhang, H. Wang, Simultaneous determination of 14 phenolic compounds in grape canes by HPLC-DAD-UV using wavelength switching detection, *Molecules.* 18 (2013) 14241–14257.
- [7] R. Sánchez-Gómez, A. Zalacain, G.L. Alonso, M.R. Salinas, Vine-shoot waste aqueous extracts for re-use in agriculture obtained by different extraction techniques: Phenolic, volatile, and mineral compounds, *J. Agric. Food Chem.* 62 (2014) 10861–10872.

- [8] L. Montero, V. Sáez, D. Von Baer, A. Cifuentes, M. Herrero, Profiling of *Vitis vinifera* L. canes (poly)phenolic compounds using comprehensive two-dimensional liquid chromatography, *J. Chromatogr. A.* (2017). In Press.
- [9] M.H. Keylor, B.S. Matsuura, C.R.J. Stephenson, Chemistry and Biology of Resveratrol-Derived Natural Products, *Chem. Rev.* 115 (2015) 8976–9027.
- [10] B. Catalgol, S. Batirel, Y. Taga, N.K. Ozer, Resveratrol: French paradox revisited, *Front. Pharmacol.* 3 JUL (2012) 1–18.
- [11] R. De La Iglesia, F.I. Milagro, J. Campión, N. Boqué, J.A. Martínez, Healthy properties of proanthocyanidins, *BioFactors.* 36 (2010) 159–168.
- [12] N. Martinez-Micaelo, N. González-Abuín, A. Ardèvol, M. Pinent, M.T. Blay, Procyanidins and inflammation: Molecular targets and health implications, *BioFactors.* 38 (2012) 257–265.
- [13] T. Vogt, Phenylpropanoid biosynthesis, *Mol. Plant.* 3 (2010) 2–20.
- [14] C. Lambert, T. Richard, E. Renouf, J. Bisson, P. Waffo-Téguo, L. Bordenave, N. Ollat, J.M. Mérillon, S. Cluzet, Comparative analyses of stilbenoids in canes of major *Vitis vinifera* L. cultivars, *J. Agric. Food Chem.* 61 (2013) 11392–11399.
- [15] T. Püssa, J. Floren, P. Kuldkepp, A. Raal, Survey of grapevine *Vitis vinifera* stem polyphenols by liquid chromatography-diode array detection-tandem mass spectrometry, *J. Agric. Food Chem.* 54 (2006) 7488–7494.
- [16] B. Houillé, S. Besseau, V. Courdavault, A. Oudin, G. Glévarec, G. Delanoue, L. Guérin, A.J. Simkin, N. Papon, M. Clastre, N. Giglioli-Guivarc'h, A. Lanoue, Biosynthetic Origin of E -Resveratrol Accumulation in Grape Canes during Postharvest Storage, *J. Agric. Food Chem.* 63 (2015) 1631–1638.

- [17] R. Hayes, A. Ahmed, T. Edge, H. Zhang, Core-shell particles: Preparation, fundamentals and applications in high performance liquid chromatography, *J. Chromatogr. A.* 1357 (2014) 36–52.
- [18] V. González-Ruiz, A.I. Olives, M.A. Martín, Trends in Analytical Chemistry Core-shell particles lead the way to renewing high-performance liquid chromatography, *Trends Analyt. Chem.* 64 (2015) 17–28.
- [19] R.J. Robbins, J. Leonczak, J.C. Johnson, J. Li, C. Kwik-Urbe, R.L. Prior, L. Gu, Method performance and multi-laboratory assessment of a normal phase high pressure liquid chromatography-fluorescence detection method for the quantitation of flavanols and procyanidins in cocoa and chocolate containing samples, *J. Chromatogr. A.* 1216 (2009) 4831–4840.
- [20] L.L. Lin, C.Y. Lien, Y.C. Cheng, K.L. Ku, An effective sample preparation approach for screening the anticancer compound piceatannol using HPLC coupled with UV and fluorescence detection, *J. Chromatogr. B Anal. Technol. Biomed. Life Sci.* 853 (2007) 175–182.
- [21] P. Franco, T. Zhang, Common approaches for efficient method development with immobilised polysaccharide-derived chiral stationary phases, *J. Chromatogr. B Anal. Technol. Biomed. Life Sci.* 875 (2008) 48–56.
- [22] J. Vial, A. Jardy, Experimental comparison of the different approaches to estimate LOD and LOQ of an HPLC method, *Anal. Chem.* 71 (1999) 2672–2677.
- [23] J. Miller & J. Miller, *Statistic Chemometrics for Analytical Chemistry* (4th edition), Prentice Hall, Madrid, 2000, pp. 125-128.
- [24] R. Moss, Q. Mao, D. Taylor, C. Saucier, Investigation of monomeric and oligomeric wine stilbenoids in red wines by ultra-high-performance liquid

chromatography/electrospray ionization quadrupole time-of-flight mass spectrometry, *Rapid Commun. Mass Spectrom.* 27 (2013) 1815–1827.

[25] R. Perestrelo, Y. Lu, S.A.O. Santos, A.J.D. Silvestre, C.P. Neto, J.S. Câmara, S.M. Rocha, Phenolic profile of Sercial and Tinta Negra *Vitis vinifera* L. grape skins by HPLC-DAD-ESI-MSⁿ: Novel phenolic compounds in *Vitis vinifera* L. grape, *Food Chem.* 135 (2012) 94–104.

[26] K. Billet, B. Houillé, S. Besseau, C. Mélin, A. Oudin, N. Papon, V. Courdavault, M. Clastre, N. Giglioli-Guivarc'h, A. Lanoue, Mechanical stress rapidly induces E-resveratrol and E-piceatannol biosynthesis in grape canes stored as a freshly-pruned byproduct, *Food Chem.* 240 (2018) 1022–1027.

[27] P. Jeandet, B. Delaunois, A. Conreux, D. Donnez, V. Nuzzo, S. Cordelier, C. Clément, E. Courot, Biosynthesis, metabolism, molecular engineering, and biological functions of stilbene phytoalexins in plants, *BioFactors.* 36 (2010) 331–341.

[28] C. Bonghi, F.M. Rizzini, A. Gambuti, L. Moio, L. Chkaiban, P. Tonutti, Phenol compound metabolism and gene expression in the skin of wine grape (*Vitis vinifera* L.) berries subjected to partial postharvest dehydration, *Postharvest Biol. Technol.* 67 (2012) 102–109.

Supplementary material Capitulo 3 sección 1:

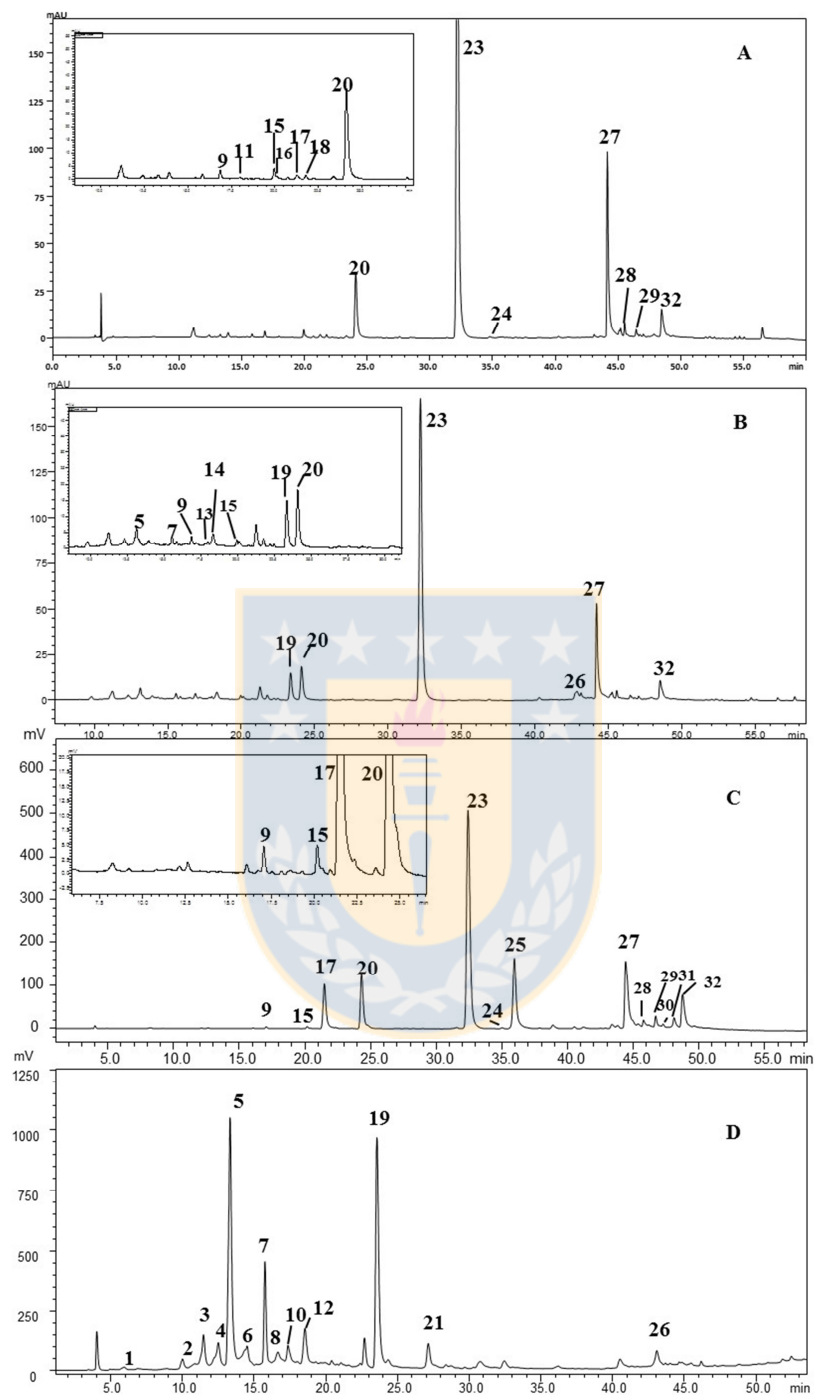


Figure S.1: HPLC-DAD-MS/MS chromatogram for identification of stilbenoids and proanthocyanidins for cane extract. (A) absorbance at 306 nm, (B) absorbance at 280 nm, (C) fluorescence detection at 330 nm and 374 nm, (D) fluorescence detection at 230 nm and 320 nm.

Table S.1: Chromatographic parameters calculated for a secondary gradient for grape cane extract development in a second C-18 core-shell column (150 x 4.8 mm, 2.6 μm of particle size, 1.6 μm of nucleus and 12% of carbon load).

Critical peak pairs	t_r' (min)	Rs	N	H (μm)	k
(+)-catechin	2.63 \pm 0.02		5167 \pm 950	29.04 \pm 1.11	2.11 \pm 0.02
Procyanidin B2	3.01 \pm 0.01	2.22 \pm 0.19	10051 \pm 212	14.92 \pm 0.31	2.42 \pm 0.03
Ampelopsin A	7.25 \pm 0.00		38820 \pm 1932	3.87 \pm 0.18	6.23 \pm 0.01
(E)-picetannol	7.40 \pm 0.00	1.05 \pm 0.01	39940 \pm 1980	3.8 \pm 0.57	6.37 \pm 0.08

N: number of theoretical plates, **Rs:** resolution, **H:** Height Equivalent to a Theoretical Plate, **k:** retention factor.

Separation conditions: The injection volume was 10.0 μL at 30°C and the flow rate was 1.3 mL/min. The %B increased from 10% to 15% in 0.3 min and subsequently to 20% at 1.8 min, 24% at 2.6 min, 28% at 5.0 min, 29% at 7.0 min, 30% at 9.0 min, 40% at 13.00 min, and 70% at 17 min. Next, the column was washed with 100% B for 3 min and equilibrated with 10% B for 3 min.

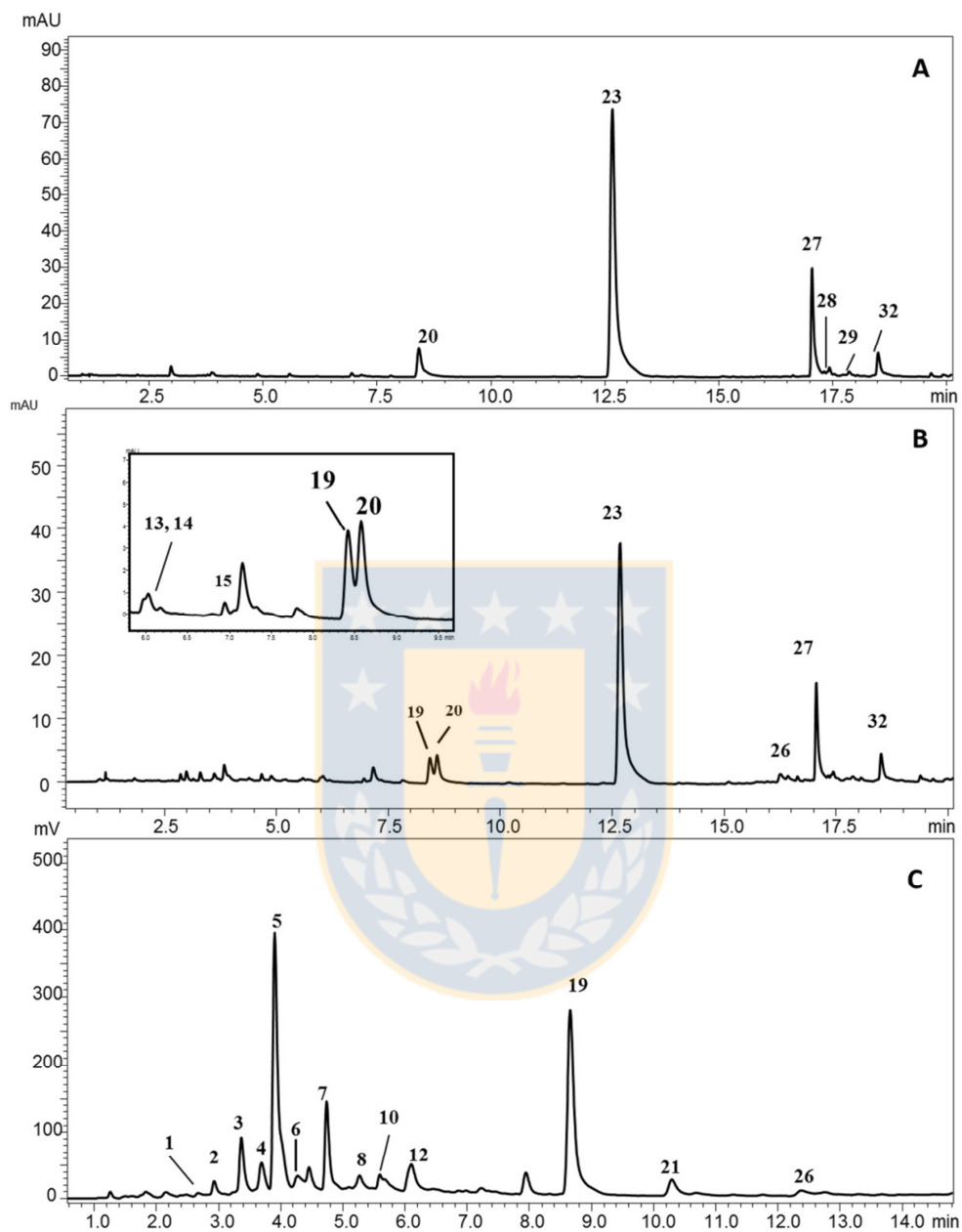


Figure S.2: HPLC-DAD-FL chromatograms for grape cane extract column I. Peaks number are in table n°1. (A) absorbance at 306 nm, (B) absorbance at 280 nm, (C) Fluorescence detection at 230 and 320 nm.

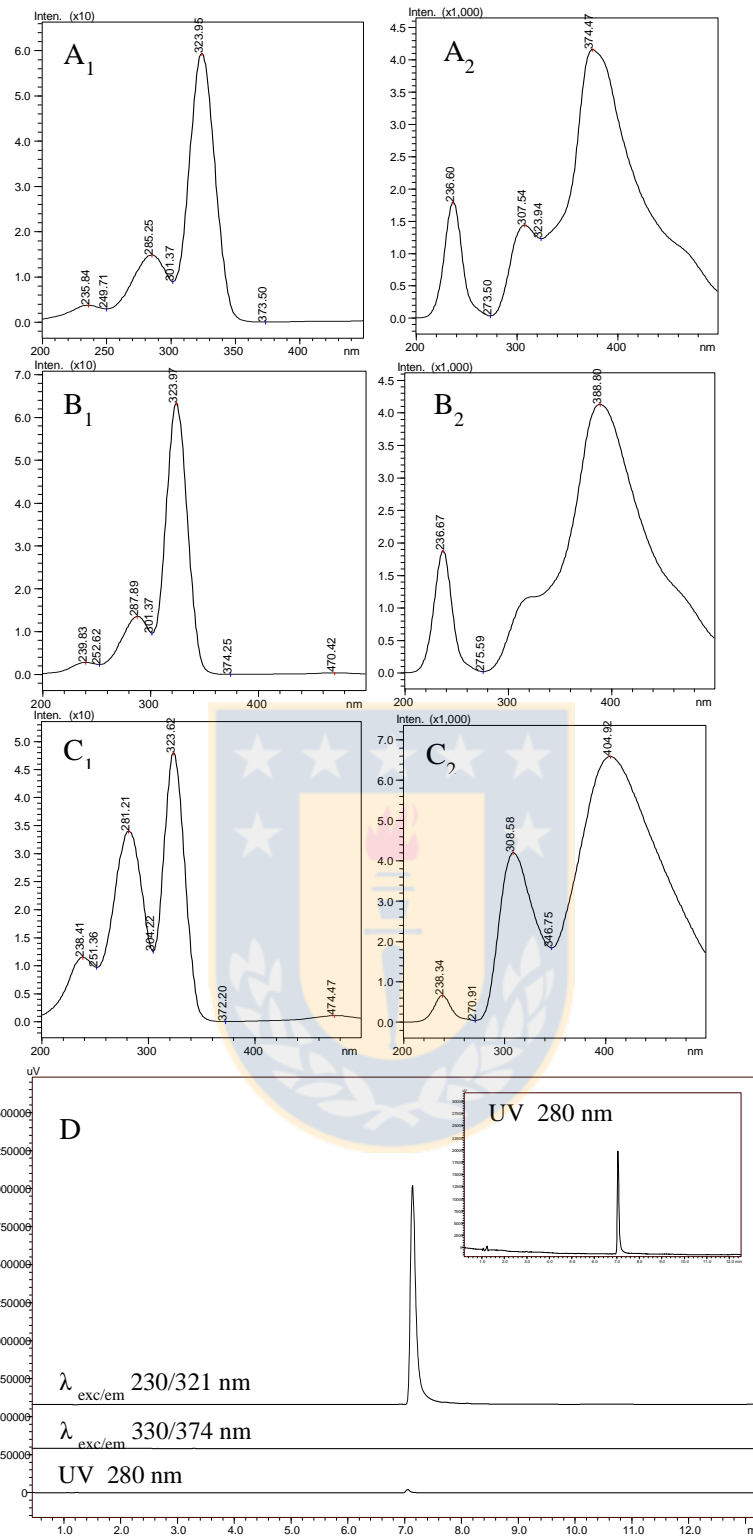


Figure S.3: Fluorescence spectra obtained in spectrum scan mode for excitation (1) and emission (2) by FL detector for: **(A)** (*E*)-resveratrol, **(B)** vitisin B and **(C)** ampelopsin A. **(D)** HPLC-DAD-FL chromatograms for ampelopsin A standard.

Capítulo 3: Sección 2

Hidrólisis alcalina, enzimática y golpe de calor aplicados en sarmientos de vides: evidencias claves que apoyan el origen biosintético de estilbenos monoméricos en sarmientos con guarda post-poda.

Resumen:

Los sarmientos son residuos lignocelulósicos con gran potencial debido a los altos niveles de estilbenoides. La guarda luego de la poda de los sarmientos de vides es clave para gatillar el incremento de estilbenoides, principalmente (*E*)-resveratrol y (*E*)-piceatanol. Se aplicó a sarmientos con 2 días de guarda procesos de autohidrólisis, hidrólisis enzimática y alcalina. Estos procesos no aumentaron los niveles de estilbenos monoméricos en sarmientos. Además se monitoreó los niveles de los estilbenoides en sarmientos a los que se aplicó un golpe de calor (2h, 60°C) previo a la guarda post-poda en condiciones de temperatura y humedad controlada. Los niveles de oligoestilbenoides no aumentaron significativamente luego de la poda, ya que no se registró un aumento de (*E*)-resveratrol ni de (*E*)-piceatanol. Los resultados apoyan el origen de los estilbenoides monoméricos se deba a la biosíntesis *de novo*.

1. Materiales y métodos:

1.1. Muestras de sarmientos para hidrólisis:

Los sarmientos de vides de la variedad Pinot Noir fueron recolectados en la viña Chillán, valle del Itata, región del Bío-Bío en invierno de 2016, luego de 2 días almacenados a temperatura ambiente fueron congelados a -20°C en bolsas plásticas, mientras que otra fracción de sarmientos fueron guardados luego de la poda por 92 días a 70% de humedad relativa a 20°C (cámara de cultivo Memmert HPP 110).

1.2. Muestras para monitorear estilbenoides luego de un golpe de calor:

Los sarmientos de vides de la variedad Pinot Noir fueron recolectados en la viña Chillán, valle del Itata, región del Bío-Bío en invierno de 2016. Inmediatamente después de la poda fueron dejados en una estufa por 2 horas a 60°C . Posteriormente fueron almacenados (cámara de cultivo Memmert HPP 110) en temperatura y humedad controladas (70% humedad relativa, 20°C) por al menos 12 semanas luego de la poda.

1.3. Extracción:

Los sarmientos fueron liofilizados, molidos y finalmente se procedió a extraer los estilbenoides acorde a la metodología descrita en el capítulo 3 en el numeral 2.3 de la sección 1.

1.4. Autohidrólisis :

Los sarmientos fueron pre-tratados para ser enzimáticamente hidrolizados. El pretratamiento consiste en una autohidrólisis (Au) del residuo de la extracción del sarmiento. Para autohidrolizar se autoclavo por una hora y media a 100°C .

1.5. Hidrólisis enzimática e hidrólisis básica:

La figura 1 ilustra los procesos hidrolíticos realizados. Una mezcla de celulasas, hemicelulasas, β -glucosidasas comercial (Cellic Ctec3, Novozyme) se utilizó para hidrolizar el residuo de sarmiento. Para saber la cantidad de enzimas a emplear acorde

al sustrato, se empleó el método de reactivo de Bradford (Biorad-Sigma) en el lector de microplacas (Synergy/ HTX). La hidrólisis enzimática se realizó en oscuridad.

Se siguieron las recomendaciones de proveedor de cellic Ctec 3 para hidrólisis. Para 0.5 g de sarmiento seco se agregó Cellic Ctec 3 (3.5 % w/w) en 5 mL de buffer citrato (pH: 4.8). Se dejó sellado en agitación continua (185 rpm) a 50°C por 3 y 6 horas. Se centrifugó por 1600 rpm durante 5 minutos extrayéndose el sobrenadante del sarmiento. Posteriormente se procedió a realizar una extracción.

Para la hidrólisis básica se utilizó 1g de residuo de sarmiento, se adicionó 8 mL de NaOH (1.13N) por 30 minutos a una temperatura de 70°C con agitación constante a 160 rpm. Posterior a la hidrólisis básica se pre concentró con sephadex LH-20 previo análisis por HPLC-DAD-FL.

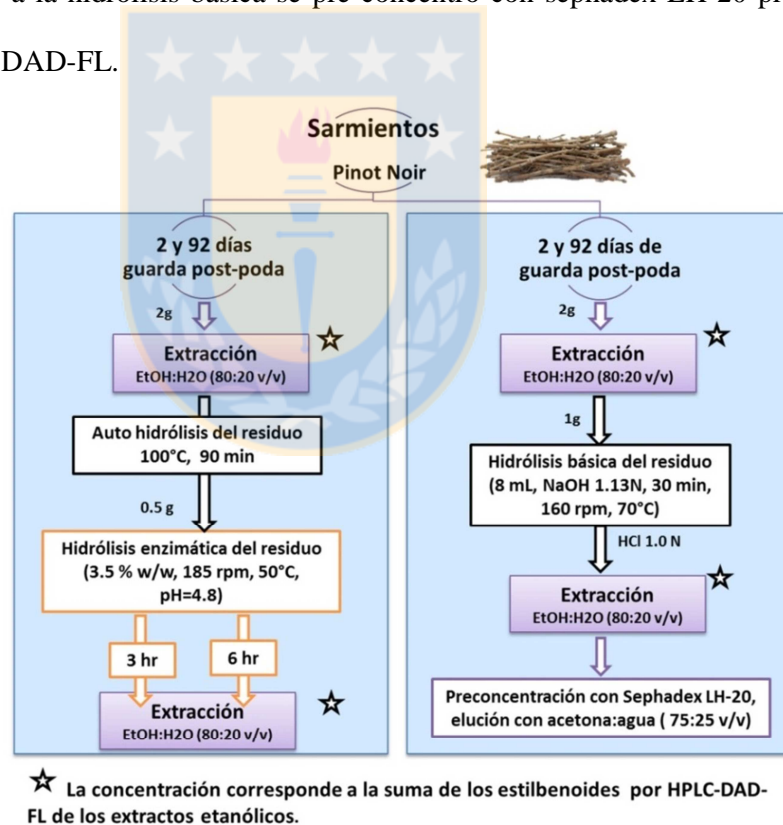


Figura 1: esquema ilustrativo de las hidrólisis efectuadas en residuos de sarmientos de vides.

1.6. Cuantificación de (poli)fenoles por HPLC-DAD-FL:

La cuantificación de los estilbenoides se realizó según la metodología descrita en la sección 1 del capítulo 3 numeral 2.5

2. Resultados y discusión:

Dado que en sarmiento fresco los estilbenoides podrían encontrarse unidos a otras moléculas como celulosa, lignina o taninos, fue requerido hidrolizar enzimáticamente. Con este fin se contempló una etapa de pre tratamiento equivalente a una autohidrólisis. Además se efectuó una hidrólisis alcalina. Esto se realizó tanto para sarmientos con 0, 2 y 92 días de guarda post-poda. Los resultados se resumen en la figura 2.

El incremento de los estilbenoides totales en sarmientos sometidos a procesos hidrolíticos no es significativo. El aumento de los niveles de (*E*)-resveratrol en sarmientos con dos días de guarda hidrolizados enzimáticamente o con hidrólisis alcalina corresponde al 1.4 % de los niveles de (*E*)-resveratrol cuantificados en sarmientos con 92 días de guarda post poda.

Si el residuo de extracción se somete a autohidrólisis sin o con hidrólisis enzimática, se observa esencialmente la aparición de un dímero oxidado de estilbenoide, pero no de los principales compuestos de interés, como (*E*)- ϵ -viniferina, (*E*)-piceatanol o (*E*)-resveratrol. Este último está prácticamente ausente en sarmientos recién cortados (0 días guarda), e incrementa a los dos días de guarda, gatillado por la poda. Existe un incremento de niveles muy significativo de (*E*)-resveratrol luego de 92 días de guarda.

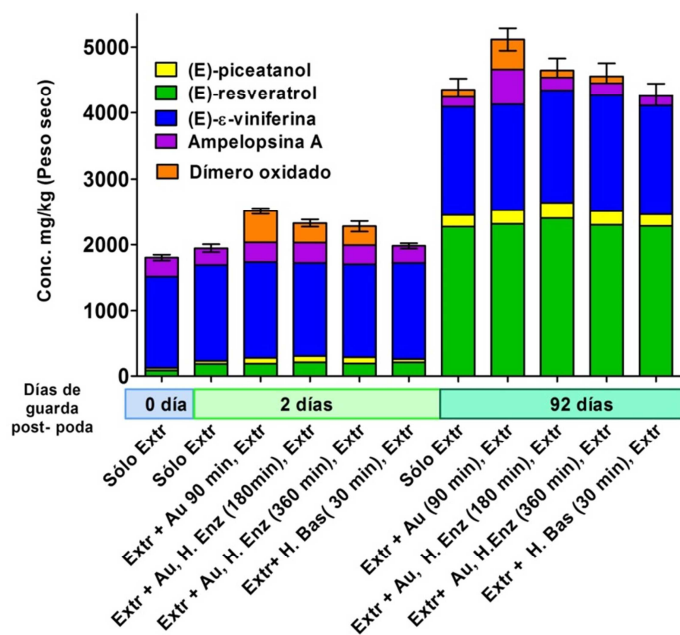


Figura 2: Niveles de estilbenoides sin y con procesos hidrolíticos del residuo de extracción de sarmientos de vides Pinot Noir con distintos tiempos de guarda post-poda. **Sólo Extr:** extracción con etanol: agua (80:20 v/v) asistida con ultrasonido, **Au:** Autohidrólisis, **H. Enz:** hidrólisis enzimática, **H. Bás:** hidrólisis básica. La barra de error corresponde a la desviación estándar de la suma de los estilbenoides.

Los sarmientos de vides aumentan los niveles de (*E*)-resveratrol y (*E*)-piceatanol luego de la poda (Vergara et al., 2012, Gorena et al., 2014, Ewald et al., 2017). Los sarmientos de vides de Pinot Noir provenientes de la viña Chillán sin el golpe de calor aumentan sus niveles de estilbenoides, principalmente de (*E*)-resveratrol (2274 ±62 mg/kg) y de (*E*)-piceatanol 179± 6 (mg/kg) (Capítulo 3, sección 1).

Al exponer los sarmientos a 60°C y luego almacenarlos en condiciones de temperatura y humedad relativa controlada no se evidencia aumento de (*E*)-resveratrol y (*E*)-piceatanol en las semanas posteriores a la poda. Los niveles de (*E*)-resveratrol se mantienen en 80 mg/kg y (*E*)-piceatanol en 30 mg/kg (Figura 3).

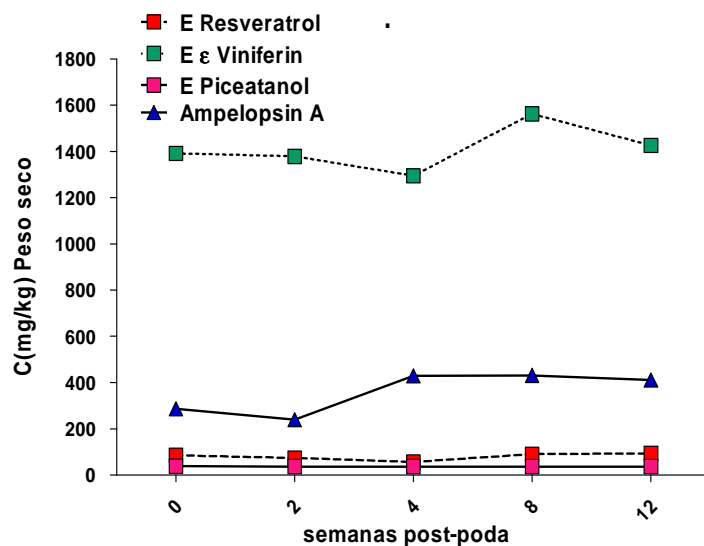


Figura 3: Estilbenoides monitoreados luego de la poda en sarmientos expuestos a un golpe de calor previo a la guarda post-poda a 70% de humedad relativa y 20°C.

Estos resultados apoyan a lo reportado por Houillé et al., 2015. El golpe de calor en los sarmientos estaría afectando a la enzima responsable de la biosíntesis de estilbenoides: la estilbeno sintasa (STS). Por lo tanto el sarmiento es incapaz de sintetizar estilbenos inducibles como (*E*)-resveratrol y (*E*)-piceatanol manteniendo los niveles bajos y constantes a diferencia de los niveles de estilbenoides no inducibles como ampelopsina A y (*E*)- ϵ -viniferina que se mantienen constantes semanas luego de la poda.

3. Conclusiones:

El monitoreo de los estilbenoides luego de la guarda post poda en sarmientos a los que se aplicó un golpe de calor apoya la evidencia de que (*E*)-resveratrol y (*E*)-piceatanol son estilbenoides inducibles. El proceso de auto hidrólisis, hidrólisis enzimática e hidrólisis básica no favorece el aumento de los niveles de estilbenoides monoméricos.

Estos resultados sumado a los antecedentes bibliográficos (Houillé et al., 2015, Ewald et al., 2017, Billet et al., 2017) llevan a concluir que el aumento de los niveles de los estilbenoides monoméricos no se deben a que estén inicialmente unidos a estructuras

celulares en sarmientos, sino a que son biosintetizados *de novo*. La clave para aprovechar íntegramente el potencial del sarmiento y gatillar la biosíntesis está en una guarda post-poda apropiada.

4. Referencia:

Billet, K., Houillé, B., Besseau, S., Mélin, C., Oudin, A., Papon, N., Courdavault, V., Clastre, M., Giglioli-Guivarc'h, N & Lanoue, A. (2018). Mechanical stress rapidly induces E-resveratrol and E-piceatannol biosynthesis in grape canes stored as a freshly-pruned byproduct. *Food Chemistry*, 240, 1022–1027.

Ewald, P., Delker, U., & Winterhalter, P. (2017). Quantification of stilbenoids in grapevine canes and grape cluster stems with a focus on long-term storage effects on stilbenoid concentration in grapevine canes. *Food Research International*, 100(August), 326–331.

Gorena, T., Saez, V., Mardones, C., Vergara, C., Winterhalter, P., & Von Baer, D. (2014). Influence of post-pruning storage on stilbenoid levels in *Vitis vinifera* L. canes. *Food Chemistry*, 155, 256–263.

Houillé, B., Besseau, S., Courdavault, V., Oudin, A., Glévarec, G., Delanoue, G., Guérin, L., Simkin, A. J., Papon, N., Clastre, M., Giglioli, N & Lanoue, A. (2015). Biosynthetic Origin of E - Resveratrol Accumulation in Grape Canes during Postharvest Storage, 63, 1631-1638.

Vergara, C., Von Baer, D., Mardones, C., Wilkens, A., Wernekinck, K., Damm, A., Macke, S., Winterhalter, P. (2012). Stilbene levels in grape cane of different cultivars in southern Chile: Determination by HPLC-DAD-MS/MS method. *Journal of Agricultural and Food Chemistry*, 60(4), 929–933.

Capítulo 4

Title:

Profiling of *Vitis vinifera* L. canes (poly)phenols compounds using comprehensive two-dimensional liquid chromatography

Lidia Montero¹, Vania Sáez², Dietrich von Baer² Alejandro Cifuentes¹, Miguel Herrero^{1}*

¹Laboratory of Foodomics, Institute of Food Science Research (CIAL-CSIC), Cabrera 9, 28049 - Madrid, Spain.

²Dept. Análisis Instrumental, Facultad de Farmacia, Universidad de Concepción, Chile.

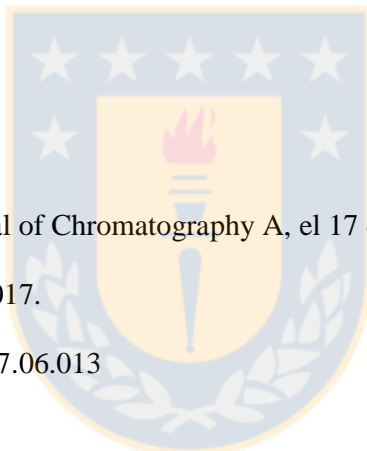
Corresponding author: m.herrero@csic.es (M. Herrero)

TEL: +34 910 017 946

FAX: +34 910 017 905

Manuscrito enviado a Journal of Chromatography A, el 17 de Octubre del 2016,
aceptado el 6 de Junio del 2017.

DOI: 10.1016/j.chroma.2017.06.013



Abstract.

Grapevine canes, a pruning-derived by-product, possess a great amount of bioactive (poly)phenolic compounds belonging to different chemical classes, thus, having a good potential for further valorization. However, in order to properly design valorization strategies, the precise chemical composition of this material has to be known. Up to now, this chemical characterization has been based on analysis of different groups of components individually due to difficulties related to their huge chemical variability. In this work, a comprehensive two-dimensional liquid chromatography-based method (LCXLC) is developed to obtain the profiles of (poly)phenolic compounds present in grapevine canes from several varieties. Three different set-ups have been tested and compared; the combination of diol and C₁₈ columns produced the best results, allowing the characterization of the (poly)phenolic profile in around 80 min. This way, 81 different components were detected in the samples; most of them could be tentatively assigned using the information provided by the DAD and MS detectors employed. Indeed, it has been possible to detect in a single run components belonging to stilbenoids, procyanidins and prodelfinidins of varying degrees of polymerization, some of them not formerly described in this natural source. The method has shown extremely good separation capabilities, and is characterized by high practical peak capacity (842) and orthogonality ($A_0 = 78\%$). The obtained results demonstrate that *Vitis vinifera* L. canes may retain a great potential to be used as an underexploited natural source of bioactive compounds, with potential applications in different fields.

Keywords: LC×LC; Grapevine canes; Stilbenoids; Phenolic compounds; Proanthocyanidins

1. Introduction.

Management of agricultural and food-related by-products and wastes is an important issue nowadays worldwide. Industrial practices related to food production are responsible for the generation of a huge amount of unwanted materials at different levels. Traditionally, these wastes have been reused for energy generation and/or feed production [1]. Nevertheless, this approach is clearly not efficient enough to deal with such a high amount of different by-products. For this reason, different alternatives have appeared in the last years proposing new ways for the valorization of agricultural and food industry by-products [2], considering that a significant part of those wastes are still rich on interesting components, such as bioactives. Indeed, at present, the complete valorization of all the residues and by-products generated is a particular production chain is ideally sought, through the application of the modern concept of biorefinery [3]. Among the different agrofood-related by products, grapevine (*Vitis vinifera* L.) canes are a promising source of different bioactive components, basically, phenolic compounds. Canes are a pruning residue which is not processed for extensive valorization as they are normally burnt or composted [4]. Among the bioactives present in this material, stilbenoids are commonly pointed out [5], although others such as proanthocyanidins are also present. Stilbenoids are non-flavonoid phenolic compounds which are related to defense mechanisms in plants as a response to different stresses. The basic structure of those found in grapevines are based on the (*E*)-resveratrol (3,5,4 trihydroxystilbene) chemical structure, which is also the most abundant compound in grapevine canes after post-pruning storage. However, reactions such as photoisomerization, glycosylation and oligomerization are responsible for the complex chemical pattern that can be found in the plant [6], including monomers ((*E*)-piceatannol, (*E*)-piceid), dimers ((*E*)- ϵ -viniferin, (*E*)- ω -viniferin, ampelopsin A,

vitisinol C), trimmers ((*E*)-miyabenolC), and tetramers ((*E*)-vitisin B, (*Z*)-vitisin B, hopeaphenol, isohopeaphenol), among others. Moreover, the levels of (*E*)-resveratrol and some other related minor stilbenoids are strongly dependent on storage conditions of canes (time, temperature) after pruning. It has been observed that pruning triggers a very significant increase in stilbenoids levels, mainly (*E*)-resveratrol, in grapevine canes [6,7], which is induced by the stress affecting the vegetal material during post-pruning storage. The increase of the activity of the stilbenoid synthesizing enzyme during this period has been already reported [7], indicating that the biosynthesis is activated. Interestingly, this increase is not observed if the vegetal material is not cut or if it is kept frozen or ground after soon after collection [5,6]. Different beneficial health effects and bioactive activities have been ascribed to (*E*)-resveratrol as well as to other stilbenoids [8], thus, highlighting the interest on these natural components.

On the other hand, proanthocyanidins, are flavan-3-ol polymers which can be linked through multiple ways and degrees of polymerization, giving rise to extremely complex patterns [9]. As for stilbenoids, proanthocyanidins are regarded as responsible for a number of bioactivities, including antioxidant, hepatoprotective, anti-inflammatory, antibacterial or anticancer effects, among others [10]. Different proanthocyanidins, mainly procyanidins, have been already described in grapevine [11], although the natural chemical variability may still be concealed due to difficulties in their analysis. Consequently, the presence of this complex array of (poly)phenolic compounds makes grapevine canes a potentially interesting material for the development of valorization processes.

However, to produce an efficient valorization of wastes, not only environmentally friendly extraction and processing techniques are needed to obtain the compounds of interest, but also an exhaustive chemical characterization of those materials is required.

In fact, it is of utmost importance to precisely know the chemical composition of a particular by-product in order to devise strategies for its valorization. In this regard, the already mentioned extremely complex pattern on bioactives present on grapevine canes implies that typically used one-dimensional separation approaches may not provide the separation and identification power enough to reveal more in detail the chemical composition of these wastes. It is precisely on this kind of complex natural samples where comprehensive two-dimensional liquid chromatography (LC×LC) may provide with the required additional separation capabilities. LC×LC is based on the coupling of two independent separation mechanisms that allow significant improvements on resolving power and peak capacity [12]. By using this on-line approach, the entire sample is subjected to two independent separation mechanisms continuously; although different combinations between separation mechanism may be applied, the one involving hydrophilic interaction chromatography (HILIC) coupled to reversed phase (RP) separations has shown a very good potential for polyphenols analysis [13]. In any case, the application of this coupling is not straightforward due to multiple factors that should be optimized [14,16], being one of the most important the transfer from the first dimension (¹D) eluent to the second dimension (²D) continuously, due to solvent incompatibility. Although, this technique has been already employed for the analysis of different types of polyphenols and matrices [17], up to now, it has not been used for the profiling of grapevine canes. Thus, the aim of this work is to profile and characterize the complex mixture of (poly)phenolic compounds contained in grapevine canes, mainly stilbenoids and proanthocyanidins, in a single run through the use of a HILIC×RP method coupled to tandem mass spectrometry. The developed method is then applied to reveal differences on the chemical composition between two red grapevine varieties stored for 3 months after pruning to foster an accumulation of stilbenoids.

2. Materials and methods.

2.1. Samples and chemicals.

Grapevine (*Vitis vinifera L.*) canes from the variety *Pinot Noir* were collected from Itata Valley (Concepción, Chile) and canes from the variety *Cabernet Sauvignon* were from Maipo Valley (Santiago, Chile) in the winter of 2013. After pruning, both samples were stored at room temperature during three months. Then, the grapevine canes were ground and frozen at -20°C. Extraction of (poly)phenolic compounds from dried canes was carried out by solid/liquid extraction. Briefly, 50 mL of acetone/water (80:20, v/v) were added to 5 g of ground grapevine canes. The solution was sonicated (Elma, Singen, Germany) for 15 min. After that, the mixture was kept in darkness during 2 h and then it was again sonicated for 15 min. Finally, the solution was centrifuged for 20 min at 8000 rpm, the acetone was evaporated under vacuum (Rotavapor R-210, Buchi Labortechnik AG, Flawil, Switzerland) and lastly, the aqueous extract was freeze-dried (Labconco Corporation, MO).

HPLC grade methanol, acetonitrile and acetone were purchased from VWR Chemicals (Barcelona, Spain), whereas acetic and formic acids were acquired from Sigma-Aldrich (Madrid, Spain) and ammonium acetate was from Panreac (Barcelona, Spain). Water employed was Milli-Q grade obtained from a Millipore system (Billerica, MA).

2.2. Instrumentation.

The LC × LC-DAD instrumentation consisted on a first dimension (¹D) composed by an Agilent 1200 series liquid chromatograph (Agilent Technologies, Santa Clara, CA) equipped with an autosampler. In order to obtain more reproducible low flow rates and to minimize the gradient delay volume of the pump, a Protecol flow-splitter (SGE Analytical Science, Milton Keynes, UK) was placed between the ¹D pump and the

autosampler. Additionally, a LC pump (Agilent 1290 Infinity) performed the second dimension (²D) separation. Both dimensions were connected by an electronically-controlled two-position ten-port switching valve (Rheodyne, Rohnert Park, CA, USA) acting as modulator equipped with two identical 30 μ L injection loops. Modulation time of the switching valve was 1.3 min. A diode array detector was coupled after the second dimension in order to register every ²D analysis. Besides, an Agilent 6320 Ion Trap mass spectrometer equipped with an electrospray interface working under negative ionization mode was coupled in series using the following conditions: dry temperature, 350 $^{\circ}$ C; dry gas flow rate, 12 L min^{-1} ; nebulization pressure, 40 psi; mass range, m/z 90–2200 Da; ultra scan mode (26000 $m/z/s$). The LC data were elaborated and visualized using LC Image software (version 1.0, Zoex Corp., Houston, TX).

2.3. LC \times LC separation conditions.

The ¹D separation was optimized using three sets of columns. The best conditions for each column after optimization were:

- i) ZIC-HILIC column (150 \times 1 mm, 3.5 μ m, Merck, Darmstadt, Germany) eluted using acetonitrile (A) and 10 mM ammonium acetate pH 5 (B) as mobile phases, using the following gradient at 15 μ L min^{-1} : 0 min, 3% B; 5 min, 3% B; 10 min, 5% B; 15 min, 10% B; 30 min, 20% B; 45 min, 20% B; 50 min, 30% B; 60 min, 30% B; 70 min, 40% B; 80 min, 40% B.
- ii) PEG column (150 \times 2.1 mm, 5 μ m, Supelco, Bellefonte, CA) eluted using methanol (0.1% formic acid, A) and water (0.1% formic acid, B) at 20 μ L min^{-1} according to the following gradient: 0 min, 40% B; 50 min, 10% B; 70 min, 2% B.
- iii) Lichrospher diol-5 (150 \times 1.0 mm, 5 μ m, HiChrom, Reading, UK) column eluted using acetonitrile (1% formic acid, A) and methanol/10 mM ammonium acetate/acetic

acid (95:4:1, B) at $18 \mu\text{L min}^{-1}$ using the following gradient: 0 min, 2% B; 10 min, 2% B; 15 min, 5% B; 30 min, 20% B; 45 min, 20% B; 50 min, 30% B; 60 min, 30% B; 70 min, 40% B; 80 min, 40% B.

On the ²D, a pentafluorophenyl column (Kinetex PFP column, 50×4.6 mm, $2.7 \mu\text{m}$, Phenomenex, Torrance, CA, USA) and a C₁₈ column (Ascentis Express C₁₈ column, 50×4.6 mm, $2.7 \mu\text{m}$, Supelco, Bellefonte, CA) were used. For LC \times LC analysis, the C₁₈ column was employed under optimized conditions depending on the stationary phase used in ¹D, as follows:

i) diol \times C₁₈ and PEG \times C₁₈ set-ups: water (0.1% formic acid, A) and acetonitrile (0.5% formic acid, B) were selected as mobile phases, eluted at 3 mL min^{-1} using the following gradient: 0 min, 2% B; 0.1 min, 2% B; 0.3 min, 10% B; 0.5 min, 25% B; 0.7 min, 40% B; 1 min, 60% B; 1.01 min, 2% B.

ii) ZIC-HILIC \times C₁₈ set-up: mobile phases employed were composed by water (0.1% formic acid, A) and acetonitrile (0.5% formic acid, B) and were eluted at 3 mL min^{-1} using the following gradient: 0 min, 0% B; 0.1 min, 2% B; 0.3 min, 5% B; 0.5 min, 15% B; 0.7 min, 25% B; 1 min, 50% B; 1.01, 0% B.

Independently of the column combinations, 2D analyses were performed maintaining a column temperature of $25 \text{ }^\circ\text{C}$. UV-vis spectra were collected in the range of 190–550 nm using a sampling rate of 20 Hz, while 254, 280 and 330 nm signals were also independently recorded. The effluent from the ²D column was splitted before entering the MS instrument, so that the flow rate introduced in the MS detector was ca. 0.6 mL min^{-1} . MS detection was performed as above indicated (Section 2.2).

2.4. Calculations.

2.4.1. Peak capacity

Individual peak capacity (n_c) for each dimension was calculated according to Eq. (1):

$$n_c = 1 + \frac{t_G}{w} \quad (1)$$

where t_G is the gradient time and w is the average peak width, equivalent to 4σ . For 1D peak capacity (1n_c) calculations, the average peak width was obtained from 10 to 15 representative peaks selected along the analysis. Likewise, for 2D peak capacity (2n_c), as much as possible peaks were considered (14–22 peaks, depending on the analysis). Additionally, 1n_c was also calculated considering the broadening factor $\langle\beta\rangle$, giving rise to a corrected 1D peak capacity (Eq.2), considering the influence of the deleterious effect of undersampling. To estimate $\langle\beta\rangle$, the sampling time (t_s) as well as the average width of 1D peaks before modulation were considered:

$$n_{c,\text{corrected}} = \frac{n_c}{\sqrt{1+0.21\left(\frac{t_s}{\sigma}\right)^2}} \quad (2)$$

For each two-dimensional set-up, different peak capacity values were estimated. First of all, theoretical peak capacity was obtained following the so-called product rule, using Eq. (3), considering the individual peak capacities obtained in each dimension:

$$2Dn_{c,\text{theoretical}} = 1n_c \times 2n_c \quad (3)$$

As Eq. (3) does not take into consideration the deleterious effects due to the modulation process as well as possible undersampling, a more realistic peak capacity value was obtained from the equation proposed by Li et al. [18], denominated here as practical peak capacity (Eq. 4):

$$2Dn_{c,\text{practical}} = \frac{1n_c \times 2n_c}{\sqrt{1+3.35 \times \left(\frac{2t_c}{1t_G}\right)^2}} \quad (4)$$

being 2t_c , the 2D separation cycle time, which is equal to the modulation time. This latter equation also includes the $\langle\beta\rangle$ parameter accounting for undersampling. Moreover, to more precisely compare among set-ups and in order to evaluate possible peak clusters along the 2D analysis and, thus, to estimate 2D space coverage, the orthogonality

degree (A_0) was considered to offer the denominated 2D corrected (also known as effective) peak capacity, as follows:

$$2Dn_{c,corrected} = n_{c,practical} \times A_0 \quad (5)$$

2.4.2. Orthogonality

Different approaches have been developed and published to quantify the orthogonality degree of a two-dimensional set-up [19]. In the present work, system orthogonality (A_0) was calculated according to the method proposed by Camenzuli and Schoenmakers [20], taking into account the spread of each peak along the four imaginary lines that cross the 2D space forming an asterisk, that is Z_1 , Z_2 (vertical and horizontal lines) and Z_3 , Z_4 (diagonal lines of the asterisk). Z parameters describe the use of the separation space with respect to the corresponding Z line, allowing to semi-quantitatively diagnose areas of the separation space where sample components are clustered, thus, reducing in practice orthogonality. For the determination of each Z parameter, the S_{Z_x} value was calculated, as the measure of spreading around the Z_x line, using the retention times of all the separated peaks in each 2D analysis.

3. Results and discussion.

Although some previous works dealt with the identification of some stilbenoids [5,21] and proanthocyanidins [22] by one-dimensional reversed phase HPLC in grapevine canes, no comprehensive method has been developed up to now to obtain the (poly)phenolic profile of this material. Consequently, a LC \times LC method has been developed to this aim. Based on the literature and our own experience, as well as considering the nature of the compounds expected to be part of that profile (see Fig.1 for examples), the combination between HILIC \times RP could be a promising alternative [17,23–25], although the application of RP \times RP has also been explored [17].

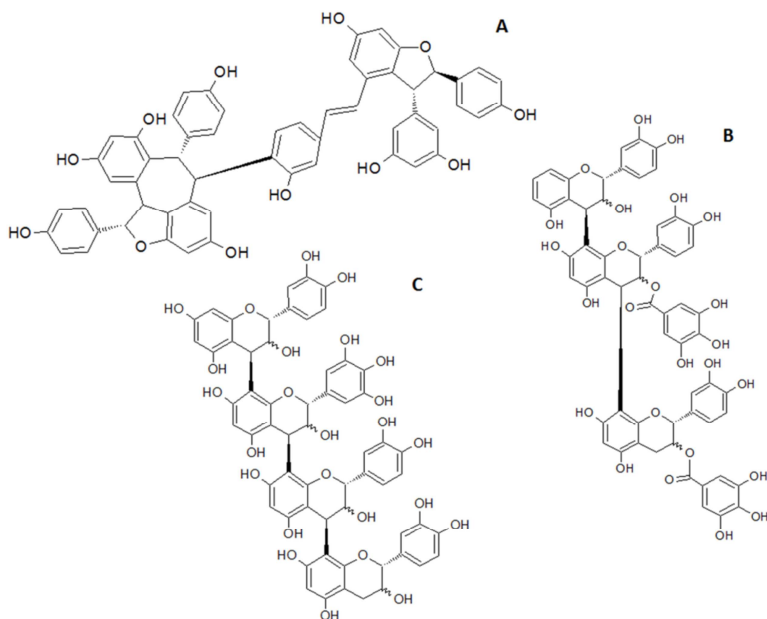


Fig.1. Chemical structure of some representative polyphenols present in grapevine (*Vitis vinifera* L.) canes. A) Resveratrol tetramer (Vitisin A); B) Procyanidin trimer digallate; C) Prodelfidin tetramer (3(E)C-(E)GC).

To perform a proper method optimization, different conditions have been tested independently, firstly looking at the performance achievable by three different stationary phases in the ¹D and then, studying their potential when combined with a C₁₈ column in the ²D. This method optimization has been performed considering the available materials and instruments, which impose some important constraints, mainly related to the maximum pressure borne by the equipment (400 bar) as well as to the scanning speed of the available detectors (DAD and MS). Thus, method development has been guided taking some compromises, as described below, not only in terms of theory but also in terms of practice (instrumental limitations). Finally, in order to select the most appropriate set-up for the separation of the grapevine cane samples, the obtained results were critically compared in terms of separation capabilities (overall resolution, peak capacity and orthogonality).

3.1 Separation method optimization

Unlike other previously investigated samples where a phenolic group of compounds was clearly predominant [23–25], the studied samples in the present work are composed of complex mixtures of varying degrees of polymerization of two different groups of polyphenols, i.e., stilbenoids and proanthocyanidins. Due to this different pattern, several stationary phases compatible with HILIC separations were evaluated for their use in ¹D separation, namely, diol, ZIC-HILIC and PEG (polyethylene glycol) columns. Diol stationary phases have repeatedly shown to provide good retention under HILIC mode [17], whereas ZIC-HILIC particles carry zwitterionic functional groups (sulfobetaine) with a charge balance 1:1, also suitable for that separation mode. On the other hand, PEG columns were initially developed for RP, although it has been demonstrated that they can also be run under HILIC conditions with satisfactory results [26]. For this reason, in this work, the performance of the PEG column was studied under both separation modes, as RP × RP has also previously shown relatively good performance in phenolic compounds analysis [13,17]. An independent optimization of the separation conditions was performed for each column, keeping in mind the basic requirements imposed by the 2D set-up used. This LC × LC set-up is based on the use two identical volume sampling loops installed in the switching valve in order to allow the continuous collection and injection of ¹D effluent on the ²D. Hence, separations as slow as possible in the ¹D are preferred (from 10 to 100 μL min⁻¹, typically) while very fast separations are needed to perform quick ²D separations (3–4 mL min⁻¹) and to maintain the modulation time (and transfer volume) as short as possible. The use of such low flow rates in the ¹D limits, in turn, the morphology of the column. It has been repeatedly reported that microbore and narrow columns can provide with the needed efficiency at low flow rates. The characteristics of the columns tested

are shown in Table 1. One of the studied grapevine samples was used as a model, and different mobile phases, gradients and flow rates (from 15 to 25 $\mu\text{L min}^{-1}$) were tested for each column, including acetonitrile/formic acid, acetonitrile/acetic acid, methanol/water/acid or methanol/ammonium acetate buffer mixtures in different proportions. After careful study of the obtained results, the optimum separation conditions for each studied column are reported in Section 2.3. The best conditions involving the use of the PEG column were found under RP conditions. When operated under HILIC-compatible conditions, the PEG column did not produce satisfactory retention of the studied compounds. In any case, it is worth noting that the internal diameter of the available PEG column (2.1 mm) was wider than those from the other tested columns. This fact implies that the used linear velocity is far from optimal values, which means that the obtained separation could be theoretically further improved, although higher flow rates, which are not practical in this application, would be required. Fig. 2 shows typical ^1D chromatograms obtained under optimum separation conditions for each column. As can be observed, good peak distributions were obtained with the three tested columns, although the diol column was the only one allowing a separation between stilbenoids and proanthocyanidins. Peak capacity values were calculated for the three optimized separations. Results are given in Table 1. The undersampling correction factor $\langle\beta\rangle$ was also considered to reduce the theoretical 1n_c as a result of undersampling (Eq. (2)), including the sampling time (t_s) later on applied in $\text{LC} \times \text{LC}$ experiments (see below). As can be observed, the diol column produced higher peak capacity values, followed by the PEG and ZIC-HILIC columns (25, 23 and 19, respectively). However, this value should not be the only one taken into consideration to select the best ^1D separation method, as increments in ^1D peak capacity do not produce enhancements in the two-dimensional peak capacity beyond a certain

point because undersampling get worse as a result of narrower 1D peaks (unless 1t_G is significantly increased) [27].

Table 1. Comprehensive two-dimensional method parameters applied to the profiling of (poly)phenolic compounds from grapevine canes.

		Diol \times C₁₈	PEG \times C₁₈	ZIC-HILIC \times C₁₈
1D	L (mm)	150	150	150
	I.D. (mm)	1.0	2.1	1.0
	Particle size (μm)	5	5	3.5
	Flow rate (μLmin^{-1})	18	20	15
	w (min)	3.01	3.60	3.40
	1n_c	32	27	23
	$\langle\beta\rangle$	1.28	1.20	1.22
	1n_c corr.	25	23	19
2D	w⁻ (s)	1.40	1.40	1.49
	2n_c	44	44	41
LC \times LC	Analysis time (min)	92	92	75
	t_s	1.73 σ	1.44 σ	1.52 σ
	Modulation time (min)	1.3	1.3	1.3
	${}^2V_{inj}$ (V 1D effluent)	30 μL (23.4 μL)	30 μL (26 μL)	30 μL (19.5 μL)
	Z_1	0.93	0.85	0.97
	Z_2	0.95	0.91	0.91
	Z_-	0.91	0.42	0.72
	Z_+	0.75	0.60	0.77
	A_0	78%	45%	70%
	${}^{2D}n_c$ theoretical	1408	1188	943
	${}^{2D}n_c$ practical	1080	961	768
	${}^{2D}n_c$ corr.	842	432	538

$\langle\beta\rangle$, average 1D broadening factor; 1n_c corr.: calculated according to Eq. (2); t_s , sampling time; A_0 , orthogonality; ${}^{2D}n_{c,theoretical}$: ${}^1n_c \times {}^2n_c$; ${}^{2D}n_{c,practical}$: calculated according to Eq. (4); ${}^{2D}n_c$ corr.: ${}^{2D}n_{c,practical} \times A_0$

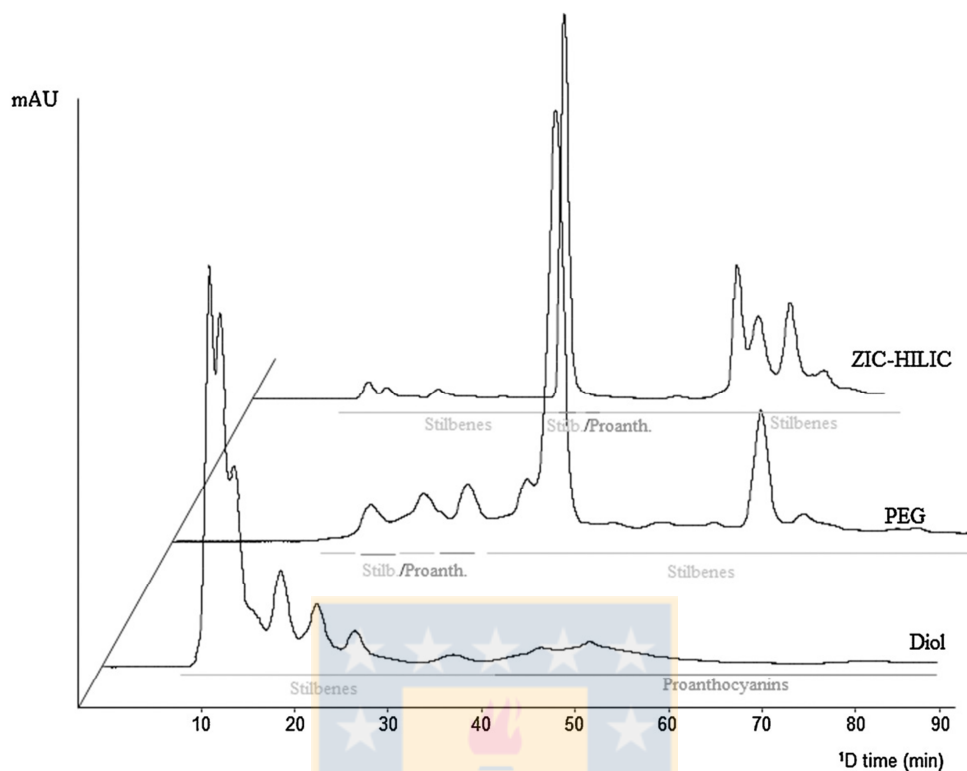


Fig. 2. First dimension chromatograms (280 nm) corresponding to the separation of the polyphenols found in a grapevine cane extract under optimum conditions for each column. For separation conditions, see Section 2.3.

The three columns studied in ¹D were then tested in a LC × LC set-up in combination with a short partially porous C₁₈ column (50 × 4.6 mm, 2.7 μm). The use of relatively short columns with partially porous materials allows obtaining high efficiency values and fast separations, significantly reducing backpressure compared to sub-2 μm columns. In our application, control of pressure as a result of the ²D separations is of utmost importance, as the available switching valve and DAD are not designed to operate at pressures above 400 bar. As can be deduced from the literature [17], C₁₈ columns offer unparalleled retention for most of published applications involving a RP separation in ²D. In spite of this, we also studied the possibility of using a PFP (pentafluorophenyl) stationary phase in ²D, maintaining column morphology, although

that column did not provide comparable results (data not shown). For each of the studied set-ups, the ²D separation conditions were independently determined; optimum separation conditions are shown in Section 2.3 Flow rate was always maintained as fast as possible in order to reduce ²D analysis time, although gradients shorter than 1 min did not produced successful separations. On the other hand, higher ²D flow rates were avoided due to increased pressure drop and lack of enough sampling rate in the DAD. For these reason, total ²D analysis times were kept at 1.3 min, in order to allow column re-equilibration for 18 s. Moreover, the transfer volume, determined by the available sampling loop volume was also considered. For the three couplings, two 30 μ L loops were employed, which provided higher volume than strictly required according to the ¹D flow rate and modulation time employed (Table 1). However, we previously demonstrated that by using this additional space, each fraction being transferred was in practice diluted at the head of the ²D column with ²D initial mobile phase. This dilution effect has been demonstrated to be effective to reduce ²D peak distortion related to solvent incompatibility between dimensions [23], considering that there was a solvent strength mismatch in every LC \times LC coupling studied here.

The results obtained after the application of each optimized LC \times LC set-up are illustrated in Fig. 3. To make a quantitative comparison of the separation capabilities of each combination, the number of separated peaks and overall resolution, peak capacity values, as well as orthogonality were considered. Firstly, it is important to note, that although 1.3 min cycles may seem too long, the conditions applied in both dimensions allowed to minimize possible negative effects due to undersampling. Considering ¹D peak widths before modulation, sampling times from ¹D to ²D were estimated; obtained values in the three studied set-ups were always faster than the recommended rate by Murphy, Schure and Foley [28] (i.e., 4 cuts per peak, thus, 2σ), as it can be observed

in Table 1. Theoretical peak capacity values derived from the application of Eq. (3) are shown in Table 1. As it can be noted, the set-up involving the use of the diol column provided the highest values (${}^2Dn_c = 1408$). Moreover, in order to give more realistic values, the practical peak capacity (according to Eq. (4)) was also calculated. This way, the effects of undersampling are also considered; these deleterious effects are related to the re-mix of already separated compounds in the 1D during the collection of the 1D effluent in the modulator. Although one of the premises of $LC \times LC$ is that none of the resolution obtained in the 1D is lost in the 2D , in practice this can never be completely achieved [27]; for this reason, the estimation of peak capacity should include the possible losses of 1D peak capacity related to undersampling. Using this approach, practical peak capacity values of the diol $\times C_{18}$, PEG $\times C_{18}$ and ZIC-HILIC $\times C_{18}$ set-ups were 1080, 961 and 768, respectively. Still, it is important to keep in mind that these peak capacity values are not the real number of peaks that could be separated along the 2D space because there are areas on the 2D chromatogram where peaks do not appear. To evaluate the 2D separation space coverage, orthogonality degree in each set-up was calculated. This parameter gives a measure of the separation quality and allows the comparison between different 2D approaches. System orthogonality (A_0) was calculated taking into account the spread of each peak along the four imaginary lines that cross the 2D space forming an asterisk, that is Z_1 , Z_2 (vertical and horizontal lines) and Z , Z_+ (diagonal lines of the asterisk) [20]. The ZIC-HILIC $\times C_{18}$ coupling provided an A_0 of 70%, due to a good spread of the peaks around Z_1 and Z_2 lines (97 and 91%, respectively). The PEG $\times C_{18}$ set-up possessed an $A_0 = 45\%$. This moderated value is related to the poor spread of peaks around the Z and Z_+ lines (42 and 60%, respectively) as can be observed in Fig. 3B, where a peak clustering occurs on the Z -axis with a low spread. The best orthogonality degree was achieved with the

diol \times C₁₈ coupling obtaining an A_0 of 78% (Fig. 3A) corresponding to a high peak spreading around the four axis (93% Z₁, 95% Z₂, 91% Z₋ and 75% Z₊). Interestingly, as expected from theory, those set-ups involving a HILIC \times RP coupling (Fig. 3A and C) provided with higher orthogonality values than the RP \times RP set-up involving the use of the PEG column (Fig. 3B), for this application. Considering orthogonality values, corrected peak capacities (eq. 5, $^{2D}n_{c,corr}$) attained in the diol \times C₁₈, PEG \times C₁₈ and ZIC-HILIC \times C₁₈ set-ups were 842, 432 and 538, respectively. The application of this correction factor allows a fairer comparison among set-ups, as the whole coupling is evaluated, not only in terms of each dimension separately but also looking at the 2D separation obtainable once coupled. Consequently, as can be deduced from Fig. 3, the best conditions were produced using HILIC \times RP using a diol column in the ¹D coupled to a C₁₈ column in the ²D. Moreover, as it can also be inferred from Fig. 3, the best ¹D peak distribution along the available analysis time was obtained using the diol column, thus, further justifying the use of the mentioned set-up in the present application.

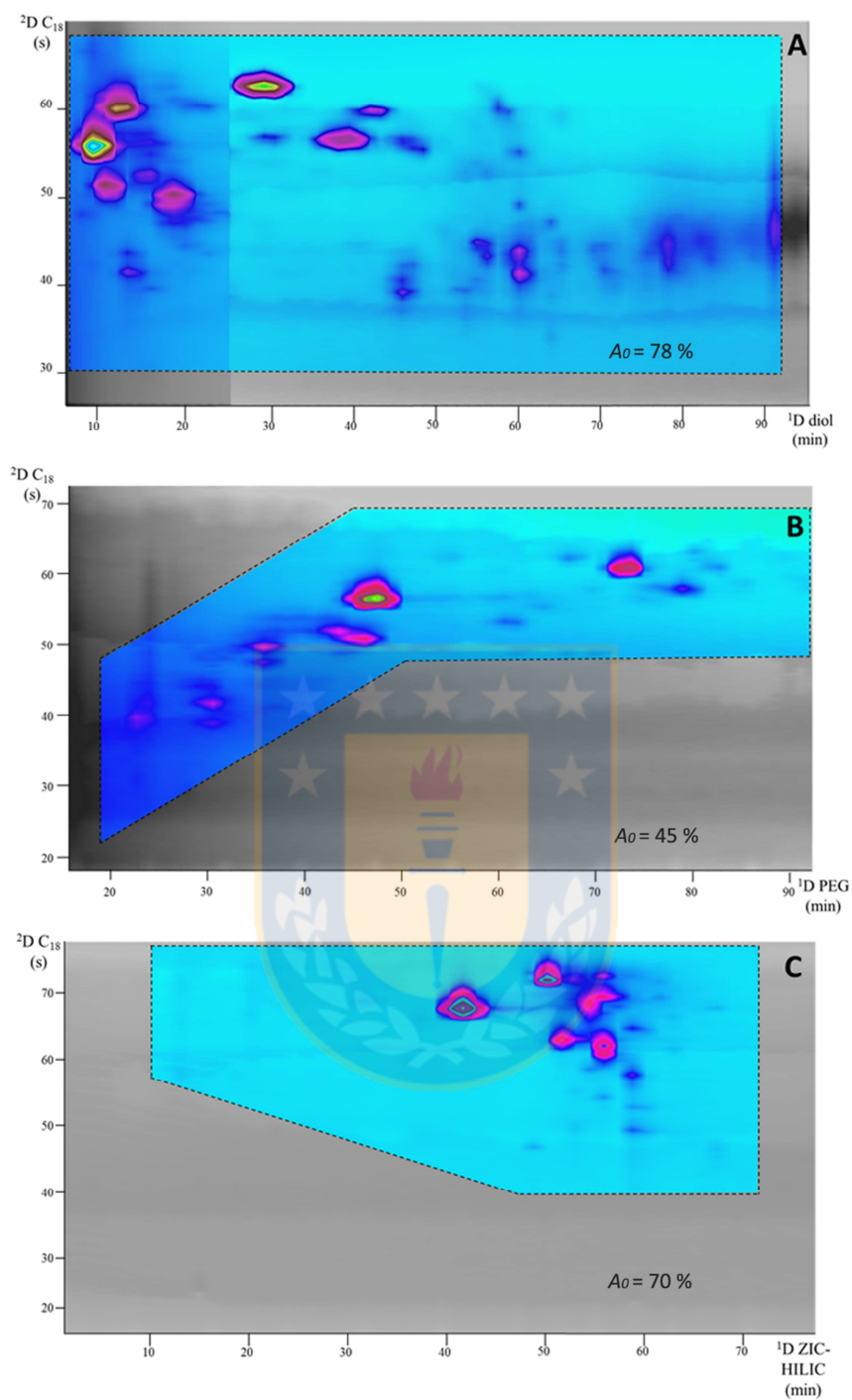


Fig. 3:Two-dimensional plots and orthogonality values (A_0) obtained using each first dimension column studied (A, diol; B, PEG; C, ZIC-HILIC) coupled to the partially porous C_{18} column in the second dimension under optimized conditions. Dotted lines define area occupied by peaks. For detailed separation conditions, see section 2.3.

3.2. Characterization of the (poly)phenolic profile of grapevine canes by HILIC × RP

The optimized method was then applied for the characterization of the (poly)phenolic profile of canes of two different grapevine varieties, specifically, *Pinot Noir* and *Cabernet Sauvignon*. The analyzed canes were derived from the pruning of different vineyards. After pruning, the canes were stored at ambient temperature for three months. This period was demonstrated to be useful to promote the synthesis of the bioactives present [6]. The 2D plots of the studied samples under the optimum conditions are shown in Fig. 4. In order to characterize the separated components, a MS detector was also hyphenated to the LC × LC instrument. The MS used consisted of an ion trap equipped with an electrospray (ESI) interface working on the negative ionization mode. Although this analyzer provided with useful MS data, this instrument does not provide with high scanning speeds, which are very desirable in LC × LC, considering the fast separations (²D) that are carried out just before detection. Table 2 summarizes the tentatively identified compounds in both grapevine cane extracts as well as the corresponding data related to their UV–vis and MS spectra. As can be observed from this Table 2 and Fig. 4, most peaks were detected in both varieties, although some others were uniquely found in just one of them. Among the assigned compounds, two families were mainly present, namely proanthocyanidins and stilbenoids. In general, compounds eluted from the ¹D according to increasing degree of polymerization (DP); monomers and smaller oligomers were predominantly found in the first section of the 2D plot (first 23 min). These compounds were the most abundant in both samples with higher intensities.

Catechin and epicatechin (peaks 5 and 6, respectively) were the only flavan-3-ol monomers detected in the studied samples. These two compounds are the basic

components of procyanidins; as can be observed in Table 2, the chemical pattern of procyanidin oligomers in grapevine canes was very complex. Moreover, catechin and epicatechin, together with (epi)gallocatechin, are part of prodelphinidins, the other group of proanthocyanidins found in the studied samples. Several procyanidins with DP 2 and DP 3 could be tentatively assigned thanks to their typical molecular ions at m/z 577, 579 and 865, depending on the type of linkage. These compounds also presented characteristic fragment ions corresponding to retro-Diels-Alder (RDA) fission (-152 Da), heterocyclic ring fission (HRF, -126 Da), and quinone methide (QM) fission (-289 Da) [29]. Moreover, other mono- and digalloylated dimers and trimers were also found (peaks 42, 62, 66 and 67). An example of the MS and MS/MS spectra of a procyanidin trimer digallate as well as its proposed fragmentation pattern can be observed in Fig. S1. The typical fragmentation pattern of these components which was already described for other samples [23] was the key for their identification, including the presence of fragments derived from different fission pathways [29]. It has to be pointed out that procyanidins are extensively present in different grape-related components, such as skins, seeds and even wine [30]. The other type of proanthocyanidins identified in these samples was prodelphinidins. In this case, different compounds containing a DP from 2 to 5 could be assigned, having also different degree of galloylation. In Table 2, the tentative monomer composition of each prodelphinidin is included in agreement with the molecular ion and main MS/MS fragments detected. For instance, both prodelphinidin dimers detected (peaks 39 and 41) possessed identical molecular ion at m/z 593 ($[M-H]^-$), producing MS/MS fragments revealing the presence of (epi)catechin (m/z 289) and (epi)gallocatechin (m/z 305) (through QM fission). However, in the case of higher molecular weight components, the chemical variability was more complex. For prodelphinidin trimers, three different

structures appeared, formed by: two (epi)catechin moieties and one (epi)gallocatechin (peaks 52, 53, 56 and 58) with m/z at 881 ($[M-H]^-$); a (epi)catechin unit with two (epi)gallocatechin moieties (peak 61) with m/z at 897 ($[M-H]^-$), and; a galloylated trimer (peak 65). Likewise, different tetramers could be described in the samples with different basic structure and degree of galloylation (peaks 68, 70, 71 and 72). Interestingly, some of these components were detected as doubly-charged ions. It is important to remark that this is the first work in which prodelphinidins are described in grapevine canes. In any case, the clarification of prodelphinidin oligomers is sometimes not possible only with the information provided by the MS and MS/MS spectra due to the fact that these complex molecules may present different degrees of galloylation as well as different number of (epi)gallocatechin molecules. This implies that some different oligomers may have the same m/z and main MS/MS fragments, making the unequivocal assignment very difficult. This is the case of peak 72 that presents a $[M-2H]^{2-}$ at m/z 828.6 and could correspond to a prodelphinidin tetramer trigallate or to a prodelphinidin pentamer monogallate. The MS and MS/MS spectra of this peak are shown in FigS1C and D, as well as the tentatively proposed fragmentation pattern of both identification options. The use of a high resolution MS analyzer would potentially improve the attainable results as well as the identification certainty through the acquisition of accurate mass values

Table 2: Main polyphenols detected in the grapevine canes samples using the optimized HILICxRP-DAD-MS/MS method. (E)C, (epi)catechin; (E)GC, (epi)gallocatechin; (E)GCG, (epi)gallocatechin gallate.

Peak	Total t_r (min)	t_r 2D (s)	[M-H] ⁻	Main MS/MS fragments	Identification proposed
1	10.03	55.80	227.2	210, 185, 159	<i>trans</i> -Resveratrol
2	10.11	60.60	453.0	435, 413, 361, 349, 335, 293, 239, 228	Resveratrol dimer
3	11.26	51.50	245.0	243, 225, 201, 175, 155	<i>trans</i> -Piceatannol
4	12.70	60.05	453.7	435, 411, 369, 359, 347, 253	Resveratrol dimer
5	13.70	41.70	289.7	246, 205, 179, 162	Catechin
6	13.73	43.90	289.2	246, 206	Epicatechin
7	15.19	53.20	523.3	503, 485, 475, 358, 243	n.i.
8	15.31	60.40	523.2	521, 503, 485, 475, 243	n.i.
9	16.27	40.05	433.7	385, 223, 205, 179, 153	n.i.
10	16.40	47.75	533.5		n.i.
11	16.42	48.85	475.0	441, 429, 379, 351, 257	n.i.
12	16.43	49.95	508.4	463, 441, 349, 193	n.i.
13	16.51	54.80	521.1	485, 476, 387, 357, 349, 177	n.i.
14	16.54	56.35	559.6	516, 485, 470, 441, 289	n.i.
15	16.54	56.55	469.3	375, 241	Stilbenoid dimer
16	18.99	47.50	475.1	454, 377, 349, 255	n.i.
17	19.03	49.65	469.4	452, 376, 364, 349, 255	Stilbenoid dimer
18	19.05	50.70	469.4	453, 432, 418, 255	Stilbenoid dimer
19	19.23	61.65	679.4	659, 586, 520, 452, 413, 345, 257	Resveratrol trimer
20	21.62	48.85	444.60	427, 402, 333, 301, 291, 285, 231, 150	n.i.
21	21.81	60.70	695.2	601, 575, 467, 453, 241	n.i.
22	29.57	58.10	906.5		Resveratrol tetramer
23	29.67	64.30	906.0		Resveratrol tetramer
24	33.25	45.00	579.9	561, 535, 453, 427, 408, 332, 289, 246, 205	Procyanidin dimer
25	33.30	48.15	549.4	521, 506, 421, 388, 311, 242	n.i.

26	34.66	57.75	906.3		Resveratrol tetramer
27	40.02	61.35	905.9		Resveratrol tetramer
28	41.05	45.05	577.6	559, 451, 425, 407, 289	Procyanidin dimer
29	42.57	58.00	905.8		Resveratrol tetramer
30	42.63	61.45	905.8		Resveratrol tetramer
31	46.16	39.30	577.7	559, 533, 469, 451, 425, 332, 290	Procyanidin dimer
32	46.18	40.80	577.7	560, 469, 452, 426, 332, 290, 233	Procyanidin dimer
33	46.21	42.45	577.6	560, 469, 452, 426, 332	Procyanidin dimer
34	46.24	44.15	577.7	559, 469, 452, 426, 332, 290	Procyanidin dimer
35	46.46	57.25	579.7	560, 547, 532, 484, 452, 425, 407, 289, 274, 187	Procyanidin dimer
36	46.47	57.95	923.4	827, 708, 612, 473, 415, 363	Stilbenoid tetramer
37	49.04	56.55	923.8	829, 696, 633, 452, 364	Stilbenoid tetramer
38	51.48	46.85	757.1	605, 509, 405, 349, 295	n.i.
39	53.96	39.50	593.6	575, 467, 441, 425, 407, 305, 289, 177	Prodelfphinidin dimer
40	54.20	53.90	939.8	906, 840, 746, 645, 578, 482, 357, 294	n.i.
41	55.28	40.75	593.4	575, 467, 441, 425, 305, 191	Prodelfphinidin dimer
42	55.36	45.25	729.3	711, 619, 603, 577, 559, 451, 441, 407, 289	Procyanidin dimer monogallate
43	55.52	55.05	839.0	821, 795, 746, 736, 677, 611, 549	n.i.
44	55.67	64.25	1045.1	1027, 1007, 999, 927, 873, 812, 722, 688, 595	n.i.
45	56.63	43.65	745.3	645, 592, 453, 341	Procyanidin dimer
46	56.79	53.55	839.8	820, 679, 593, 532, 1443, 1355, 1222,	n.i.
47	58.22	61.40	790.9*	1131, 1038, 1009, 906, 792, 743, 697, 679, 604, 545, 451	Resveratrol heptamer
48	59.44	56.25	777.6	615, 454, 1439, 1351, 1040,	Viniferin diglycoside
49	59.52	61.20	781.8*	949, 887, 825, 774, 735	n.i.
50	60.49	41.35	865.6	847, 739, 713, 695, 577, 449, 287, 245	Procyanidin trimer
51	59.52	43.35	865.8	848, 821, 801, 715,	Procyanidin trimer

52	60.54	44.30	881.3	663, 591, 518, 475 861, 753, 727, 711, 591, 577, 547, 439, 287	Prodelphinidin trimer (2 (E)C--1 G(E)C)
53	59.80	47.15	881.5	729, 711, 591, 577, 559, 547, 439	Procyanidin dimer digallate
54	60.63	49.95	897.7	877, 801, 725, 605, 589, 578	Dp-3-p-coumaroilglucoside- (epi)catechin
55	60.74	56.25	1359.7	1265, 1196, 1043, 937, 906, 813, 722, 628, 523, 480	Resveratrol hexamer
56	61.87	46.00	881.5	861, 753, 727, 709, 791, 547	Prodelphinidin trimer (2 (E)C--(E)GC)
57	61.97	52.00	1195.7	1043, 997, 948, 905, 803, 743, 707, 547, 357	n.i.
58	64.26	33.75	881.3	863, 755, 729, 711, 695, 593, 575, 287	Prodelphinidin trimer (2 (E)C--(E)GC)
59	64.50	47.80	1027.6	905, 782, 724, 659, 575, 313	
60	64.70	59.90	1175.1	1137, 1027, 944, 843, 729, 592, 493, 381	n.i.
61	65.71	42.60	897.9	838, 769, 743, 727, 607, 591, 467, 303	Prodelphinidin trimer ((E)C+ 2(E)GC)
62	65.74	44.25	1017.0	999, 955, 891, 866, 847, 740, 729, 696, 678, 602, 559, 451, 407, 289	Procyanidin trimer monogallate
63	65.76	45.35	1015.2	997, 967, 851, 789, 713, 610, 427	n.i.
64	66.01	60.60	922.7*	1811, 1555, 905, 875 827, 799	n.i.
65	69.53	37.95	1035.2	1015, 907, 881, 863, 847, 755, 745, 729	Prodelphinidin trimer monogallate (2 (E)C--(E)GCG or (E)CG--(E)C--(E)GC)
66	69.65	44.65	1169.6	1151, 1043, 1017, 999, 881, 865, 847, 729, 577	Procyanidin trimer digallate
67	70.90	42.05	1167.7	1152, 1017, 999, 877, 865, 742, 729, 591	Procyanidin trimer digallate
68	76.06	39.70	1171.8		Prodelphinidin tetramer (3 (E)C--(E)GC)
69	76.14	44.10	751.9*	1241, 1129, 993, 834, 753, 733, 674, 586, 528, 445	n.i.
70	77.30	36.15	1186.5		Prodelphinidin tetramer (2 (E)C--2(E)GC)
71	78.71	42.80	735.0*	1443, 1339, 1154, 1017, 865, 651, 578, 455, 289	Prodelphinidin tetramer digallate (2(E)CG--(E)C--(E)GC or (E)CG--2(E)C--(E)GCG)

72	78.75	45.20	828.6*	1576, 1492, 1370, 1291, 1178, 1080, 1016, 865, 831, 811, 745, 571, 487	Prodelphinidin tetramer trigallate ((E)CG--2(E)GCG--(E)GC or (E)C--3(E)GCG // Prodelphinidin pentamer monogallate ((E)CG--4(E)GC or (E)C--(E)GCG--3(E)GC)
73	81.34	44.45	917.9*	1541, 1487, 1361, 1255, 1087, 1029, 983, 918, 841, 762, 678, 629, 576, 480 1647, 1568, 1483, 1426, 1316, 1192,	n.i.
74	82.66	45.55	884.3*	1065, 995, 864, 807, 739, 591, 531, 465, 413, 246 1746, 1618, 1495, 1375, 1316, 1179,	n.i.
75	82.67	46.05	894.9*	1062, 816, 749, 603, 530, 465, 332 1490, 1425, 1339, 1191, 989, 881, 863,	n.i.
76	83.92	43.30	881.4*	806, 755, 728, 711, 695, 594, 577, 543, 287 1648, 1618, 1579, 1483, 1354, 1179, 1169, 1153, 1017,	n.i.
77	84.66	45.60	886.0*	995, 887, 865, 808, 741, 666, 615, 598, 577, 453, 386, 244	n.i.
78	86.54	44.25	1163.7		n.i.
79	86.57	46.30	1171.7		n.i.
80	86.44	38.10	1028.9		n.i.
81	89.16	45.35	1163.5		n.i.

n.i., Not identified; *ions detected as [M-2H]²⁻

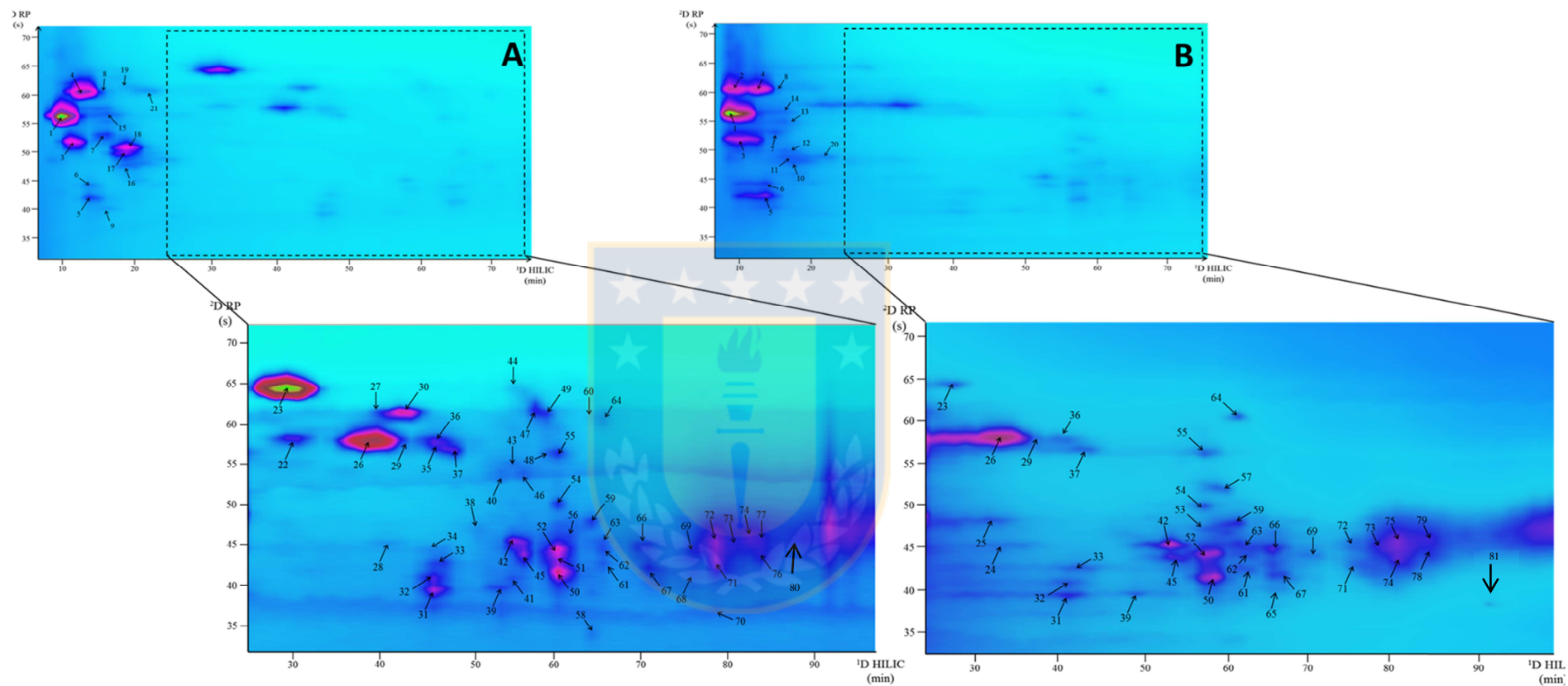


Fig. 4: Two-dimensional HILIC \times RP plots (280 nm) corresponding to the (poly)phenolic profile of Pinot Noir (A) and Cabernet Sauvignon (B) grapevine canes under optimum separation conditions. For peak identification, see Table 2. For detailed separation conditions, see Section 2.3.

The other main group of phenolic compounds in grapevine canes are stilbenoids. As can be observed from Table 2, the chemical composition on these compounds was also very complex, involving a great number of different but closely related chemical structures. These components eluted from the ¹D according to their increasing size. The most abundant among them was (*E*)-resveratrol (3,5,4'-trihydroxystilbene, peak 1), which was also the most intense peak in general in both samples. Piceatannol (peak 3) was also present in high amounts. Stilbenes monomers, such as resveratrol and piceatannol, present the same MS/MS fragmentation behavior. The fragmentation occurs in the resorcinol ring, which loses two consecutive C₂H₂O, corresponding to one and two neutral losses of 42 Da, respectively [31]. This way, the fragmentation of resveratrol (peak 1, *m/z* 227) is characterized by the production of fragments at *m/z* 187 and 143. Likewise, the fragmentation of piceatannol (peak 3, *m/z* 243) produced fragments at *m/z* 201 and 159. The rest of stilbenoids detected in the grapevine canes samples were formed by more complex structures, with varying degree of polymerization. UV-vis maxima were also useful to assign the separated components as resveratrol presents a UV absorption maximum at 310 nm, whereas, as the size of stilbenoid oligomers increases, the UV maximum shifts to ca. 280–290 nm [32]. The above-commented loss of C₂H₂O under MS/MS fragmentation is also characteristic of stilbenoid oligomers; besides the neutral loss of 42 Da, oligomers may also present typical losses corresponding to 94 Da (C₆H₆O), 106 Da (C₇H₆O) and 110 Da (C₆H₆O₂) [31]. For instance, peak 4 (*m/z* 453.7, [M–H][–]) was tentatively identified as a resveratrol dimer, being the most important fragments derived from this ion those with *m/z* 411 (loss of 42 Da), 359 (loss of 94 Da) and 347 (loss of 106 Da). In the same way, peak 2 was also assigned as a resveratrol dimer. These two compounds were related to

viniferin, although an unequivocal identification could not be reached with the available tools.

Interestingly, a di-glycosylated derivative of this compound was also found in *Pinot Noir* canes (peak 48). This compound, not reported previously in grapevine canes, has been detected in Riesling wine [33]. Viniferin diglycoside was characterized by a molecular ion at m/z 777, showing MS/MS fragments corresponding to the loss of one or both glycosidic residues (m/z 615 and 454). Moreover, three other dimeric stilbenoid derivatives were also detected (peaks 15, 17 and 18). These possessed an ion at m/z 469, which was in agreement of a structure based on the combination of (*E*)-resveratrol and piceatannol. Only one resveratrol trimer was detected (peak 19) in the *Pinot Noir* sample (m/z 679, Fig. 4A) which contrasts with the detection of 6 different resveratrol tetramers (peaks 22, 23, 26, 27, 29 and 30). All these possessed molecular ions at m/z 905 and their structure would be related to hopeaphenol and vitisin [34]. Additionally, two other stilbenoid tetramers were detected at m/z 923 (peaks 36 and 37); their fragmentation pattern indicated that were related to viniferol E, including an additional hydroxyl group in their structure compared to the other tetramers. Moreover, two bigger oligomers, i.e., a resveratrol hexamer (peak 55) and a resveratrol heptamer (peak 47, Fig. S1A), were detected in these samples. The generated fragments corresponding to less polymerized resveratrol derivatives helped to assign these components. This is the first report of the presence of these big oligomers in grapevine canes.

Besides these components, other compounds were separated and their MS and MS/MS information collected, although no specific assignment could be obtained (see Table 2). Comparing both samples, quite similar profiles were achieved (Fig. 4), being (*E*)-resveratrol, piceatannol and resveratrol dimers the most abundant compounds. Although the

precise composition changed between *Pinot Noir* and *Cabernet Sauvignon* canes, from a qualitative point of view all the groups of compounds were similarly represented on both samples. In any case, the variability on the (poly)phenolic composition and content in grapevine canes from different varieties has been already reported [5,34]. However, this method allows to obtain the (poly)phenolic profile of these complex materials involving different groups of polyphenol oligomers, which gives a clear idea of the satisfactory separation power of the developed HILIC \times RP method. Furthermore, this application confirms the good possibilities that grapevine canes may have for valorization and attainment of valuable natural components with potential applications in the food, nutraceutical and cosmetic industries.

4. Conclusions

In this work, a new HILIC \times RP-DAD-MS/MS method is developed for the profiling of (poly)phenolic compounds present in grapevine canes from several varieties. By combining a diol column in the 1D with a C_{18} column in the 2D , it is possible to obtain their (poly)phenolic profile in around 80 min. The method has shown extremely good separation capabilities, and is characterized by high effective peak capacity (842) and orthogonality ($A_0 = 78\%$). 81 different components were detected in the samples; most of them could be tentatively assigned using the information provided by the MS and DAD detectors employed. Two main (poly)phenolic groups are represented, proanthocyanidins and stilbenoids. Thanks to this development, some components, such as prodelfinidins as well as some highly polymerized stilbenoids have been described for the first time in grapevine canes. Consequently, the interest of the application of LC \times LC-based approaches to study complex natural mixtures has been once more confirmed. From the obtained results, it can

be deduced that *Vitis vinifera* L. canes have a great potential to be used as an underexploited natural source of bioactive compounds, with potential applications in different fields. The developed methodology might also be a very effective tool to better understand the ongoing mechanisms in grapevine canes triggering the significant increase of the concentrations of some stilbenoids after pruning and during cane storage, thanks to its improved separation capabilities.

Acknowledgements

The authors would like to thank Projects AGL2014-53609-P (MINECO, Spain), Grant 1150721 (FONDECYT, Chile) and Project Basal PFB-27 (CONICYT, Chile) for financial support. V.S. thanks CONICYT (Chile) for a Doctoral Fellowship.



References

- [1] D.S. Martin, S. Ramos, J. Zufía, Valorisation of food waste to produce new raw materials for animal feed, *Food Chem.* 198 (2016) 68–74.
- [2] R. Ravindran, A.K. Jaiswal, Exploitation of food industry waste for high-value products, *Trends Biotechnol.* 34 (2016) 58–69.
- [3] F. Cherubini, The biorefinery concept: using biomass instead of oil for producing energy and chemicals, *Energy Convers. Manag.* 51 (2010) 1412–1421. [4] R. Devesa-Rey, X. Vecino, J.L. Varela-Alende, M.T. Barral, J.M. Cruz, A.B. Moldes, Valorization of winery waste vs the costs of not recycling, *Waste Manag.* 31 (2011) 2327–2335.
- [5] C. Vergara, D. von Baer, C. Mardones, A. Wilkens, K. Wernekinck, A. Damm, S. Macke, T. Gorena, P. Winterhalter, Stilbene levels in grape cane of different cultivars in Southern Chile: determination by HPLC-DAD-MS/MS method, *J. Agric. Food Chem.* 60 (2012) 929–933.
- [6] T. Gorena, V. Sáez, C. Mardones, C. Vergara, P. Winterhalter, D. von Baer, Influence of post-pruning storage on stilbenoid levels in *Vitis vinifera* L. canes, *Food Chem.* 155 (2014) 256–263.
- [7] B. Houillé, S. Besseau, V. Courdavault, A. Oudin, G. Glévarec, G. Delanoue, L. Guérin, A.J. Simkin, N. Papon, M. Clastre, N. Giglioli-Guivarc'h, A. Lanoue, Biosynthetic origin of E-resveratrol accumulation in grape canes during postharvest storage, *J. Agric. Food Chem.* 63 (2015) 1631–1638.
- [8] R. Flamini, F. Mattivi, M. De Rosso, P. Arapitsas, L. Bavaresco, Advanced knowledge of three important classes of grape phenolics: anthocyanins, stilbenes and flavonols, *Int. J. Mol. Sci.* 14 (2013) 19651–19669.

- [9] C. Santos-Buelga, C. García-Viguera, F.A. Tomás-Barberán, On-line identification of flavonoids by HPLC coupled to diode array detector, in: C. Santos-Buelga, G. Williamson (Eds.), *Methods in Polyphenol Analysis*, The Royal Society of Chemistry, Cambridge, UK, 2003.
- [10] D. Bagchi, A. Swaroop, H.G. Preuss, M. Bagchi, Free radical scavenging: antioxidant and cancer chemoprevention by grape seed proanthocyanidin: an overview, *Mutat. Res.* 768 (2014) 69–73.
- [11] T. Püssa, J. Floren, P. Kuldkepp, A. Raal, Survey of grapevine *Vitis vinifera* stem polyphenols by liquid chromatography-diode array detection-tandem mass spectrometry, *J. Agric. Food Chem.* 54 (2006) 7488–7494.
- [12] D.R. Stoll, Recent progress in online:comprehensive two-dimensional high-performance liquid chromatography for nonproteomic applications, *Anal. Bioanal. Chem.* 397 (2010) 979–986.
- [13] F. Cacciola, P. Donato, D. Sciarrone, P. Dugo, L. Mondello, Comprehensive liquid chromatography and other liquid-based comprehensive techniques coupled to mass spectrometry in food analysis, *Anal. Chem.* 89 (2017) 414–429.
- [14] X. Li, P.W. Carr, Effects of first dimension eluent composition in two-dimensional liquid chromatography, *J. Chromatogr. A* 1218 (2011) 2214–2221. [15] S.R. Groskreutz, M.M. Swenson, L.B. Secor, D.R. Stoll, Selective comprehensive multi-dimensional separation for resolution enhancement in high performance liquid chromatography. Part I—principles and instrumentation, *J. Chromatogr. A* 1228 (2012) 31–40.
- [16] P. Donato, F. Cacciola, P.Q. Tranchida, P. Dugo, L. Mondello, Mass spectrometry detection in comprehensive liquid chromatography: basic conceptsinstrumental aspects, applications and trends, *Mass Spectrom. Rev.* 31 (2012) 523–559.

- [17] F. Cacciola, S. Farnetti, P. Dugo, P.J. Marriott, L. Mondello, Comprehensive two-dimensional liquid chromatography for polyphenol analysis in foodstuffs, *J. Sep. Sci.* 40 (2017) 7–24.
- [18] X. Li, D.R. Stoll, P.W. Carr, Equation for peak capacity estimation in two-dimensional liquid chromatography, *Anal. Chem.* 81 (2009) 845–850.
- [19] M.R. Schure, J.M. Davis, Orthogonal separations: comparison of orthogonality metrics by statistical analysis, *J. Chromatogr. A* 1414 (2015) 60–76. [20] M. Camenzuli, P.J. Schoenmakers, A new measure of orthogonality for multi-dimensional chromatography, *Anal. Chim. Acta* 838 (2014) 93–101.
- [21] A. Zhang, L. Wan, C. Wu, Y. Fang, G. Han, H. Li, Z. Zhang, H. Wang, Simultaneous determination of 14 phenolic compounds in grape canes by HPLC-DAD-UV using wavelength switching detection, *Molecules* 18 (2013) 14241–14257. [22] N. Vivas, M.F. Nonier, N. Vivas de Gaulejac, C. Absalon, A. Bertrand, M. Mirabel, Differentiation of proanthocyanidin tannins from seeds:skins and stems of grapes (*Vitis vinifera*) and heartwood of Quebracho (*Schinopsis balansae*) by matrix-assisted laser desorption/ionization time-of-flight mass spectrometry and thioacidolysis/liquid chromatography/electrospray ionization mass spectrometry, *Anal. Chim. Acta* 513 (2004) 247–256.
- [23] L. Montero, M. Herrero, M. Prodanov, E. Ibáñez, ~ A. Cifuentes, Characterization of grape seed procyanidins by comprehensive two-dimensional hydrophilic interaction × reversed phase liquid chromatography coupled to diode array detection and tandem mass spectrometry, *Anal. Bioanal. Chem.* 405 (2013) 4627–4638.

[24] L. Montero, M. Herrero, E. Ibáñez, ~ A. Cifuentes, Profiling of phenolic compounds from different apple varieties using comprehensive two-dimensional liquid chromatography, *J. Chromatogr. A* 1313 (2013) 275–283.

[25] L. Montero, M. Herrero, E. Ibáñez, A. Cifuentes, Separation and characterization of phlorotannins from brown algae *Cystoseira abies-marina* by comprehensive two-dimensional liquid chromatography, *Electrophoresis* 35 (2014) 1644–1651.

[26] B. Buszewski, S. Noga, Hydrophilic interaction liquid chromatography (HILIC)—a powerful separation technique, *Anal. Bioanal. Chem.* 402 (2012) 231–247.

[27] D.R. Stoll, P.W. Carr, Two-dimensional liquid chromatography: a state of the art tutorial, *Anal. Chem.* 89 (2017) 519–531.

[28] R.E. Murphy, M.R. Schure, J.P. Foley, Effect of sampling rate on resolution in comprehensive two-dimensional liquid chromatography, *Anal. Chem.* 70 (1998) 1585–1594.

[29] H.J. Li, M.L. Deinzer, Tandem mass spectrometry for sequencing proanthocyanidins, *Anal. Chem.* 79 (2007) 1739–1748.

[30] Y. Hayasaka, E.J. Waters, V. Cheynier, M.J. Herderich, S. Vidal, Characterization of proanthocyanidins in grape seeds using electrospray mass spectrometry, *Rapid Commun. Mass Spectrom.* 17 (2003) 9–16.

[31] R. Moss, Q. Mao, D. Taylor, C. Saucier, Investigation of monomeric and oligomeric wine stilbenoids in red wines by ultra-high-performance liquid chromatography/electrospray ionization quadrupole time-of-flight mass spectrometry, *Rapid Commun. Mass Spectrom.* 27 (2013) 1815–1827.

[32] R.H. Cichewicz, S.A. Kouzi, Resveratrol oligomers: structure, chemistry, and biological activity, in: Atta-ur-Rahman (Ed.), *Studies in Natural Products Chemistry*, vol.

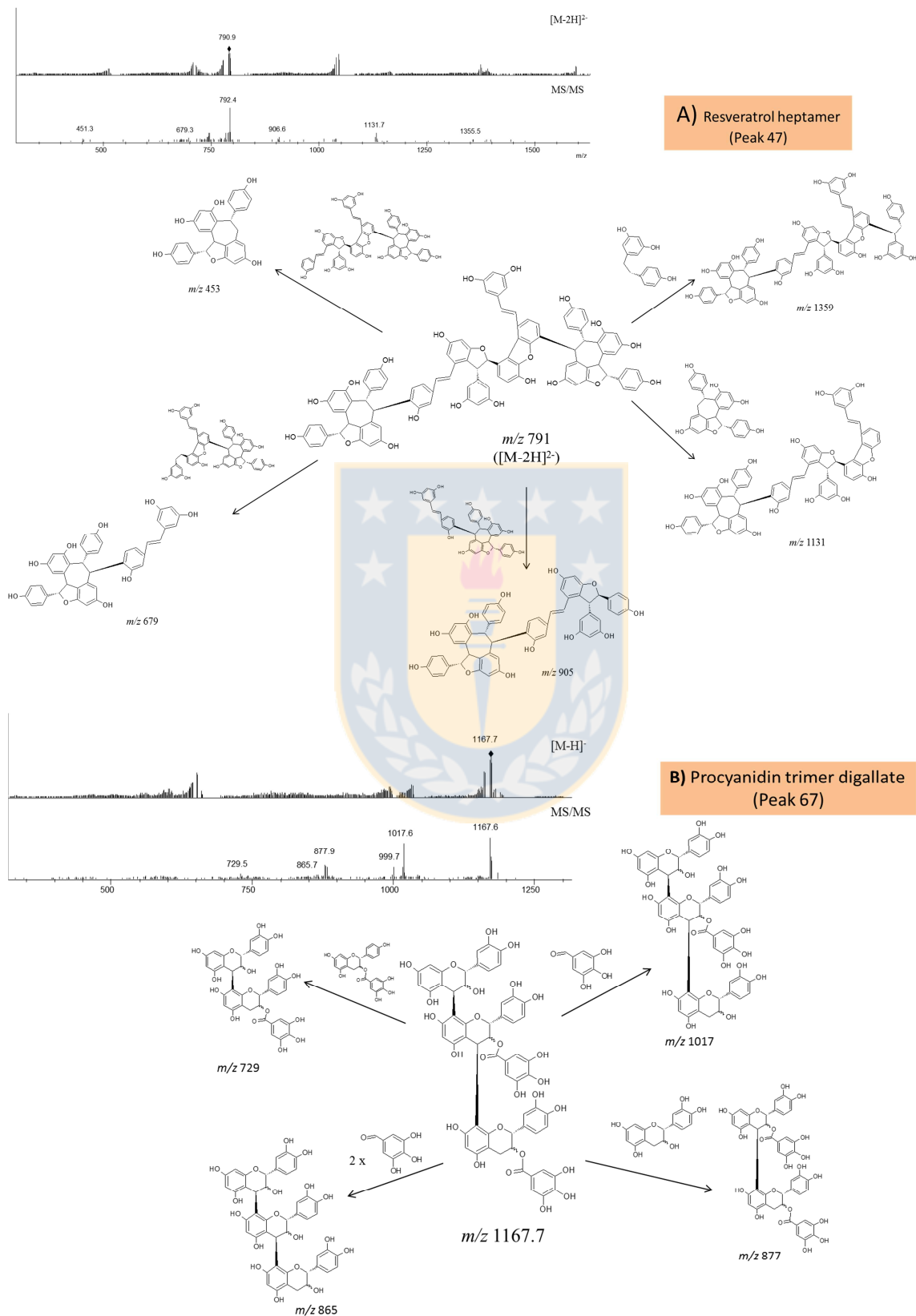
26, Bioactive Natural Products (Part G), Elsevier Science B.V., Amsterdam, The Netherlands, 2002.

[33] B. Baderschneider, P. Winterhalter, Isolation and characterization of novel stilbene derivatives from Riesling wine, *J. Agric. Food Chem.* 48 (2000) 2681–2686.

[34] C. Lambert, T. Richard, E. Renouf, J. Bisson, P. Waffo-Teguo, L. Bordenave, N. Ollat, J.M. Merillon, S. Cluzet, Comparative analyses of stilbenoids in canes of major *Vitis vinifera* L. cultivars, *J. Agric. Food.*



Supplementary data :



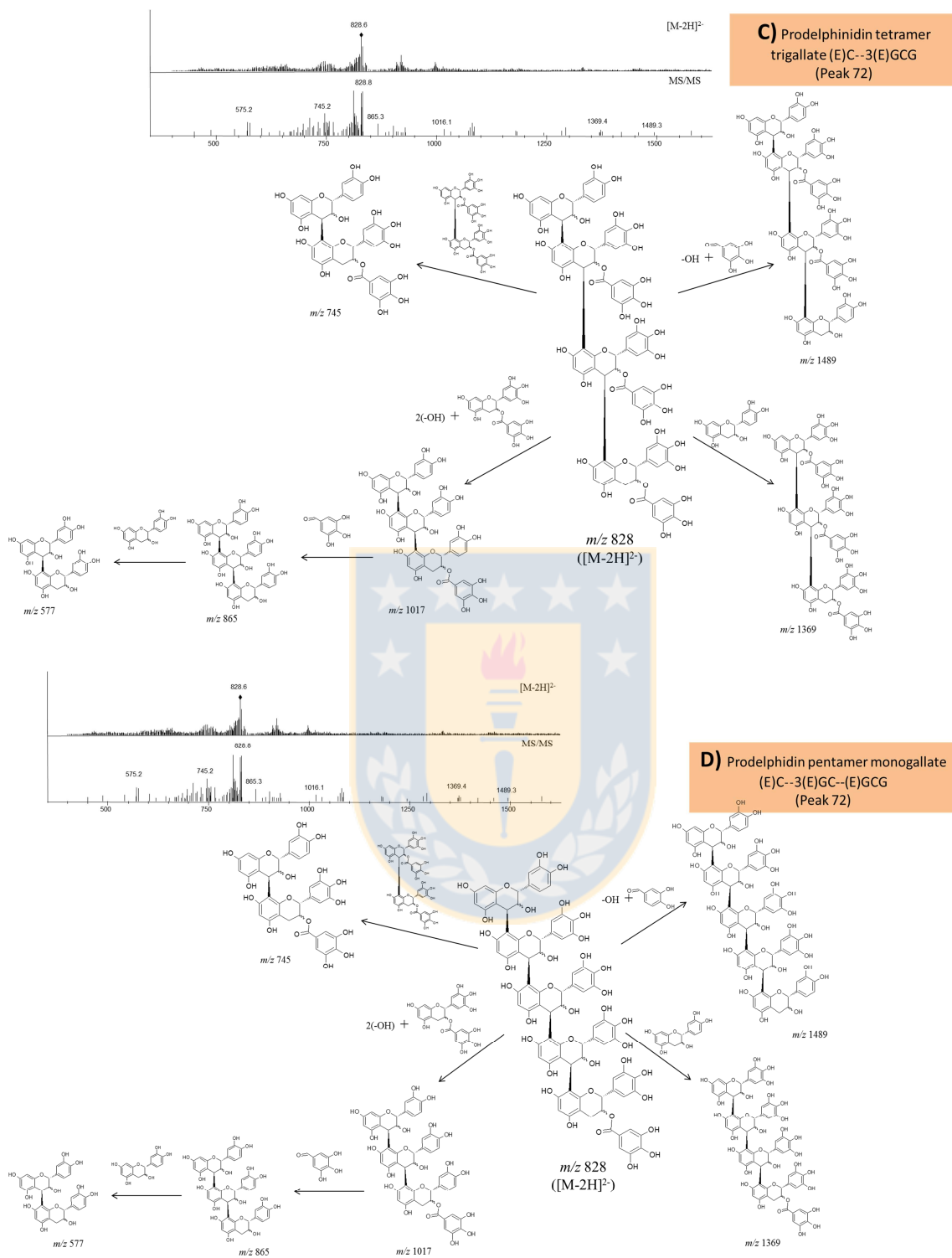


Fig.S1. MS spectra and MS/MS fragmentation patterns as well as tentatively proposed chemical structure of A) resveratrol heptamer (peak 47), B) procyanidin trimer digallate

(peak 67), and C) prodelphinidin tetramer trigallate (peak 72) and its alternative identification D) prodelphinidin pentamer monogallate (peak 72).



Capítulo 5 :Conclusiones finales.



1. Desde sarmientos de Pinot Noir se aisló e identificó (*E*)-resveratrol, (*E*)- ϵ -viniferina, (*E*)-piceatanol, ampelopsina A y vitisina B (94-99 %) y estilbenoides minoritarios como como pallidol, (*E*)-*trans-cis*-miyabenol C, (*E*)- ω -viniferina, (*E*)- δ -viniferina, isorapontigenina, scirpusina A y un heterodímero, no reportado anteriormente, denominado iso-scirpusina A
2. Mediante ensayos *in vitro* se demostró la capacidad antioxidante de los estilbenoides de sarmientos. La capacidad antioxidante (ORAC-FL) *in vitro* de (*E*)-resveratrol es sobrepasada por los oligómeros minoritarios aislados.
3. En un ensayo *in vitro* con líneas celulares cancerosas destaca el efecto antiproliferativo de (*E*)-piceatanol. Este no es apreciable en una línea celular normal. Ampelopsina A y el extracto de sarmiento completo poseen efecto antiproliferativo en una línea celular de adenocarcinoma de vejiga (J82).
4. La combinación de una columna de núcleo sólido con un detector de absorbancia DAD y uno de fluorescencia en serie son una herramienta analítica muy útil en el monitoreo de la evolución de los niveles de estilbenoides y proantocianidinas durante la guarda de los sarmientos.
5. Estos son una fuente de estilbenoides, cuyo potencial depende directamente de las condiciones de guarda post-poda. Los monómeros (*E*)-piceatanol, (*E*)-resveratrol y (*E*)-piceido aumentan notablemente durante la guarda, no así los oligómeros.
6. Un incremento de 60 % a 70% de humedad relativa durante la guarda afecta la concentración de estilbenoides, disminuyen el potencial de utilización de los sarmientos, pues la concentración máxima, principalmente de (*E*)-resveratrol y (*E*)-piceatanol son significativamente menores. Se establece así una nueva variable,

aparte de tiempo, temperatura y longitud del sarmiento para lograr un adecuado manejo del residuo luego de la poda.

7. La humedad relativa también afecta los niveles de proantocianidinas. (-)-epicatequina disminuye hasta un 75 % en sarmientos guardados luego de la poda, en menor grado procianidina B1 y un dímero de prodelfinidina, tiende a disminuir progresivamente sus niveles en sarmientos. (+)-catequina no presenta una tendencia definida.
8. Por LC x LC (HILIC (diol) x RP (C18)) de mayor poder de resolución además de las proantocianidinas ya descritas, se detectaron numerosos dímeros y trímeros de procianidinas, dímeros mono-galoilados y di-galoilados. El grado de polimerización de las prodelfinidinas presentes es de 2 hasta 5, con diferente grado de galoilación, además de estilbenoides complejos con elevado grado de polimerización (hasta heptámeros), viniferinas mono-glicosiladas y di-glicosiladas, además de heterodímeros.

